2022-12-01

Using Ultrasonication For The Improvement Of Grade And Recovery In Molybdenum Sulfide Flotation

Wayne Alexander Campbell
University of Texas at El Paso

USING ULTRASONICATION FOR THE IMPROVEMENT OF GRADE AND RECOVERY IN MOLYBDENUM SULFIDE FLOTATION

WAYNE ALEXANDER CAMPBELL

Doctoral Program in Materials Science and Engineering

APPROVED:

Guikuan Yue, Ph.D., Chair

Stella Quinones, Ph.D.

Antonio Arribas, Ph.D.

Stephen L. Crites, Jr., Ph.D.
Dean of the Graduate School

Dedication

This work is dedicated to my wonderful wife Olga, who always makes me strive to be the best version of myself, and our daughter Aurora.

USING ULTRASONICATION FOR THE IMPROVEMENT OF GRADE AND RECOVERY IN MOLYBDENUM SULFIDE FLOTATION

by

WAYNE ALEXANDER CAMPBELL

DISSERTATION

Presented to the Faculty of the Graduate School of

The University of Texas at El Paso

in Partial Fulfillment

of the Requirements

for the Degree of

DOCTOR OF PHILOSOPHY

Doctoral Program in Materials Science and Engineering

THE UNIVERSITY OF TEXAS AT EL PASO

December 2022

Acknowledgements

I first would like to acknowledge my advisor, Dr. Guikuan Yue, for all his help and insight as I pursued this research. He has helped me develop my skills as a metallurgist in the mining industry and I greatly appreciate his encouragement and guidance. I would not hold the position I have today without his support.

I would also like to thank my committee members, Dr. Guikuan Yue, Dr. Stella Quinones, and Dr. Antonio Arribas for their valuable contributions and suggestions for my research. I hold them in very high regard and can not think of a better group to have guided me. I want to acknowledge the hard work done by all of the MMBME department. The faculty as well as the students have made my experience at UTEP a great one that I will always remember. It was an honor to study here as well as teach. I want to especially thank Dr. Stephen Stafford, Dr. Shailendra Varma, Dr. David Roberson, and Dr. Christopher Bradley for such a wonderful graduate experience. I want to also thank Truman Word, Diego Bermudez, Yamile Urquidi, Joy Hamilton, and all the other teaching assistants in the department, from whom I learned so much as we worked together. Moving forward in my career is tough as I am leaving a place full of such hard-working and kind-hearted people all destined for greatness. I have learned so much from you all and grew with you during such a challenging time.

I also want to thank Freeport-McMoRan for giving me an opportunity to work with their fantastic company and help me finish this work, financially and practically. I especially want to thank Bradford Wesstrom for taking the time to get UTEP students involved with Freeport and drawing my attention to the company in the first place. In addition, I want to thank William Lambert, Denita Kippers, Jay Williams, and Nick Schade for all of their help and knowledge. I also want to acknowledge the hard work of Mitchell Stashick, Michael Opitz, Joshua Ryks, and

Shelby Epperson for helping me accomplish this research, and especially Robert Schempp, from whom I learned how to operate the flotation machines, assaying techniques, and mostly all of the practical knowledge behind experimenting with molybdenum. A special thank you to Meredith Bahe, who taught me mostly all of the operational aspects and intricacies of the mill as I completed this work.

I have the deepest gratitude that I had the opportunity to know you and work with you all.

Abstract

Experimentation was performed on molybdenite slurry by using ultrasonication to elucidate the effects of ultrasonic-induced bubble cavitation on the grade, recovery, and gangue reduction during small-scale flotation tests and was followed by a topographical analysis of quartz particles using SEM. Ultrasonic waves at 20-80 kHz that propagate through a liquid medium cause microbubbles to form, grow, and implode. The cavitation bubble's implosion causes brief extreme local conditions where temperatures can reach 5,000 K and pressures of 1,000 bar. The resulting microjets create mechanical and chemical changes to the system and were directed at improving flotation dynamics in these experiments.

Through experimentation with a float cell immersed in an ultrasonic bath as well as the utilization of an ultrasonic probe, a clear reduction in gangue recovery was found after subjecting the slurry to a 2-minute pretreatment of ultrasound at 24 kHz and continuing for the duration of an 8-minute test. While the ultrasonic bath at 37 kHz did not reveal clear improvements, the ultrasonic probe embedded directly into the slurry did show benefits to gangue reduction and molybdenite grade in the concentrate, while the process did slow the kinetics of flotation. Subjecting the slurry to only a pretreatment of ultrasound revealed similar results to the testing involving using the probe for the entire duration of the float test. The effects of ultrasonication in regard to its deagglomeration capabilities is suspected as the cause of these results. While gangue is released from agglomerates and allowed to be rejected in the system, fine molybdenite particles benefit from agglomeration. A topographical survey of quartz particles using an SEM revealed craters and dimples in ultrasonicated slurry, potentially causing a reduction in contact angle and reduced quartz floatability.

Table of Contents

List of Tables

List of Figures

Chapter One: Introduction

1.1 Molybdenum Production

Molybdenum (Mo) concentrate production in the United States reached 41,100 metric tons in the year of 2021. Worldwide, that figure was estimated to be 300,000 metric tons with the greatest producer being China with 130,000 tons in 2021. Molybdenum resources in the U.S. total about 5.4 million tons, with resources equaling 20 million tons worldwide [1, 2]. Concentrates of molybdenum ore production are typically molybdenum sulfide which originate from porphyry molybdenum deposits or as a secondary product from porphyry copper deposits. The leading producers of molybdenum from primary molybdenum ore in the USA were the Climax mine and Henderson mine located in Colorado, both owned by Climax Molybdenum, a subsidiary of Freeport-McMoRan, which produces approximately 80 million pounds of a year.

The Henderson mine is an underground mine which operates as a block caving operation where the ore body is blasted by dynamite and allowed to collapse under its own weight. The broken ore is collected, placed in a gyratory crusher and conveyed to the mill site 15 miles away. The Climax mine is an open-pit operation which has the mill on site. The ore body possesses more oxide material than the Henderson mine as it is collected near the surface. By-product mines such as Bagdad, Sierrita, Morenci, or Cerro Verde are open-pit mines which mine primarily copper ore but produce molybdenum concentrate albeit at a lower quality. This lower quality concentrate must first be leached to remove impurities before it can be roasted to produce chemical grade molybdenum oxide.

Molybdenum is used in a wide variety of applications; the great majority of the metal being used as catalysts in the petroleum industry and as additives in steels and superalloys as it can increase toughness and corrosion resistance at elevated temperatures. The metal contributes to improving

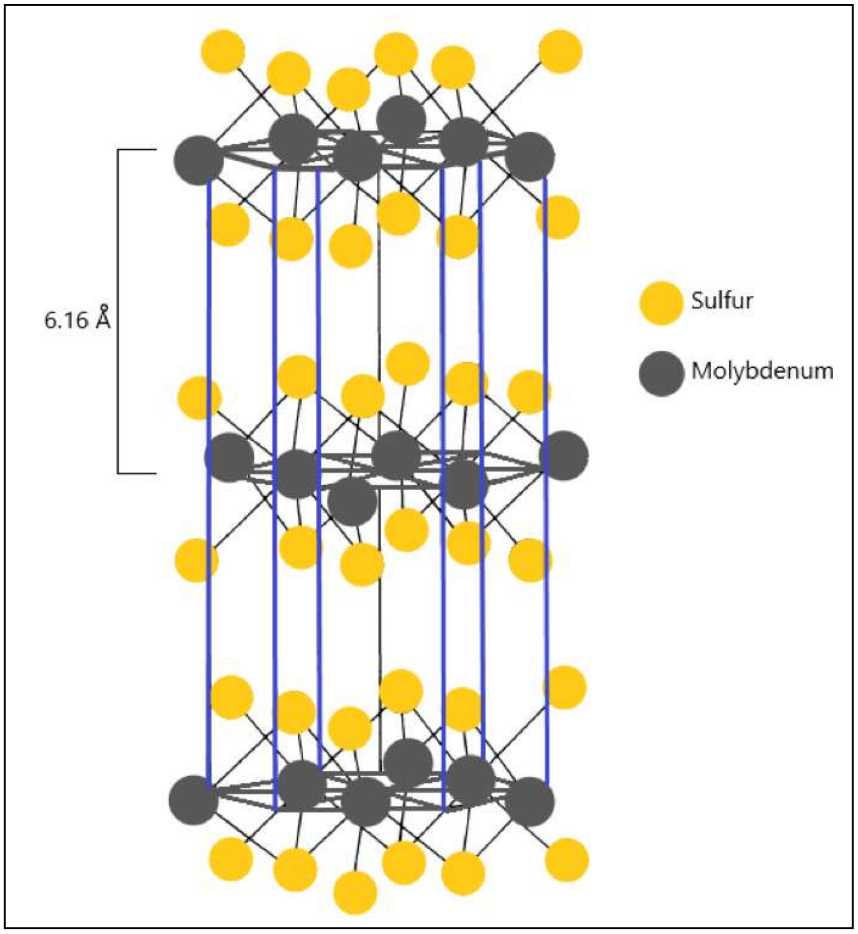

Figure 1: the structure of molybdenum disulfide. Each molybdenum atom, surrounded by six sulfur atoms, form layered sheets in a hexagonal structure.

the environment as 70% of its chemical uses are as a catalyst in the hydrodesulfurization process in petrochemical refining, leading to less sulfur emissions. There will also be a greater demand for high grade molybdenum steels in coal powered plants, as they would need to run their plants at significantly higher temperatures in order to lower carbon dioxide emissions. Global consumption of molybdenum was over 264,000 tons in 2018, with structural steels leading the end use for the metal [3].

Molybdenum is also a key component in fertilizers and lubricants. Molybdenum disulfide is a very effective lubricant and can reduce machine wear at high pressures and high temperatures. These properties manifest due to MoS_2 forming layered sheets in a hexagonal

structure. As the sheets slide past each other, there exists an uncommonly low coefficient of friction. This phenomenon occurs first through a transfer of MoS_2 to the opposing material with good adhesion, as well as a friction-induced re-orientation of the basal planes in the MoS_2 grains to parallel of the sliding direction. These lubricating effects can be hindered by contaminants [4]. MoS_2 can be typically added as a blend with oils or greases, and since the lubricity is retained even when no oil remains, the product is used in aircraft engines and other critical applications.

Concentrate production from molybdenite (MoS_2) ore occurs through a series of grinding and milling, rougher flotation, and cleaner flotation [5, 6]. The ore is recovered from the deposit by blasting and is then crushed. The crushed ore is delivered by truck or conveyor to be milled to the consistency of sand and the resulting slurry, which would have a low grade of <0.2% Mo, would be next sent to a series of flotation cells to produce high grade concentrate.

To reduce the MoS_2 concentrate into the base metal, it is processed further by roasting to produce molybdenum oxide, which is then extracted with ammonia to produce ammonium molybdate (**Figure 2**). This ammonium solubilization is done to further purify the material, since impurities will remain as solids and can be removed. Ammonium molybdate is filtered, crystallized, dried, and then converted to ammonium dimolybdate. The material then undergoes calcination to produce molybdenum trioxide. By reducing the oxide with hydrogen, molybdenum metal is produced [5].

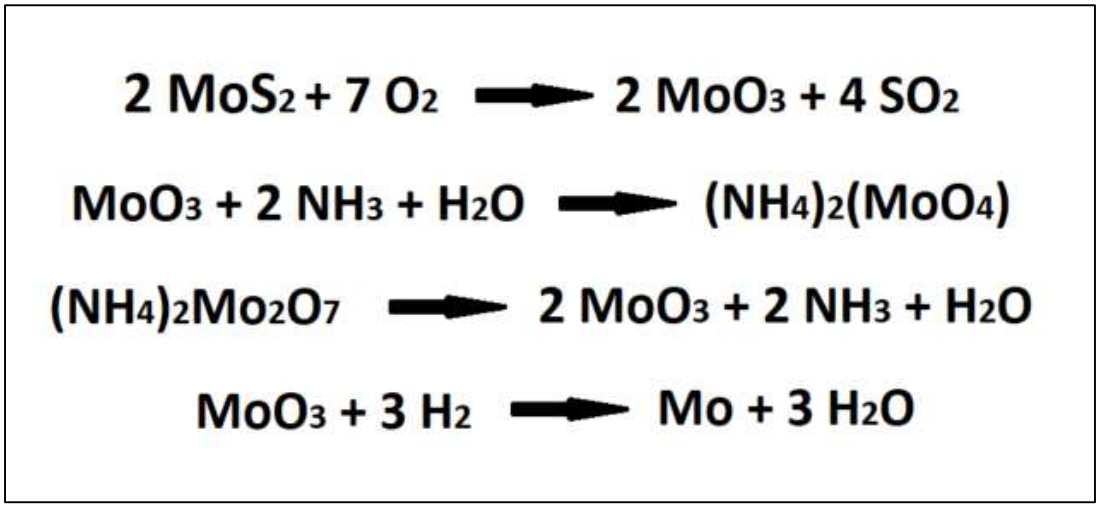

Figure 2: The chemical reactions involved in the production of molybdenum metal from molybdenum disulfide concentrate.

1.2 Froth Flotation

MoS_2 froth flotation, like other sulfide flotation, is a means of separation of the sulfide mineral from gangue and occurs in a series of roughers and cleaners. The roughers act as the first stage to quickly remove as much gangue material as possible from the desired mineral. Cleaners are another stage of float cells that further remove undesired material and improve grade as much as possible. These stages are usually set in a series, or parallel, and can return back as a circuit depending on the operation's goals. Froth flotation takes advantage of the hydrophobicity of sulfide minerals by using air bubbles to attract the mineral and separate them from unwanted gangue [7]. The flotation cell is agitated and air is run at the bottom of the cell. As the air bubbles rise, hydrophobic MoS_2 adhere themselves to the bubble surface and are concentrated in a foam at the flotation cell's surface. This foam then pours over the side of the cell into a launder as a MoS_2 concentrate [8]. Three routes by which material is recovered through froth flotation are by selective attachment to the air bubble, becoming entrained in the water as it passes

through the froth, and particles becoming aggregated between the mineral attached to bubbles [9].

Froth flotation is a complex system that separates the desired mineral from unwanted material by incorporating the three phases of solids, liquids, and gases, with physical and chemical interactions [10, 78]. The physical variables of the system include ore particle size, the extent of mineral liberation, along with the agitation rate (physical mixing of the slurry to prevent settling), air flow rate, and bubble size [11]. Chemical interactions by added reagents are used to control the hydrophobicity of the elements and minerals in the system. Chemical reagents can include collectors, frothers, and regulators [12, 13]. Fundamentally, these variables come together to constitute the floatability of the system, or probability of particle/bubble collision and their continual adherence [14,15].

1.2.1 Particle Size

Froth flotation relies on ore particle size being relatively fine so that the adhesion force between the particle and the froth bubble is greater than the gravitational force of the particle, otherwise the particle will detach [16]. However, there is a limit to the effectiveness of flotation if the particle becomes too small [17, 19]. Molybdenum sulfide minerals are naturally hydrophobic up to a certain size. The faces of the MoS_2 sheets, consisting of an arrangement of the sulfur atoms, are hydrophobic while the edges of the sheets are hydrophilic. As the particle size gets smaller and smaller, the ratio of edges to sheet faces increases and therefore will reduce its natural hydrophobicity. The contact angle between a bubble and a face surface would be approximately 80^o where it would become 30^o on an edge surface [5]. Larger contact angles increase the particle/bubble adhesion and will be discussed later [20]. In addition, as a particle becomes smaller, the probability of bubble collision decreases as well.

1.2.2 Mineral Liberation

The liberation of the desired mineral from gangue also affects the efficiency of froth flotation, as the system is greatly based on the particle surface. Gangue materials are not as hydrophobic as a sulfide mineral and will not tend to adhere to bubble surfaces. As more mineral is liberated, the greater the ratio of hydrophobic surface exists for a bubble to interact with. In addition, an unliberated mineral which is completely surrounded by gangue, or locked, will not have access to a bubble and will be rejected in the system [17].

1.2.3 Air Rate

Increasing air flow rate will increase mineral recovery up to a maximum limit. Once above this critical rate, large undispersed air bubbles will pass through the froth and burst at the surface, causing the froth to be disrupted and will tend to collapse, resulting in a lower recovery [18]. The maximum air rate will depend on the percent solids in the slurry, with the lower percent solids having a higher maximum air rate [8]. Research by Cooper et al. [21] showed that decreasing air rate improved the grade of concentrate by reducing entrainment. The reduction in gangue recovery by entrainment was attributed to a lower water recovery resulting from the lower air rate.

1.2.4 Bubble size

Decreasing bubble size is a more effective means to improve flotation kinetics than increasing air rate [22]. The reduction of a flotation bubble's size will increase the bubble surface area and therefore improve the real estate at which a hydrophobic mineral can attach [23]. A typical flotation machine produces an average 4mm diameter bubble and if that size is reduced to 1 mm would constitute an increase in the total number of bubbles by 64, with a total bubble surface area by 16 times. In addition, the longer a bubble remains in the slurry zone of the

flotation cell, the higher the probability of particle/bubble collision [24]. The smaller a bubble becomes, the slower it moves through the slurry, most likely due to surface tension gradients increasing fluid drag around the bubble [25]. The reduction of bubble size and rise velocity is achieved through the use of a frother reagent, whose mechanisms will be explained with other chemical interactions [5]. An optimum range is called for by Yianatos and Henriqez [26] for mean bubble diameter being between 1-1.5 mm (if air rate equals 1-2 cm/s) with sizes above that resulting in a lower bubble surface area flux, lower mineral carrying capacity, larger disturbances at the slurry-froth interface, and a larger entrainment in the froth. Sizes below 1 mm result in the loss of the slurry-froth interface, known as flooding, a lower bubble surface area flux, and a lower mineral carrying capacity [26].

1.2.5 Collectors

Collectors are a class of chemical reagent which act as a surfactant that modulates the hydrophobicity of the desired mineral. In the case of molybdenum sulfide, an added collector would amplify the natural hydrophobicity. Typical collectors are organic compounds, insoluble and strongly hydrophobic themselves, usually oils. These oils will adsorb by combining with the mineral through hydrophobic interaction against the water and reduce the stability of the hydrating layer between the particle and bubble [12, 27]. For example, the main collector used at the Climax mine in Colorado is vapor oil at 0.8-0.9 lb/ton [5]. Vapor oil can also be referred to as naphthenic oils and possess saturated cyclic hydrocarbons in the molecular structure.

1.2.6 Frothers

Frothers are also surfactants which aid in the formation of froth, aid in forming small bubbles, and therefore reducing the speed at which the bubble rises to the surface. Whereas both frothers and collectors have a polar and non-polar region as part of their molecular structure, a

good frother possesses a polar structure that has an affinity to water only and a non-polar structure that has an affinity to air only. The polar structure of a collector should have an affinity for the mineral [5]. The heteropolar nature of the molecule causes them to accumulate at the air-water interface, where the hydrophilic group is pointed toward the water in its attraction through hydrogen bonding, and the hydrophobic toward the air. In this way, the frother molecules can greatly influence the bubble dynamics. Interestingly, rather than reducing the bubble's size, frother molecules will alternatively slow down the coalescence of smaller bubbles into larger ones and stabilize them at that small siz. [12, 28, 29]. Frother used at Climax operations is pine oil in minimal doses [5].

1.2.7 Regulators/Modifiers

Regulators will modify the action of a collector in order to increase the selectivity of a desired mineral [12]. In actuality there may be two or more sulfide minerals in a certain slurry where only one is wanted. There is then a need to depress other sulfide minerals or enhance the hydrophobicity of one over the other. Regulators can be:

- Activators: which alter the mineral surface to engage with a collector.
- Depressants: which cause certain minerals to become hydrophilic and prevent flotation.
- Dispersants: which prevent or remove aggregation of particles as well as disperse reagents.
- pH modifiers: alters the acidity or alkalinity of the slurry.

Climax's operations typical reagents of these types include Arctic Syntex L as an emulsifier at 0.04-0.05 lbs/ton, Nokes reagent as a depressant at 0.027 lbs/ton, and lime as a pH adjustor at 0.3-0.4 lbs/ton [5].

1.2.8 Surface Charge and Zeta Potential

Surface charge and zeta potential have a large role in the stability of a colloidal system and can affect bubble-particle attachment angle [30]. Particles with zeta potentials greater than positive 30 mV or less than -30 mV are generally unstable as the particles will tend to repel each other with no inclination to come together. Main factors that influence the zeta potential of molybdenite would be pH and particle size [31]. Surface charges are different for the two types of molybdenite surfaces: the basal surface and the edge surface. The point of zero charge for the basal surface occurs at a pH lower than the edge surface (with edge surface zero charge occurring at 3 pH), with both surfaces becoming more negative as pH increases. At alkaline conditions, the edge surface possesses a much more negative surface potential than the basal surface, possibly due to molybdate ions at the edge surface [32]. Wang et al. [33] describes the edge surfaces having a higher electrochemical reactivity than the basal surfaces and research suggests that the edge surfaces are more likely to oxidize [34].

Zeta potentials for molybdenite are negative above 2 pH and become more negative as solution becomes more alkaline. Edge surfaces possess a much more negative zeta potential at elevated pH (-40mV to -75mV), and overall zeta potential of the mineral will get more negative the smaller the average particle size becomes. This is due to a greater ratio of edge to basal surfaces as particle size decreases. The high electrochemical reactivity of the edge surface may contribute to its sensitivity to pH changes on surface potential [31].

1.2.9 pH

Froth flotation in modern plants is almost all conducted in alkaline conditions. There are different optimum pH ranges for any given ore to maximize recoverability. pH controls the surface charge which will control the reactions involving chemical reagents. Selectivity of a

specific mineral in froth flotation depends on a balance between pH and reagent concentrations. As pH increases, the mechanism of the collector is slowed and the sulfide is depressed. Each mineral has a different pH at which depression occurs, allowing for a certain pH window at which a specific desired mineral can be selected for flotation. If pH is too low, selectivity is reduced and unwanted minerals will float.

1.3 Flotation Recovery, Thermodynamics, and Kinetics

The first instances of mineral flotation described a process where the desired hydrophobic mineral was poured out on the surface of water, sometimes aided by oil, and the mineral layer that remained floating on the surface was removed. This process eventually replaced by introducing agitation and air into the system, allowing ore particles to attach to bubble surfaces as they float through the pulp. As the desired ore particles transition to the froth phase from the pulp phase, the froth can then be separated and collected as a concentrate. The advancement into froth flotation dramatically reduced the amount of oil needed as well as greatly improved recoveries and grade.

Concentration ratio and recovery are important indices when calculating the efficiency of the float operation [9]. The heads, H, represents the slurry feeding into the system. The weight percent of the heads, $\mathbf{H_w}$, with the grade, **h**, as well as $\mathbf{T_w}$, $\mathbf{C_w}$, **t**, & **c** as the weight percentages of the tails, concentrate, and their grades respectively, one can create a balance for the system as a closed circuit in the following two equations:

$$H_w = T_w + C_w$$

$$H_w \cdot h = (T_w \cdot t) + (C_w \cdot c)$$

The first equation represents a balance of the overall ore components, and the second creates a balance for a specific component within the ore. These equations make the basis for further analysis such as the concentration ratio (R_c) and recovery of the system:

$$R_c = (c - t) / (h - t)$$

$$\text{Recovery percentage} = 100 \cdot c(h - t) / h(c - t)$$

These equations allow a calculation of the efficiency of the system using only their grades, their chemical assays of a specific component of the ore In addition, one can make the deduction that concentration ratio and recovery are inversely related with:

$$\text{Recovery} = (C_w \cdot c) / (H_w \cdot h) = c / (R_c \cdot h)$$

The principles of flotation thermodynamics and kinetics can be considered first by way of chemical thermodynamics and kinetics. In the latter, the reaction in question can be predicted using thermodynamics to proceed or not under certain parameters, ie. pressure and temperature. However, while this can be used to fundamentally find the feasibility of a reaction, chemical kinetics is required to uncover the rate of reaction as it relates to changes in temperature or other parameters.

For a given reaction, $aA + bB \leftrightarrow cC + dD$, with A,B,C and D the reactants and products, and with a, b, c, and d their respective molar quantities, one can find their standard change in free energy as:

$$\Delta G^o = -R_o \cdot T_K \cdot \ln [(C^c \cdot D^d) / (A^a \cdot B^b)]$$

With R_o as the gas constant and T_K as absolute temperature, this equation can be used to find the rate of forward reaction as:

$$\text{Forward Reaction Rate} = k_f (A^a \cdot B^b)$$

$$\text{Reverse Reaction Rate} = k_r (C^c \cdot D^d)$$

The concentration of the reactants and the products, with their rate constants, k_f and k_r, can describe the rate of reaction. This reaction rate is dependent on the temperature condition by way of the Arrhenius equation in the rate constant:

$$k_{(f,\,r)} = A \cdot \exp\left(-G/\left(R_o \cdot T_K\right)\right)$$

where A is described as the frequency factor for the reaction and G is the free energy of activation for the reaction. The system must be provided with this energy of activation in order to achieve a new arrangement of the system.

As chemical thermodynamics and kinetics shed light on the principles behind froth flotation, there exists additional mechanics that must be explained in order to describe particle/ bubble interactions and their probabilities of collision, namely the interactions of surface energies between the solid, liquid, and gas states in the system. The tensile forces holding the bubble to a particle involve the surface tensions between the solid-gas, solid-liquid, and liquid-gas interfaces (γ_{sg}, γ_{sl}, γ_{lg}) and will develop a contact angle Θ at the particle surface [35]:

$$\gamma_{sg} = \gamma_{sl} + \gamma_{lg}\cos\Theta$$

The work of adhesion (W_{sg}) is referred to as the force necessary to break the particle-bubble interface, represented by the work needed to separate the solid-gas interface and create separate liquid-gas and solid-liquid interfaces:

$$W_{sg} = \gamma_{lg} + \gamma_{sl} - \gamma_{sg}$$

When combined with the equation for contact angle:

$$W_{sg} = \gamma_{lg}\left(1 - \cos\Theta\right)$$

One can see that the larger the contact angle, the larger the work of adhesion becomes and will therefore result in a tighter bond between the particle and bubble with a greater energy needed to break them apart [9].

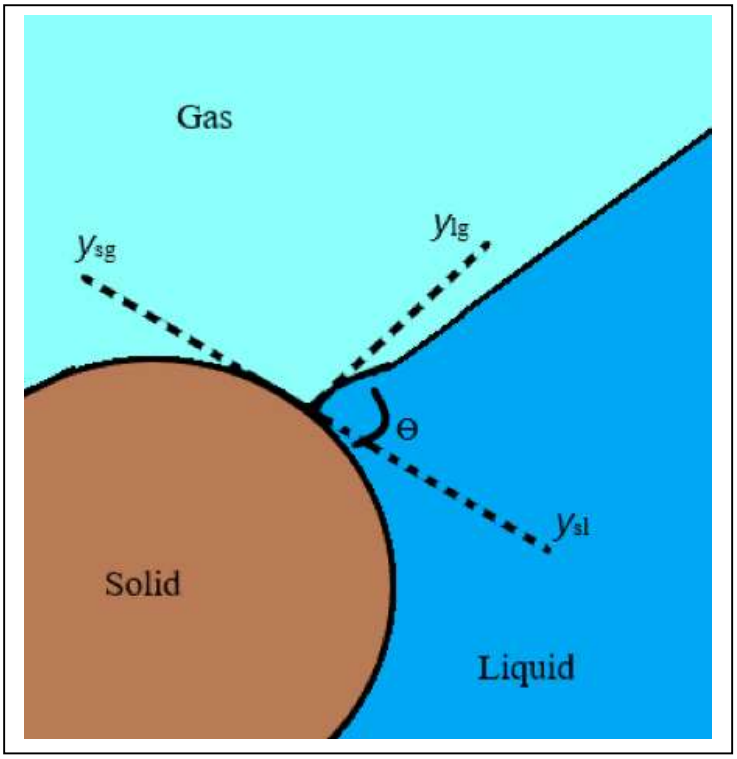

Figure 3: Contact angle which forms from particle in contact with a bubble.

Classically, the possibility of particle/bubble collision is on the basis that the free energy change, ΔG, of the system becomes negative as the particle attaches to the bubble. This can be described as:

$$\Delta G = E_2 - E_1 = \gamma_{sg} - \gamma_{sl} - \gamma_{lg}$$

where E_1 and E_2 represent the Gibbs free energy before and after attachment and γ_{sg}, γ_{sl}, γ_{lg} are each of the solid, liquid, and gas interfacial tensions. By introducing Young's equation with the contact angle, Θ, a deduction is made that the greater the contact angle, the greater the particle/bubble adhesion:

$$\Delta G = \gamma_{lg} \cdot (\cos \Theta - 1)$$

The rate of the flotation process has not been standardized and is not directly correlated with the contact angle. The rate may be dependent on the concentrations of particles/ bubbles and flotation time using first order kinetics [36]:

$$\ln (x_t / x_o) = -kt$$

$$x_t = x_o \cdot \exp(-kt)$$

where air supply is constant and x_o and x_t are the concentration of particles at time 0 and time t. There are some other factors to consider in the kinetics of particle/bubble adhesion and kinetics, such as a disjoining microfilm which segregates the interfaces between liquid and gas, and solid and liquid. The controlling mechanism of adhesion of the particle to the bubble surface depends on the thinning of the microfilm as it becomes unstable and ruptures. This requires the particle and bubble to have sufficient time in which they come into contact, allow for film rupture and subsequent attachment time. Whereas contact time can be manipulated by the hydrodynamics of the system, the attachment time can be altered by the chemistry involved on the surfaces between the particle and bubble along with the presence of reagents. Floatability becomes favorable when the attachment time is less than or equal to the contact time.

1.3.1 Flotation Cells, Circuits

Most flotation cells are mechanically agitated using an impellor which prevents the slurry from settling as well as disperses air into smaller bubbles. The air in the system can either be introduced by the slurry aerating itself as it travels through the cell, it can be caused by the impellor's depression, or it can be injected into the cell by a blower. There are different brands of flotation machines which can have their own advantages or disadvantages. Flotation columns have also been developed mainly in their advantage as cleaner cells. The column allows for a

greater froth depth as well as a good implementation of a wash water system. Wash water is added to the froth zone at the top of the column and entrainment recovery is greatly reduced.

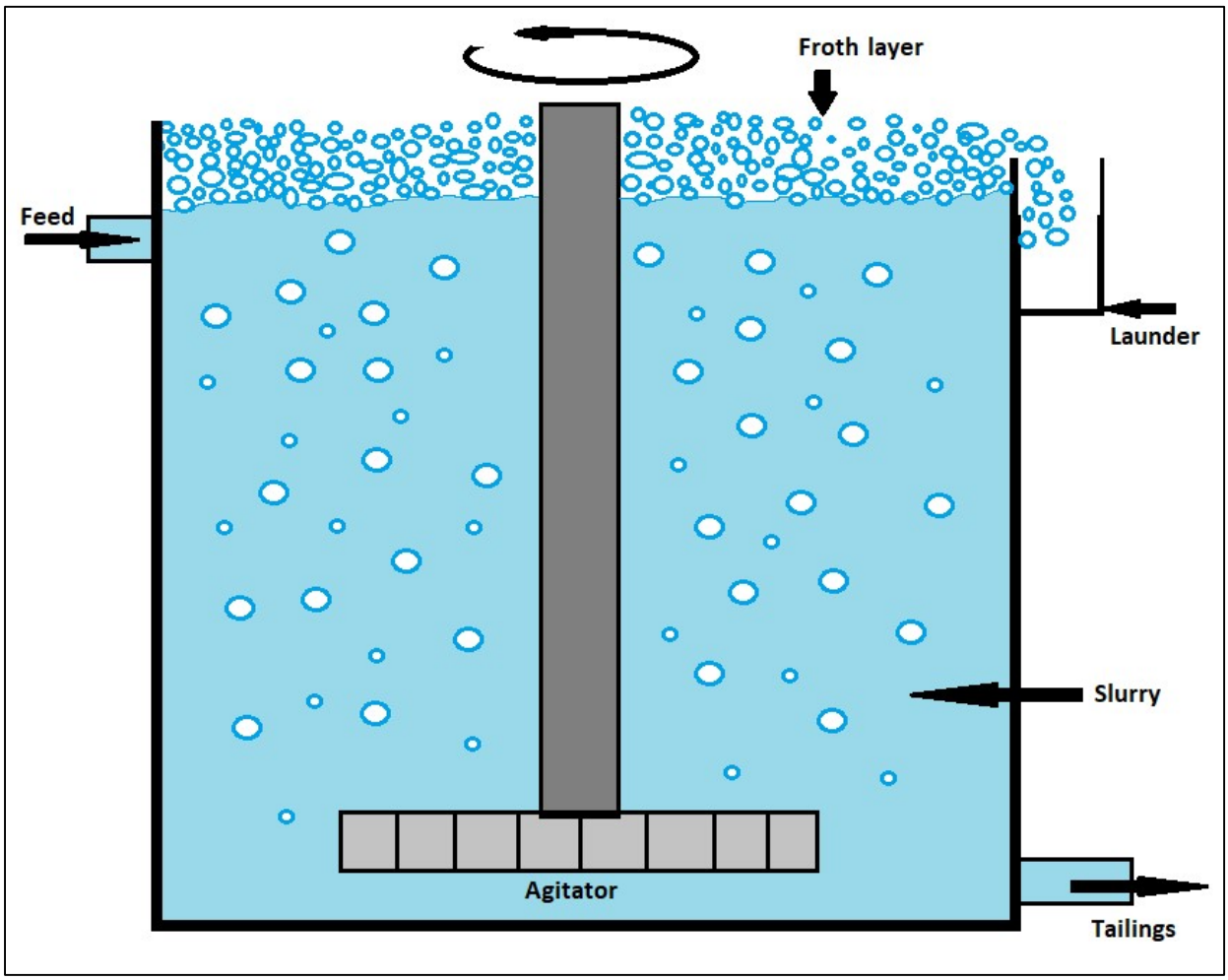

Figure 4: A Denver-type flotation machine float cell. An agitator's impellor will keep particles in suspension as air is diffused to generate bubbles. Froth gathers at the surface and spills into a launder as concentrate.

A typical flotation plant has a great number of flotation cells in their operation in order to optimize their capabilities as grade increases and particle size decreases. The cells can be arranged as a rougher/scavenger and cleaner type circuit [5, 8, 9]. A rougher will quickly concentrate easily floatable material and pass it to the cleaner cells. The scavenger cells will attempt to capture any remaining material that is slower to float and pass it along the circuit. Any

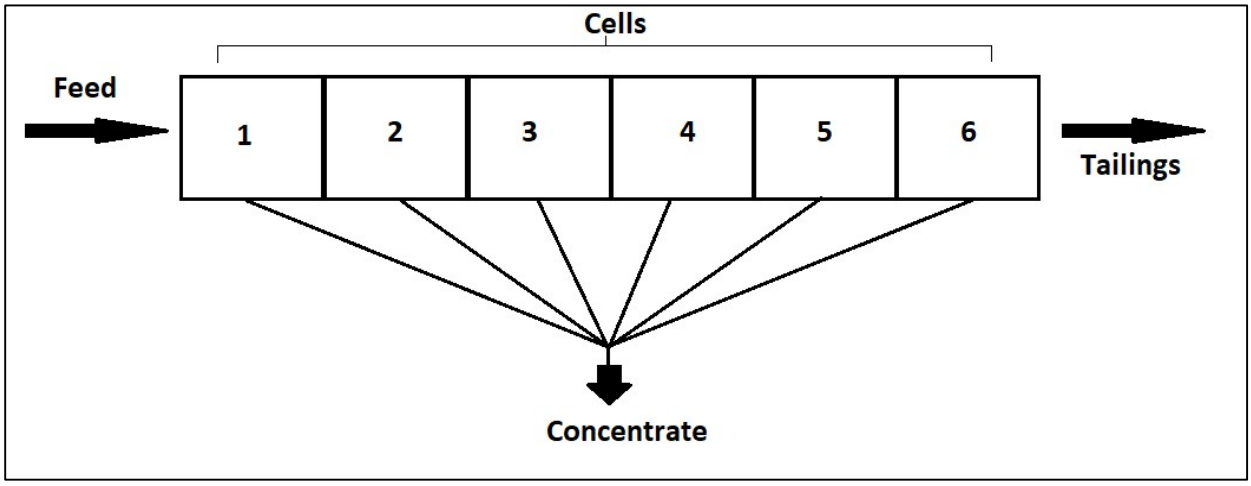

Figure 5: A typical stage in a flotation circuit. A series of cells through which the feed flows, each cell forming a concentrate gathered in launders, with remaining slurry finally flowing out as tailings.

material that is not passed along is lost in the tail line. The scavenger cell's objective is to maximize recovery of desired material before it can be lost. The rougher stages can contain many more cells than the cleaner circuit as less solids make its way through the plant. The most

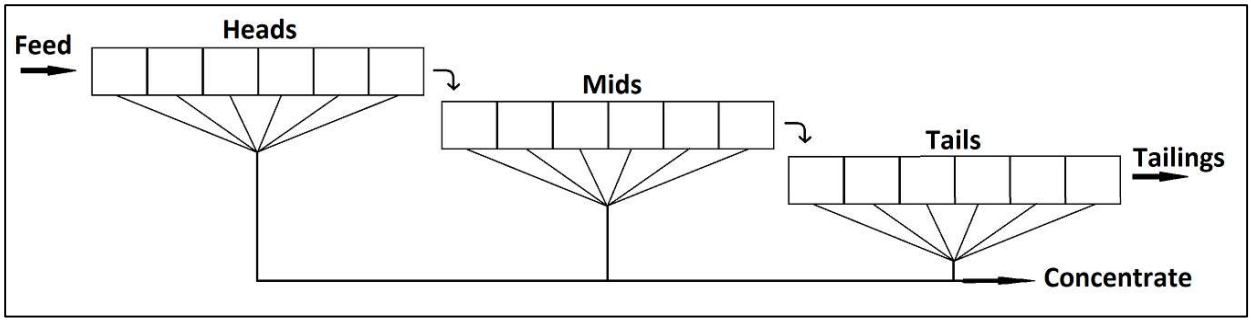

Figure 6: A typical rougher circuit. A series of stages (heads, middlings, and tails/scavenger) which combine concentrate to continue processing.

amount of gangue is attempted to be removed in the rougher stages as not only the fact that the grade of rougher material affects final product grade, but also excessive gangue in the cleaner circuit can cause unnecessary energy consumption in regrinding the material.

A cleaner circuit, which can be preceded or followed by regrinding of the material, attempts to refine and improve the grade to the desired value by floating the material additional times. The tails of the cleaner cells can then be looped back to previous parts of the circuit rather than be lost. In this way, any remaining gangue can pass through the circuit many times and its potential to be removed is increased. Material that travels through the circuit in this way is referred to as a circulating load, and the control of this load can have a large impact on the final quality of the product as well as the speed at which it is produced.

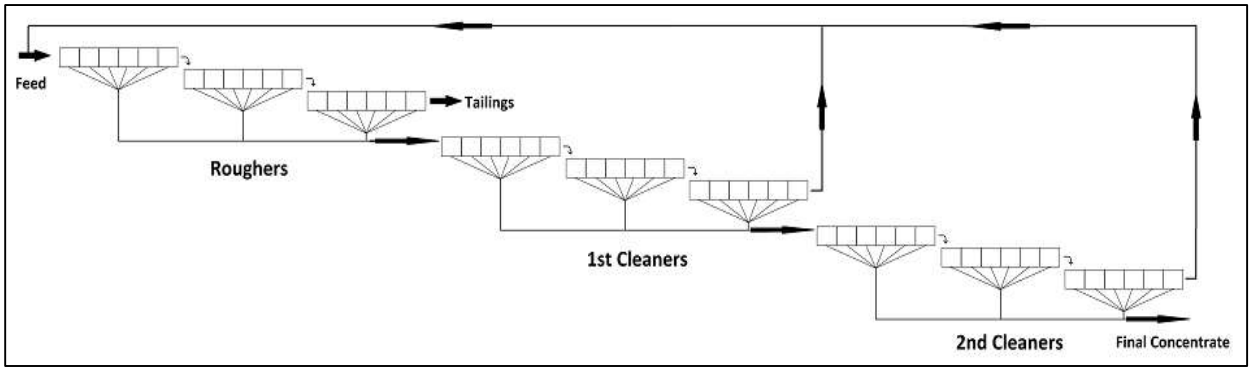

Figure 7: A typical cleaner circuit. The tailings from the cleaners can recirculate as the feed to a stage further back in the circuit.

1.3.2 Gangue in Final Concentrate and Entrainment

After enough flotation cycles, the final concentrate can be upwards of 99% molybdenum sulfide and can be classified in different grades. While Molybdenum sulfide is an efficacious lubricant, there remains a certain percentage of gangue that remains in the finished product. Even though this percentage can be small, <0.4%, the remaining material, comprised mainly of quartz, can have a detrimental effect of the efficacy of the lubricant as quartz is extremely hard and

abrasive. A main goal of a producer is to remove this material in the floatation stages as much as possible. Grade B molybdenum sulfide is of lessor purity (97- 98%) than Grade 1 molybdenum sulfide (99.0- 99.9%). Grade 1 molybdenum sulfide can be sold at a premium in relation to Grade B and so the reduction of gangue in the final product can be greatly beneficial financially.

Even through many stages of flotation, there remains gangue material in the end product. Research predicts that this remaining gangue material can arrive in the finished product through several routes [37, 38]. One route is by quartz remaining on an unliberated mineral whose hydrophobicity allows the attached quartz to travel with the mineral into the concentrate. Another way is from molybdenum sulfide particles agglomerating around small quartz particles and traveling through the cell. A third possibility is quartz particles becoming entrained in the torrential nature of the water and the bubbles as they quickly rise to the top of the cell and spill over into the concentrate. If the intended product is Grade 1 molybdenum sulfide and the gangue material reaches over specifications, the product must then be reclassified as lower purity Grade B and financial losses could incur.

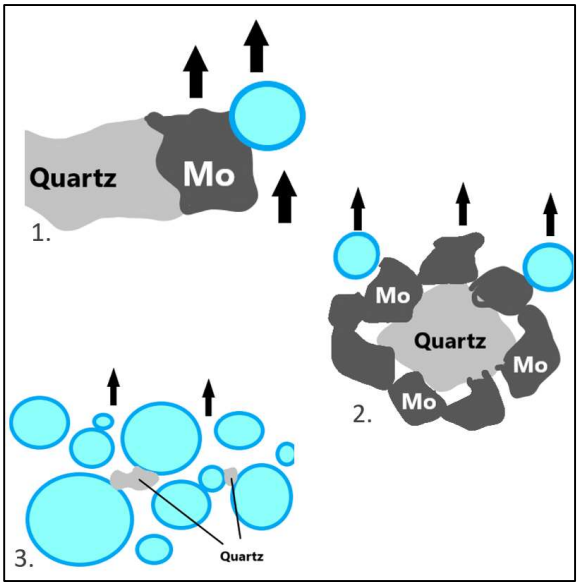

Figure 8: Three routes by which quartz or gangue can travel to the molybdenite concentrate. 1) on an unliberated mineral, 2) in an agglomeration, or 3) entrained in the froth.

The mechanism by which particles are recovered through froth entrainment is based upon three different theories: the Boundary Layer Theory, the Bubble Wake Theory, and the Bubble Swarm Theory. The Boundary Layer Theory proposed that entrained particles become trapped in a thin layer of water surrounding bubbles as they rise into the froth. The Bubble Wake Theory describes particles becoming transported to the froth by way of the wake in a rising bubble. The Bubble Swarm Theory proposes that water draining from the froth phase will encounter rising bubble layer swarms which will consistently push the entrained particles suspended in the water back into the froth [38, 39].

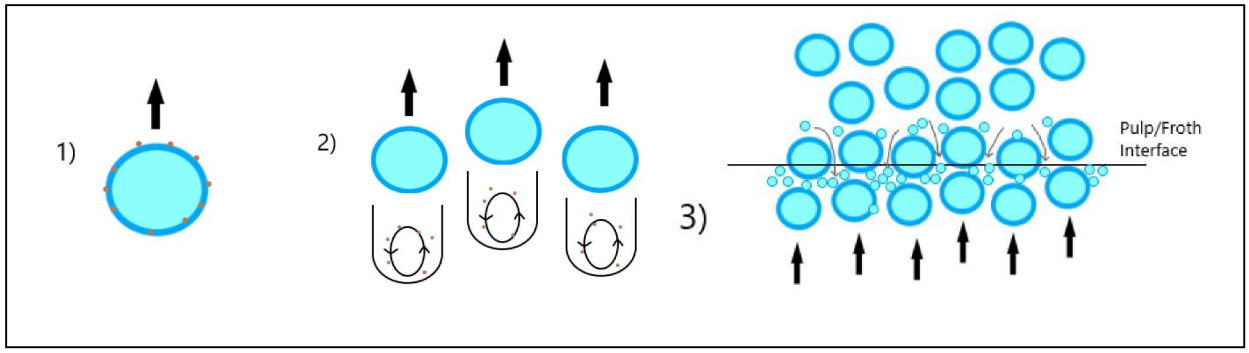

Figure 9: Three theories of particle entrainment mechanisms in froth. 1) The Boundary Layer Theory 2) The Bubble Wake Theory 3) The Bubble Swarm Theory.

1.3.3 Water Recovery

The amount of entrainment in concentrate has been shown to be linked with water recovery in the flotation cell. The more water that is recovered in the concentrate, the more undesired particles that are entrained in that water are recovered. Efforts to reduce water recovery in the concentrate have been taken to reduce undesired fines in entrainment recovery. These efforts include increasing pulp dilution, additional cleaner stages, increasing froth depth, and addition of wash water [9].

As water recovery has been linked to the recovery of entrained gangue material in flotation concentrate, models have been proposed for the mechanism of water transport from the slurry to

the concentrate. Water is thought to enter the froth by way of a film surrounding the rising bubbles, modeled as a function of bubble surface area and film thickness. [40, 41] The transport of water into the concentrate is greatly influenced by bubble size and in that regard the frother reagent.

1.3.4 Small Scale Flotation Experiments

Improvement in a plant's froth flotation process or research into improving flotation kinetics can be elucidated with small scale experimentation using flotation machines in a laboratory setting [42, 43]. A small-scale flotation machine mimics a plant scale machine by including an impellor and air injection, both of which can be manipulated of their rotation rate and air rate. Approximately 1 to 2 liters of slurry is deposited into a float cell which the impellor is then placed into. Reagents can then be added as needed and the impellor activated for approximately 2 minutes to allow for reagent dispersal. The test itself can be 7 to 30 minutes depending on the study. Froth will form as the air injection is activated and is recovered in a collection bin as the concentrate. Kinetics testing can be performed by making separate collections of concentrate at different time markers, i.e. 1, 2, 4, and 8 minutes. After the test, the remaining slurry in the float cell (treated as the tails), the collection bin froth (the concentrate), and a sample of the original feed (heads) can all be assayed and analyzed to generate a model of recovery for that system. Changing variables can easily be performed for these experiments, and many can be performed in a short amount of time.

This research has aimed to reduce the remaining gangue material that is being captured in flotation cell concentrate through agglomeration and entrainment by using ultrasonication in small-scale flotation experiments.

1.4 Ultrasonication

Ultrasonication, or sonochemistry, is the application of high frequency sound waves in a liquid medium with the aim of generating mechanical or chemical effects that result from bubbles cavitating under the sound waves' influence. As ultrasound propagates through the liquid, a series of compression and rarefaction waves cause an expansion of microbubbles in the medium up to a point where they become unstable and implode. The resulting implosion causes a dramatic increase in local temperature and pressure, with temperatures exceeding 5,000 Kelvin and pressures reaching 1,000 bar. A jet stream will also occur at the site of implosion with speeds at over 100 meters/sec. [44,45,46] This phenomenon can produce various effects and are taken advantage of in the production or extraction of a wide variety of materials. Sonochemistry is becoming an emerging field of research in chemical synthesis, bioengineering, and nanomaterials. This research has drawn interest due to the efficient way sound waves can create these local conditions through bubble cavitation.

1.4.1 Bubble Growth and Cavitation

In any given liquid in regular atmospheric conditions, there exists nanobubbles or microbubbles that usually form on impurities in the solution. As sound waves perpetuate through the liquid medium at a certain frequency, there are fluctuations in pressure that cause these nanobubbles to expand in size and eventually cavitate. At lower ultrasonic frequencies, 20-80 kHz, the cavitation of these bubbles will cause mainly physical phenomenon like shockwaves and microjets. At higher frequencies, 150-2,000 kHz, there begins to produce chemical effects due to the emergence of radicals from the intense conditions that the cavitation causes. Frequencies above 2,000 kHz do not produce these cavitation effects [46].

The ultrasonic sound waves will cause an expansion/compression cycle in the liquid medium. During expansion, there is a negative pressure exerted on the medium which draws out the molecules from each other and can create cavities. When the intensity of the wave is high enough, the negative pressure will become greater than the liquid's tensile strength and will form small gas bubbles. These gas bubbles grow and compress as they are subjected to the continual ultrasonic waves and at high enough energies will expand faster than they can compress, causing the bubble to grow in size over the course of the acoustic cycles. There reaches a critical size when the bubble no longer is able to absorb the energy from the sound wave efficiently enough to continue its growth and will subsequently collapse or implode.

Noltingk and Neppiras' work [47] on cavitation theorize a critical bubble radius (R_0) above which cavitation does not occur, given by:

$$\rho\omega^2 R_0^2 = 3\gamma(P_A + 2S/R_0) - 2S/R_0$$

where ρ is liquid density, ω is the frequency, γ is the specific heat ratio of the bubble's gas content, P_A is the hydrostatic pressure, and S is the liquid's surface tension. As the radius increases beyond this mechanical resonance, the change in radius (ΔR) is minimal and oscillations form a sinusoidal pattern. There also exists a lower critical bubble radius below which cavitation does not occur and the bubble is stable. This is due to the dynamics between the bubble's gas pressure, surface tension forces, and pressure conditions right outside the bubble. This model is represented by this equation of the pressure right outside the bubble (p):

$$p = (P_A + 2S/R_0)(R_0/R)^3 - 2S/R$$

where a minimum p with respect to a minimum R_0 (as a radius threshold R_T) can be verified by:

$$R_T = [3R_0^3(P_A + 2S/R_0)/2S]^{1/2}$$

and if the minimum value for p is greater than the minimum value for the pressure that exists in the liquid beyond the bubble's locality: $P_A + P_0 \sin\omega t$ or $P_0 - P_A$, (where P_0 is the alternating pressure amplitude) the conditions which exist are not balanced with the liquid pressure right outside the bubble and rapid expansion occurs. The bubble's radius is not stable when the difference in hydrostatic pressure and the alternating pressure amplitude is greater than the minimum liquid pressure right outside the bubble:

$$(P_0 - P_A) > (P_A + 2S/R_0)(R_0/R_T)^3 - 2S/R_T > 0$$

By substitution of R_T, we will get:

$$(P_0 - P_A) > 4S/3R_T \quad \text{or} \quad (P_0 - P_A) > (8/9)[3S^3/2R_0^3(P_A + 2S/R_0)]^{1/2}$$

In this equality, if P_A is constant, there exists a minimum R_0 for each value of P_0 which the bubble's radius is unstable and radii lower than that value are stable. This model details a range of bubble radii which cavitation occurs. As frequency increases, this range is reduced by lowering the upper threshold radii. If frequency continues to increase past the point where the lowering upper threshold meets the lower threshold, cavitation does not occur and an upper threshold for frequency is obtained.

Other studies have produced models which can predict the values at which the bubble transitions from oscillation to growth, and from growth to collapse [48-52]. The transition from bubble radius oscillation to growth is determined by a minimum pressure, called the rectified diffusion threshold (P_{DT}), is represented by

$$(P_{DT}/P_i)^2 = 3/2\ [1 - (c / (1+2\sigma/RP_i)][(1 - f^2/f_D^2)^2 + f^2b^2/f_D^2]$$

Where P_i is the initial pressure, c is the gas saturation in water, R is the bubble radius, σ refers to the ratio of the speed of sound in the particle to the speed of sound in the liquid, f is the frequency, f_D is the resonance frequency, and b is the damping factor. As pressure increases, the

transition from growth to collapse as the pressure passes a point called the Blake threshold (P_B) [87]:

$$P_B = P_0 + 8\sigma/9\ [3\sigma / 2(P_0 + 2\sigma/R)R^3]^{1/2}$$

When the bubble implodes, the surrounding liquid rapidly fills the cavity, causing extreme local conditions at the site of collapse. The temperatures in this region can reach up to 5,000 K and pressures up to 1,000 bar. Shockwaves form around the area as well as microjets of liquid that can reach velocities of up to 100 m/sec. These extreme conditions are the source of the desired effects of ultrasonic processing: either the mechanical effects (shockwaves and microjets) or the chemical effects (formation of chemical radicals) that result. In their previous work, Neppiras et al. [53] found the maximum pressures and jet stream velocities that are created will increase as the radius of the cavitation bubbles decrease. Since there is a lower limit to the bubble radius where cavitation can occur this creates a limit to the magnitude of the cavitation pressures.

1.4.2 Frequency and Amplitude

Frequency refers to the rate at which a sound wave cycles per second. The differences in effects between higher or lower frequencies (chemical effects and physical effects, respectively) is theorized to be due to low frequencies (20-80 kHz) producing larger but fewer cavitation bubbles while higher frequencies (150-2,000 kHz) producing many smaller cavitation bubbles. The numerous small bubble cavitations will generate a large number of radicals that depend on the liquid medium. In the case of water as the medium, sonolysis will occur as a result of the high local temperatures and pressures, producing H^+ and OH^+ species. These radical species will quickly react with other substances or materials in the system and some researchers and

operations take advantage of this effect by using sonication for molecular synthesis and/or chemical degradation.

Lower frequencies which cause fewer yet larger bubbles will emphasize a physical or mechanical effect on the substances in the system. The shockwaves and jet streams can cause a great physical force on surfaces of materials in the system. Many laboratories use these lower frequencies in ultrasonic baths for cleaning of glassware or other materials. The cleaning effect comes from the jet streams focusing a large force on the surface of materials. This effect can also be used as to deagglomerate particles and has been shown to break and erode tough surfaces. Amplitudes, referring to the maximum displacement of vibrations in the medium, must be at a high enough intensity for cavitation effects to occur. At lower amplitudes, the expansion and compression phases in bubble growth will more or less be equal and will not occur in a large cavitation as the bubble is not allowed to have significant growth. As amplitude reaches higher intensities, the rapid expansion will result in a substantial subsequent collapse at high speeds, causing the cavitation effects.

1.4.3 Conversion of Electrical to Acoustical Power via a Transducer

The creation of the ultrasonic waves from electrical power is typical done through the application of a transducer. A transducer takes advantage of the piezoelectric effect in certain materials (quartz or doped ceramics) by machining them into discs or plates and fixing them with electrodes. The material will then expand or compress as a voltage is applied to the electrodes which causes the vibrations that produce sound waves. The transducer will create a maximum displacement from its resonance frequency. The resonance frequency of a transducer will depend on its geometry. An electrical voltage equal to the transducer's resonance frequency is applied by

way of an electric generator. The efficiency of converting the electrical power into acoustical power has yet to be above 40% and is a challenge for further research in this field.

1.4.4 Ultrasonic Baths and Probes

Ultrasonic baths are very common in laboratories and are used for cleaning glassware, deagglomerate materials, dissolve compounds, etc. The ultrasound transducer is typically at the bottom or the sides of the tank and sound waves are indirectly propagated through the metal walls of the tank through a liquid medium the target material is immersed in. These baths are usually of a low acoustical intensity in order to prevent damage to the tank over time. The ultrasonic field inside the bath is also not homogenous and can limit experimental reproductions.

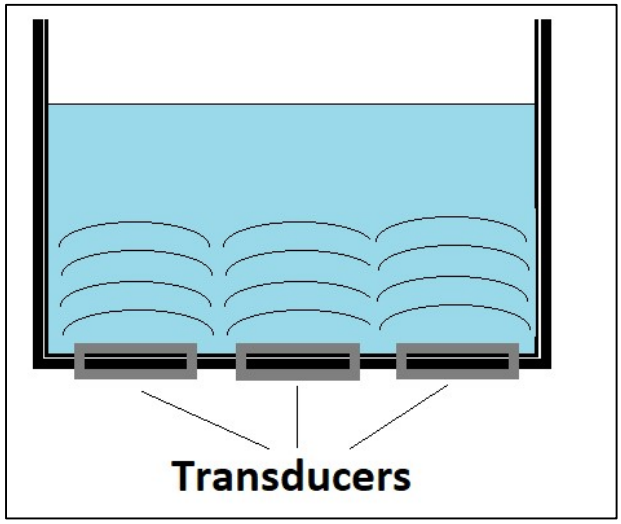

Figure 10: The typical construction of an ultrasonic bath. It will usually have transducers placed on the bottom or sides of the tank and sound waves propagate through a liquid medium.

Ultrasonic probes allow intense direct sound propagation, almost 100 times greater intensities than an ultrasonic bath. The probe consists of a transducer connected to an electrical generator with an amplification probe and a detachable ultrasonic probe. After the application of voltage to the transducer, it will create mechanical vibrations. The amplification probe will

increase the amplitude of the sound wave and the ultrasonic probe is in contact with the liquid and propagates the resulting waves into the medium.

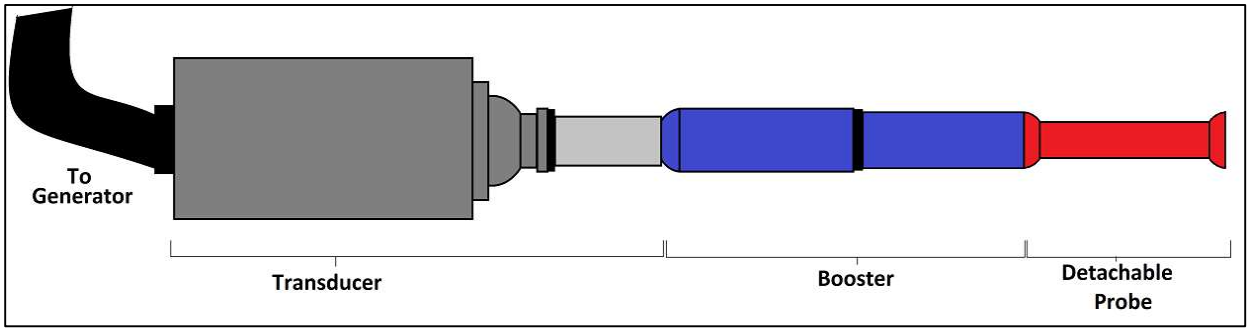

Figure 11: The arrangement of an ultrasonic probe. A generator provides electrical power, the transducer converts voltage to vibratory energy, the booster will increase amplitude, and the probe propagates the sound waves through a contacted medium.

1.5 Ultrasonication in Froth Flotation

Zhou at al. [54, 75] evaluated the benefits of using mechanically induced cavitation bubbles to improve flotation kinetics. His research touched upon experiments from Wrobel in 1952 [55] which elucidated how gas nuclei adsorbed onto hydrophobic minerals was the key to the quick attachment of the larger flotation bubbles. These results were further explicated in Klassen's experiments in the 1960's [55,56] which showed amplified flotation kinetics by supersaturating the slurry with air and generated mechanical cavitation bubbles. Ultrasonication proves to be an excellent way of efficiently creating cavitation bubbles in froth flotation without need for mechanical generation.

While there have been several decades of study on ultrasonication in froth flotation, there have been relatively few studies which concerned solely molybdenite ore and its reduction in quartz in the final concentrate. Researchers have used the effects of ultrasonication to aid in

mineral flotation in various ways. A study involving zinc flotation proved that recovery and grade was increased after the slurry was subjected to an ultrasonic pretreatment [57]. This improvement in recovery may have been due to the ultrasound fostering dispersion of the particles, the enhancement in the adsorption of collectors, and the cavitation bubbles forming on the zinc mineral's surface increasing the contact angle and chance of attachment. After an ultrasonic pretreatment, in multiple stages of column flotation the zinc grade was increased by 20% and the recovery increased by 5%. One recent study on the effects of ultrasonication on quartz was conducted by Hassanzadeh et al. They found that ultrasonication for 90 seconds diminished the contact angle at the surface of quartz and reduced its hydrophobicity, thereby reducing the recovery. Their study suggests that the topography of quartz, altered by the ultrasonic waves, is the main factor in reducing the recoverability of the mineral. However, not many studies delve into this topographical aspect and further research is needed to theorize the mechanical and chemical effects of ultrasonication at the surface of quartz [58].

Utilizing the effects of ultrasonication in regard to mineral flotation should first take into account the fundamentals of the effects of ultrasound on solutions. These effects are categorized as the result of cavitation, with both physical and chemical effects. Cavitation is a term that describes bubble dynamics in regard to growth, oscillation, and collapse. These resultant effects can assist with a variety of issues encountered in mineral flotation, including slime coating and oxidation film removal, desulfuration, tiny bubble generation, flotation reagent dispersion, and aggregation. [59, 60].

1.5.1 Slime Coating

A slime coating can exist which surrounds desired minerals during froth flotation. This coating typically consists of very fine clay or gangue particles and will demonstrate hydrophilic

behavior. This behavior inhibits the floatability of normally hydrophobic minerals and causes detriment to recovery. Ultrasonic treatments of the slurry have shown that the cavitation effects which produce high powered jet streams can strip away this outer slime layer and reveal the hydrophobic mineral underneath. Bandini et al. [61] used an ultrasonic bath to effectively remove iron oxide slime coatings from quartz particles. The 10-minute treatment at 150 W increased the fraction of removal from 20% to 95%. His research also found that the effects of sonication were improved by 5 times when used in conjunction with a reagent. Others have suggested that the effectiveness of a collector is improved due to the cleaning of the mineral surfaces [62]. SEM and XRD analysis involving the flotation of oil shale showed that an ultrasonic treatment cleaned the surfaces of the shale and removed impurities embedded in the crevices on the surface of the concentrate, reducing ash contents in the final concentrate by an average of 29% [63]. Studies performed on coal flotation showed that gangue entrained within the slime coatings on the coal surfaces was removed with ultrasonic treatment at 50 W using four plate transducers surrounding the float cell during the flotation experiments [64, 65, 66]. Using a sonication pretreatment as well as during the flotation experiment improved the recovery of copper in tailings by 3.5% with conclusions that the treatment minimized slime coatings and that ultrasound applied at any stage will improve final recovery and kinetics [67].

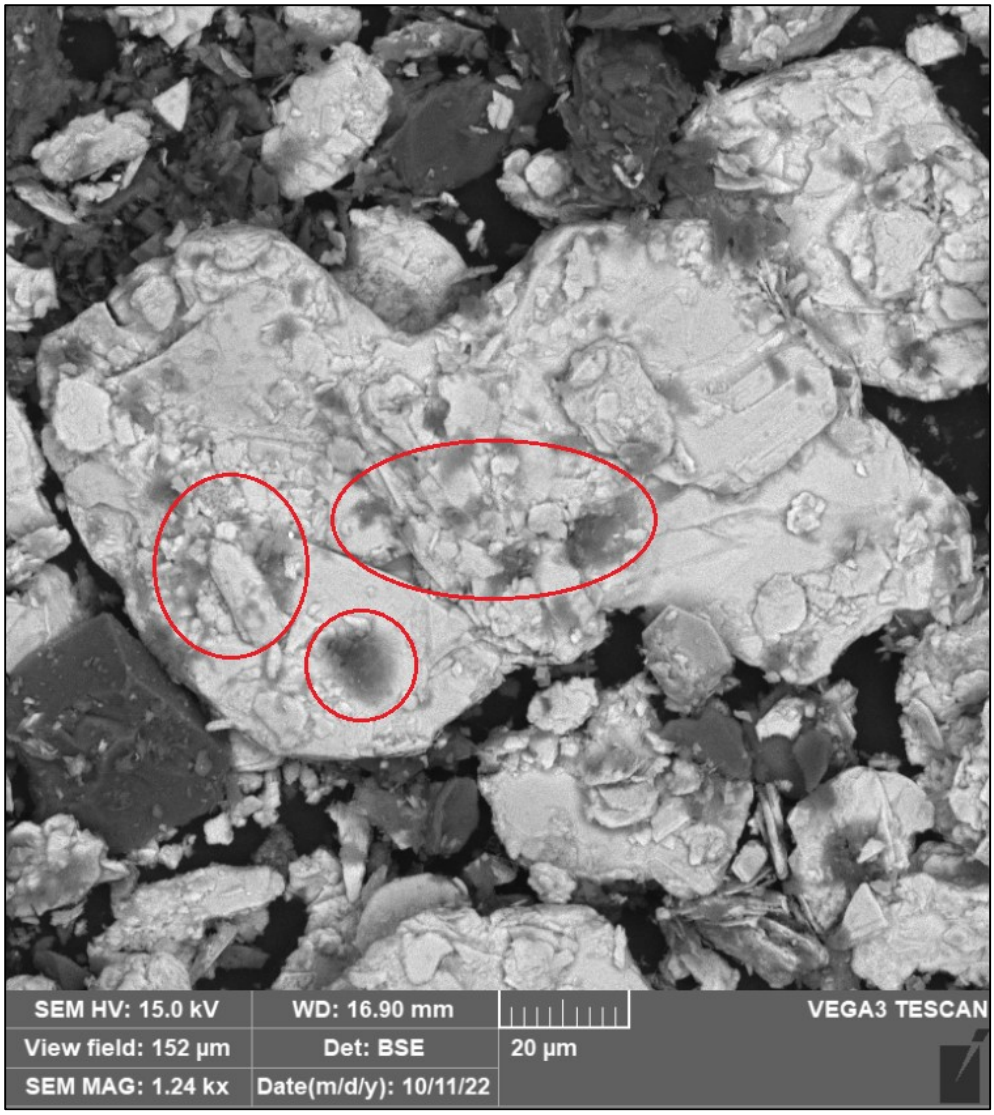

Figure 12: BSE SEM image showing slime coatings, dark regions circled red, covering molybdenite particles.

1.5.2 Oxidation Films

Many sulfide mineral flotation operations which rely on the hydrophobic nature of the sulfide can be hindered by an oxidation layer that can form over the sulfide surface before the mineral can be processed. The oxidation layer will cover the sulfide surface with hydrophilic oxides and will therefore lower the hydrophobicity of the mineral and reduce floatability. Similar to slime removal, ultrasonic treatments have proved to be effective in removing the oxidation

layer. In the floatation of arsenopyrite, the oxidation layer was thinned or removed by analysis of the zeta potential using a 40 second ultrasonic pretreatment. The arsenopyrite flotation recovery increased from 25% to 85%. Increasing the pretreatment time to 10 minutes caused recovery to almost 100% [68]. Cao et al. found several advantageous effects of sonication on the flotation of oxidized pyrite, with a focus on its ability to remove the oxidation layer and observe its surface cleaning abilities [69]. Sufficient surface cleaning and oxidation layer removal occurred within 40 seconds. Beyond that time, the radicals that were created from the cavitation bubbles re-oxidized the surface of the pyrite. They discovered that the beneficial effects of sonication are embedded in the power and not the length of time the material was subjected to the treatment. Recovery was improved from 61% to 81% in the flotation in the rougher and cleaner cells with ultrasonication. They concluded this was most likely due to the decrease in hydrophilicity from the removal of the oxides from the mineral surface.

Other studies confirmed the possibility that with too long of an ultrasonic treatment can cause the reoxidation of the mineral surface [70]. They revealed that there exists an optimum treatment time for maximum recovery at 10 minutes on their studies of coal flotation. Beyond that time, continual ultrasonication caused a shift in the beneficial effects of the physical phenomenon that cleaned the oxidation layer to the chemical phenomenon where hydroxide radicals begin to form and subsequently re-oxidize the mineral surface, thereby decreasing flotation recovery. Manipulation of a mineral's hydrophobicity using the chemical effects of ultrasonication was also explored in Feng and Aldrich's work on the flotation of talc [71]. They found that ultrasonication could hinder the hydrophobicity of talc by causing the adhesion of water molecules to surface defects caused by the sound waves, creating silicon hydroxl species on talc surfaces. This resulted in a lower recovery rate especially when used in conjunction with

depressants, the effects of which were enhanced with sonication. This shows promise in the reduction of flotation recovery of silicates, of which talc is categorized. Another work by this group showed that ultrasonic treatment improved the floatability of platinum group sulfide minerals as the silicates were depressed [72].

1.5.3 Small Bubble Effects

There may also be beneficial effects to flotation involving the formation of microbubbles due to ultrasonic cavitation on the surface of hydrophobic particles. A study by Filippov et al. used a model to show that these microbubbles formed on the hydrophobic mineral surface would promote the attachment of the mineral to the larger flotation bubbles produced by the sparger due to the coalescence of the two bubbles [73, 74]. In addition, the larger flotation bubbles' radii may become reduced under the external vibrational forces and would increase the chance of particle-bubble collision. More experimental work needs to be done to confirm these predictions. Studies by Zhou et al. [76] show that hydrodynamically induced cavitation bubbles, created through increasing the velocity of the slurry through a nozzle, will form on hydrophobic minerals and show a beneficial effect to flotation kinetics by way of aggregating the bubble/particle complexes and bridging with larger particles, increasing the collection rate.

1.5.4 Improvement of Reagent Efficiency

Several studies have concluded that ultrasonic treatment has a positive effect on the efficiency or consumption of flotation reagents. One investigation involving the flotation of galena showed that the consumption of a collector, potassium ethyl xanthate, could be reduced by 50% by applying a pretreatment in an ultrasonic bath [77]. Another study showed that the required collector was reduced in the flotation of coal and recovery increased up to 35% after an ultrasonic pretreatment [64]. Another study with a 5-minute ultrasound pretreatment improved

recovery of zinc by 7% and increased grade by 10%, with a conclusion that considered an improvement in collector dispersion due to the effects of ultrasound [57]. This is indicative that flotation operations utilizing reagents can have amplified beneficial effects with used in conjunction with an ultrasonic treatment. The cavitation bubbles, upon implosion, will cause oil reagent droplets to disperse into many smaller droplets, effectively improving the chances of adsorption on mineral surfaces [59].

Chapter Two: Research Problem

2.1 Introduction

The need for improving the grade and recovery during metals production grows more each year, as energy efficiency is becoming more important and as demand for raw materials increases. As infrastructure and construction projects demand a greater number of structural steels and requirements for catalysts in the petroleum industry grow higher, molybdenum poses to maintain its vital role in the world's appetite for raw materials. Novel and efficient methods of metal extraction along with their development are important to companies as they seek to incrementally improve their output.

2.2 Statement of the Problem

While the production molybdenum sulfide creates a high-grade product that is upwards of 99% pure, there still exists a small amount of gangue in the final product. This gangue, mostly quartz, is detrimental to final uses as molybdenum sulfide is slated for use as an industrial lubricant. Quartz is notoriously hard and abrasive, and any reduction in the final MoS_2 product will improve its performance. Furthermore, slightly lower grades of MoS_2 which previously could not be further refined would have an opportunity to do so and then subsequently be sold at a higher premium. The gangue in the final product has several routes. Firstly, unliberated gangue particles can rise with the attached molybdenite and be collected. Secondly, liberated gangue can become agglomerated with molybdenite surrounding the particle and become carried with the molybdenite into the froth concentrate. Lastly, the gangue can become entrained in the torrential nature of the froth as it quickly rises to the surface and is collected in the concentrate. Methods to improve end grade have aimed to target the entrained gangue by deagglomerating, creating rinse water channels in the froth, slowing float times, etc. This study intends to reduce the gangue

material traveling through the second route by deagglomerating the particles and releasing trapped gangue within them so they may be rejected in the system. Ultrasonication has been proven to improve recovery, grade, and floatability in studies of other minerals, and it should prove to be just as effective with molybdenite. However, very few studies have been performed regarding the effects of ultrasonication on molybdenite despite its naturally hydrophobic surfaces that would attract cavitation bubble formation without the need for reagents. Molybdenite has a relatively higher natural hydrophobicity compared to other sulfide minerals due to its face surface structure. Smaller molybdenite particles command a lower face to edge surface ratio and therefore become less hydrophobic.

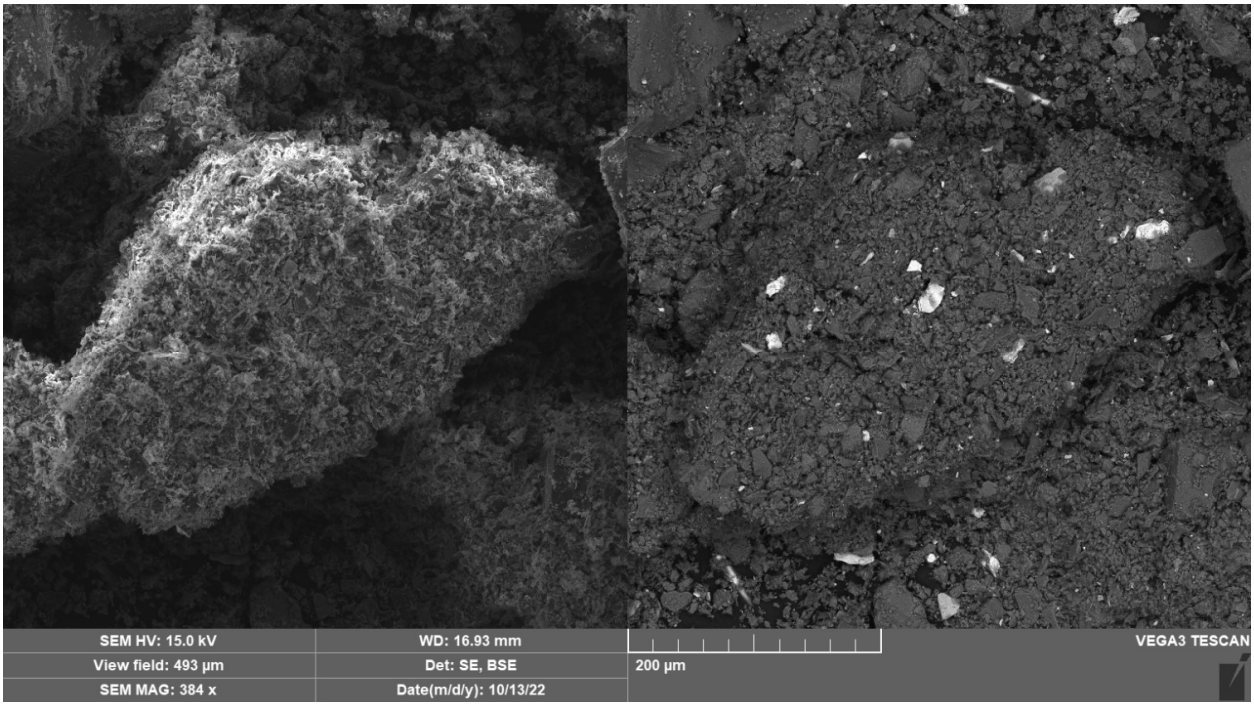

Figure 13: SE (left) and BSE (right) SEM images of an agglomerate of molybdenite and gangue material.

2.3 Significance of the Study

This research intends to be beneficial to the industry by attempting to improve grade and recovery. This would improve economic feasibility of certain ore grades and open doors to

facilities that are unable to improve their product grade based on their current process flow. Moreover, if the deagglomeration tendencies of the ultrasonic treatment prove feasible, this could potentially replace the need for certain regrind mills. Some mills do not serve to reduce particle size but rather to polish and deagglomerate the particle surfaces of slime to improve floatability after the mill. This same process could be achieved instead by ultrasonication. Replacing a mill would cut significant operating and maintenance costs. Ultrasonication during flotation would also show that reagents and the costs associated with them could be cut back due to the resulting effects of the treatment: increasing the diffusion of reagents as well as cleaning the mineral surface to make way for reagent binding sites. Not only could this research have implications that would improve molybdenum production, but every mineral produced by flotation could show improvement since the mechanisms are similar. For an operation which produces 20,000 lbs of product per day at 19 dollars a pound, an increase of 5% float recovery would equate to an increase in production value of upwards of 6 million dollars.

2.4 Research Objectives

This research intends to elucidate the effects of ultrasonication on the flotation of molybdenum sulfide ores with the aim of reducing gangue material in the end product. The research hopes to achieve this through the physical effects of ultrasonic cavitation. The goal and topic of this research is to achieve a higher grade and recovery of a molybdenum sulfide flotation cell using ultrasonication and will seek to answer the following:

- Will ultrasonication improve recovery and/or grade in a small-scale flotation experiment with molybdenite slurry?
- How does ultrasonication treatments affect the kinetics of molybdenite flotation?

- Can gangue material in molybdenite concentrate be reduced through using an ultrasonication treatment?
- Will ultrasonication treatment during flotation liberate and remove gangue material that is trapped in agglomerated particles?
- How does the length of treatment affect kinetics in molybdenite flotation?

Agglomerated molybdenite surrounding quartz particles have been observed under the SEM in preliminary analysis of the feed samples in this study (Figure 12). Samples will be prepared following the ultrasonic treatment and will be reevaluated to see if the quartz particles have been released and agglomerations have been reduced in comparison to controls. Trapped gangue material may be coerced out of the froth using the ultrasonicator and a comparison of the collected froth with the control froth may show if there is any improvement without affecting recovery. In addition, different intensities of sonic waves at different time intervals may show varying results. Where some intensities may be inadequate to deagglomerate, others may be more effective. Too long of a time in ultrasonication treatment could show a detriment to recovery after a certain point due to chemical radical formation. This research will perform small scale flotation experiments at differing degrees of sonic intensity and time intervals with the resulting collected froth assayed, gangue material quantified, and with SEM observations.

Chapter Three: Experimental Methods

3.1 Obtaining Molybdenite Slurry

Molybdenite slurry was obtained at the Henderson Mine site at their mill operations in Grand County, Colorado. Collections of the slurry were taken during operation of the circuit at various points prior to each test. Samples were taken of the second cleaner feed as well as the rougher concentrate. Slurry contained active reagents that are added throughout the Henderson mill circuit and were not manipulated before the small-scale float tests.

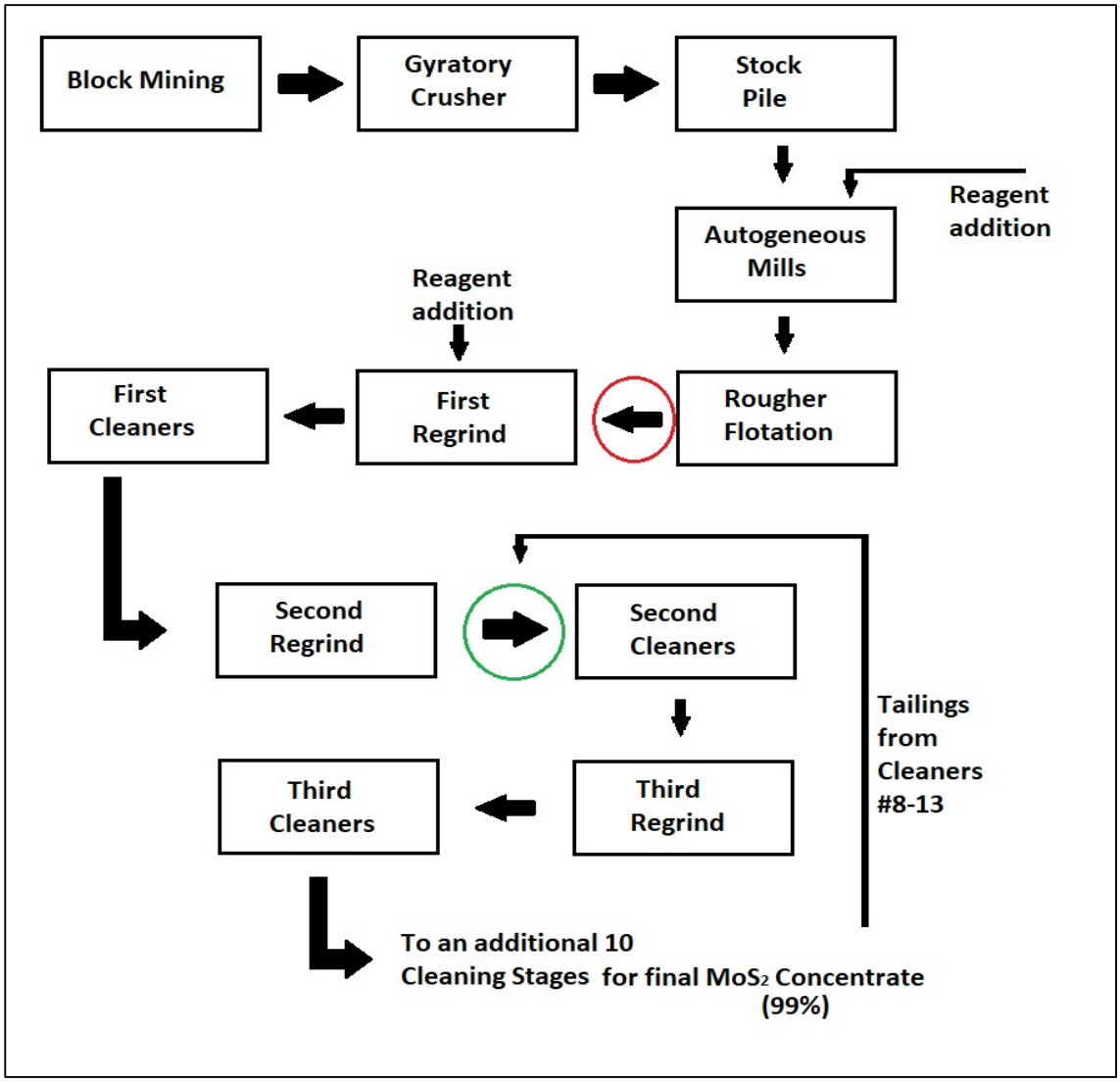

Figure 14: Process flow sheet of Henderson Mill showing the samples pulled for these experiments: the rougher concentrate (red circle) and the second cleaner feed (green circle).

3.2 Characterization of Molybdenite Slurry

Characterization of the molybdenite slurry feed, and subsequent concentrates and tailings of each experiment, was performed using inductively coupled plasma optical emission spectrometry (ICP-OES). Samples for assay were first dried using a pressure chamber and placed in a drying oven until all moisture was evaporated. The samples were then de-oiled with acetone and then prepped for a 3-acid digestion. Samples were first dissolved in nitric acid at elevated temperature until off gassing ceased. Sulfuric acid was then added at elevated temperatures to further dissolve the material. After the sulfuric acid mixture had mostly evaporated, hydrochloric acid was added and then diluted to perform the assay. Additionally, samples of this acid digestion were filtered and prepped for an insol (insoluble material) analysis. The solution was filtered with an ashless filter and that filter was placed in a crucible in an oven at 900 degrees Celsius for one hour. The residue material in the crucible was characterized as the insoluble material (i.e. quartz) that remained in the molybdenite slurry and is a measure of the gangue material. The insoluble material was weighed and compared to the original mass of the molybdenite sample for a percentage insol calculation.

3.3 Small-Scale Float Tests

Small-scale float experiments were performed using a Denver Cell D12 Lab Flotation machine at time lengths of 8 minutes long with a 2-minute pretreatment of the slurry using the agitator (without air addition) and the ultrasonication during some tests. The agitator was set at 1200 RPM with an air injection rate of 5 liters per minute (LPM). Pine oil reagent was added to the float cell by way of the makeup water (2 drops/liter). As froth is collected, makeup water is

added to the cell in order to maintain the slurry level at approximately 8 inches height with a 1-inch froth depth. The froth collection was aided by use of a hand paddle periodically running along the top of the slurry surface, typically drags that were 5 seconds long. Froth was collected in a container and labeled as concentrate. The remaining slurry left in the float cell was labeled as the tailings.

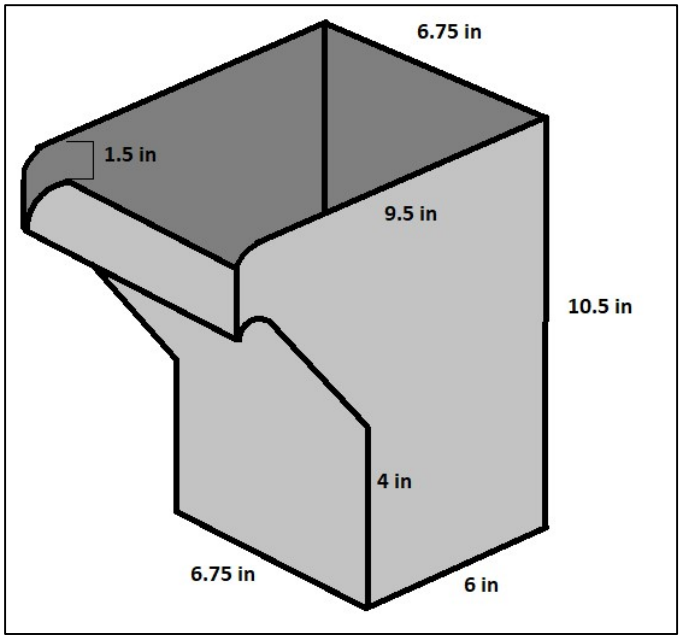

Figure 15: Dimensions of small-scale float cell used for these experiments.

Prior to the test, a representative slurry feed sample was obtained from the bulk. These feed, concentrate, and tail samples were then prepared for assay and insol analysis using methods described in section 3.2.

Two different float cells were used for these experiments: a plexiglass and a stainless-steel float cells. Although both had the same dimensions, the different materials were chosen due to their properties depending on the type of test. One, made of stainless-steel, was used for the experiments in which the cell was submerged in the ultrasonic bath. The stainless-steel cell was favored for those experiments due to steel's low attenuation rate for ultrasonic waves as opposed to plexiglass' ability to absorb sound waves. The ultrasonic waves would originate at the bath's transducers located on the sides of the bath and would pass through about one inch of water, then

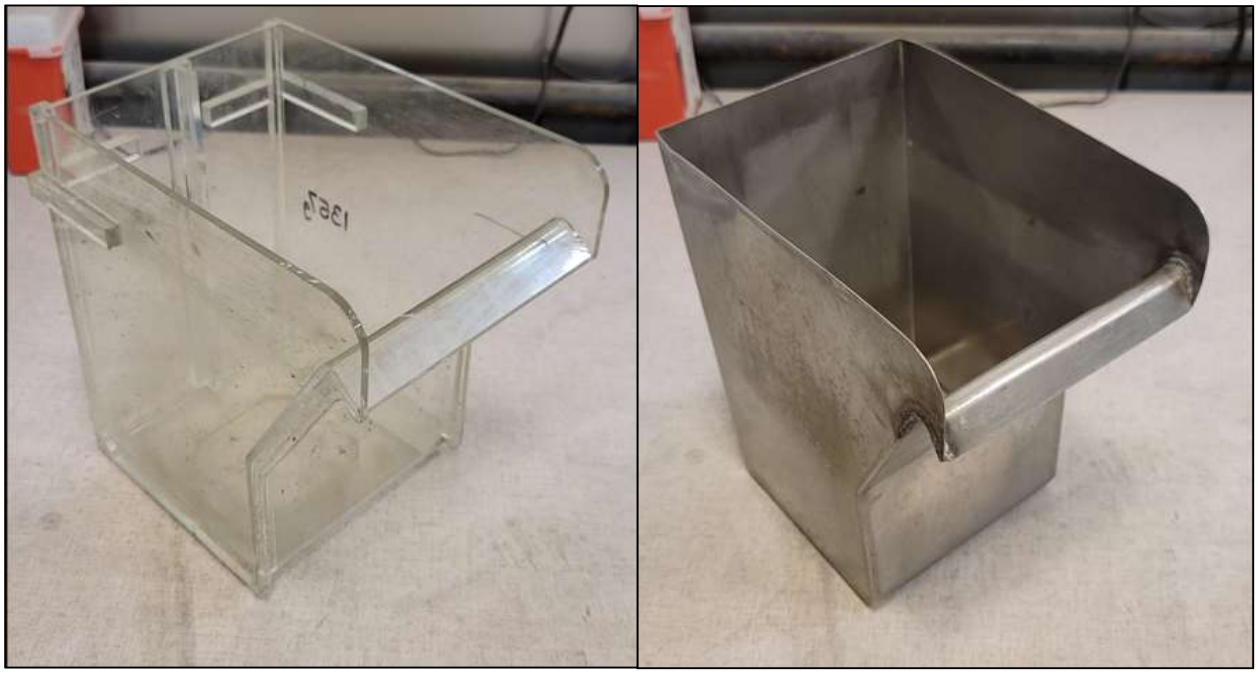

Figure 16: The plexiglass (left) and stainless steel (right) float cells used in these experiments

through the 1 mm thick steel float cell's walls, and then into the slurry. The other float cell, made of plexiglass, was used for the experiments in which the ultrasonic probe was inputted directly into the slurry. The plexiglass cell is favored since it is transparent; it is more easily able to distinguish the level of the slurry versus the froth level than the steel cell.

Figure 17: The Denver Cell D12 Lab Flotation machine used in these experiments.

3.4 Feasibility Study Using Ultrasonic Bath

A feasibility study using ultrasonication implemented by way of an ultrasonic bath was performed. The same set up and slurry preparation as described in section 3.3 was followed with the steel float cell being submerged inside of an ultrasonic bath filled with water. To maintain homogenous slurry, the slurry was placed in a bucket and agitated for two minutes using a spare Denver flotation machine and siphoned into the float cell using a peristaltic pump. The 8-minute test was run with the bath producing ultrasound at 37 kHz without being run at the 2-minute pretreatment. The agitator was run at 1200 RPM and the air rate was set to 5 liters per minute (LPM). Froth concentrate was hand-paddled into a container at 5-second sweeps. Samples of feed, concentrate, and tailings were collected subsequent to the tests and prepared for assay and insol analysis.

Figure 18: The ultrasonic bath used for the experiments, an Elmasonic P 120 H ultrasonic bath.

3.5 Feasibility Study & Kinetics Study Using Ultrasonic Probe

A feasibility study using an ultrasonic probe was performed. The 24 kHz 2000W Ultrasonic Processor was obtained from Great Wall Instruments and used as the ultrasound source in the remaining experiments. The 20mm diameter probe was clamped in the center of the flotation cell and run at 90% power capacity. The frequency ran at 24 kHz during each test. The feasibility study consisted of running the probe during the 8-minute float test as well as throughout the 2-minute pretreatment before air was added. Feed, concentrate, and tailing samples were collected from the test and were subsequently assayed and analyzed for insoluble material. Following the feasibility study, a kinetics study was performed using the ultrasonic probe. Froth was collected at 1-minute, 2-minute, 4-minute, and 8-minute time intervals during

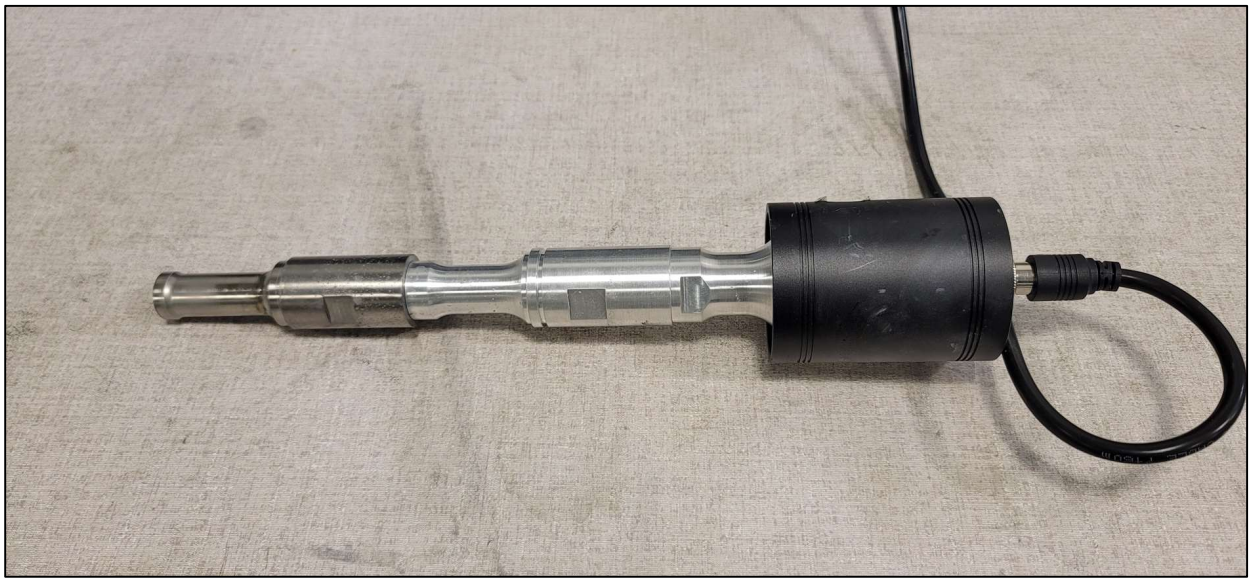

Figure 19: The 2000W 24 kHz Ultrasonic probe used in these experiments.

the float test in order to obtain a kinetics profile of the system. Each concentrate, along with the feed sample and tailings, were dried and assayed with insol analysis.

3.6 Topographical Analysis Using SEM

Topographical information regarding the quartz particles following an ultrasonic treatment were obtained via SEM analysis. Both of the two streams of slurry in the previous experiments were analyzed. Each stream was collected and subjected to a ten-minute-long ultrasonic treatment using the 2000W ultrasonic probe at 24 kHz while inside the float cell used in the flotation experiments. During the ultrasonic treatment, the float cell was agitated at 1200 RPM but was not aerated. Samples with and without the treatment were dried and de-oiled using acetone. Pin stub specimens of each sample were carbon coated to prevent charging and prepared for SEM analysis. Images of the topography of quartz particles were obtained with the goal of finding ultrasonic effects to the surface of quartz.

Chapter 4: Experimental Results and Discussion

Molybdenite slurry was tested in small-scale flotation experiments to gauge the effects of ultrasonic treatments on flotation performance. The slurry chosen was taken from the feed distribution box for a second cleaner stage. In addition, another slurry stream from rougher concentrate was taken for testing. The second cleaner feed was chosen as one of the slurries to perform experiments on for several reasons. This stream lies in the circuit as one that captures all of the tailings from the upper cleaner stages. Tail streams from the high-grade stages cycle back to a clarifier, the underflow of which is funneled to the second cleaner feed distribution box. It was this that drove the choosing of this stream. While there is still considerable flow from the first stage concentrate, the mixing of the streams' rejected material in second cleaner feed prompted this choice as one that could benefit most from an ultrasonic treatment to improve its floatability. In addition, the rougher concentrate stream was chosen due to its larger particle size and greater percentage of gangue material, a contrast to the second cleaner feed stream. If gangue is able to be reduced early in the production circuit, it will result in a better-quality final product overall with a less energy expenditure. If floatability and quality were improved significantly, some stages could be removed or maneuvered into a parallel circuit instead of continuous, allowing a greater tonnage throughput in the circuit (**Figure 20**).

Slurry was first tested in a stainless-steel float cell that was submerged in an ultrasonic bath run at 37 kHz for the duration of the test. Subsequent tests were performed using a 2000 W ultrasonic probe submerged directly in the slurry. The aim of these tests was to elucidate the effects of ultrasound on the flotation kinetics and see whether an improvement to grade and/or recovery could be achieved. Previous literature describes a substantial improvement to recovery on other types of mineral flotation and molybdenite's natural hydrophobicity should aid in the

formation of cavitation bubbles on the mineral's surface. This will theoretically improve flotation kinetics through the cleaning of the surface of slimes and oxides, the coalescence of cavitation bubbles with flotation bubbles, a more efficient dispersion of reagents in the float cell and deagglomeration of molybdenite covered gangue particles. The results of the tests and SEM analysis are presented here.

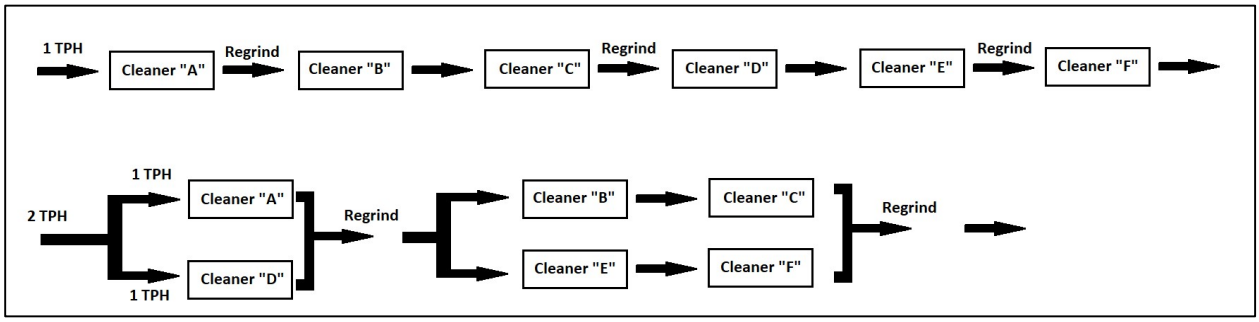

Figure 20: If floatability is improved, the existing circuit in series can be rearranged in parallel to increase throughput from 1 ton per hour (TPH) to 2 tons per hour.

4.1 Characterization of Molybdenite Slurry

The slurry tested was evaluated for particle size distribution using sieves and chemical analysis using an ICP-OES. Particle size distribution for the slurry shows a majority of fines beyond 635 mesh. This stream, second cleaner feed (2CF), was chosen due to its important positioning in the plant's circuit. The tails from the cleaner circuit stages report back to this feed and so the hope was to liberate or deagglomerate the rejected material from the high-grade circuit and improve its floatability. The presence of so many fines is indicative of the many regrinds that this material has gone through. The slurry had on average a 12% solids ratio to water.

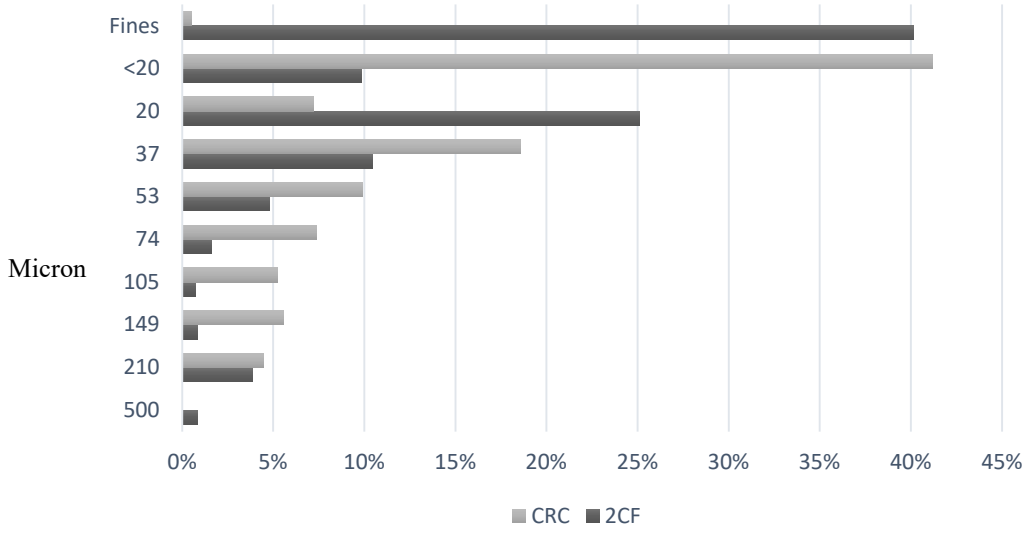

Figure 21: Particle size distributions for second cleaner feed (2CF) and rougher concentrate (CRC).

Chemical analysis was performed using an ICP-OES following acid digestion. In addition, gangue analysis (insol testing) of the insoluble material following the acid digestion was also performed and quantified. The chemical analysis is shown with molybdenum being majority molybdenum disulfide; the percentage of molybdenum in pure molybdenum sulfide being 59.94%, along with major trace metals, which are typically sulfides in the slurry.

Table 1: Elemental distribution of second cleaner feed (2CF) and rougher concentrate (CRC) found from ICP-OES.

	Al	Ca	Cu	Fe	K	Mg	Mn	Mo	Na	Ni	Pb	Sn	Ti	W	Zn
2CF	0.51	0.768	0.0103	1.5806	0.1803	0.0116	0.1038	37.076	0.0163	<0.0001	0.099	<0.0001	0.0065	0.007	0.115
CRC	0.4091	0.9459	0.0045	3.1694	0.155	0.0115	0.1365	2.8281	0.022	0.0001	0.0294	<0.0001	0.002	0.0054	0.073

Insoluble gangue material in the 2CF stream was quantified to be on average 32.5%. This gangue material, which is mainly quartz particles, will be characterized later in this chapter. The mineralogy of this stream from TIMA analysis shows a majority molybdenite followed by quartz and orthoclase. Molybdenite was found to be 91% liberated.

Table 2: The major constituents of second cleaner feed (2CF) and rougher concentrate (CRC) mineralogy from TESCAN Integrated Mineral Analyzer (TIMA).

2CF		CRC	
Mineral	**Mass %**	**Mineral**	**Mass %**
Molybdenite	76.172	**Quartz**	45.102
Quartz	14.181	**Orthoclase**	23.049
Orthoclase	3.936	**Muscovite**	10.251
Muscovite	2.137	**Molybdenite**	9.487
Pyrite	1.283	**Pyrite**	3.829
Fluorite	0.565	**Topaz**	2.065
Topaz	0.423	**Anorthoclase**	1.506
Siderite	0.159	**Fluorite**	1.447
Zinnwaldite	0.141	**Albite**	0.683
Anorthoclase	0.134	**Zinnwaldite**	0.479
Albite	0.101	**Iron oxides**	0.340
Iron oxides	0.085	**Siderite**	0.311

Figure 22: 2CF (left) and CRC (right) samples under an optical microscope. CRC possesses larger particle sizes and a larger percentage of gangue.

The other stream chosen for these experiments represents a larger particle size and a greater ratio of unliberated mineral. The concentrate from the rougher circuit (CRC) was collected and analyzed using the same methods for the previous stream. Insoluble mass on average was found to be 83% and mineralogy analysis shows that quartz and orthoclase feldspar is the majority material. Liberated molybdenum accounts for 73% of total molybdenum in the slurry.

4.2 Characterization of Gangue

Gangue material is isolated after an acid digestion of the molybdenite concentrate which is then filtered through an ashless filter and heated in a furnace at 900°F for one hour. The insoluble gangue material residue left in the crucible is quantified in the determination of product grade. As the material is detrimental to the final product use as a lubricant, the characterization of this gangue is important to understanding its removal during the floatation process. XRD analysis of the gangue shows a large majority quartz (SiO_2) followed by cristobalite. Cristobalite is a polymorph of SiO_2 and is likely a product of the assaying process.

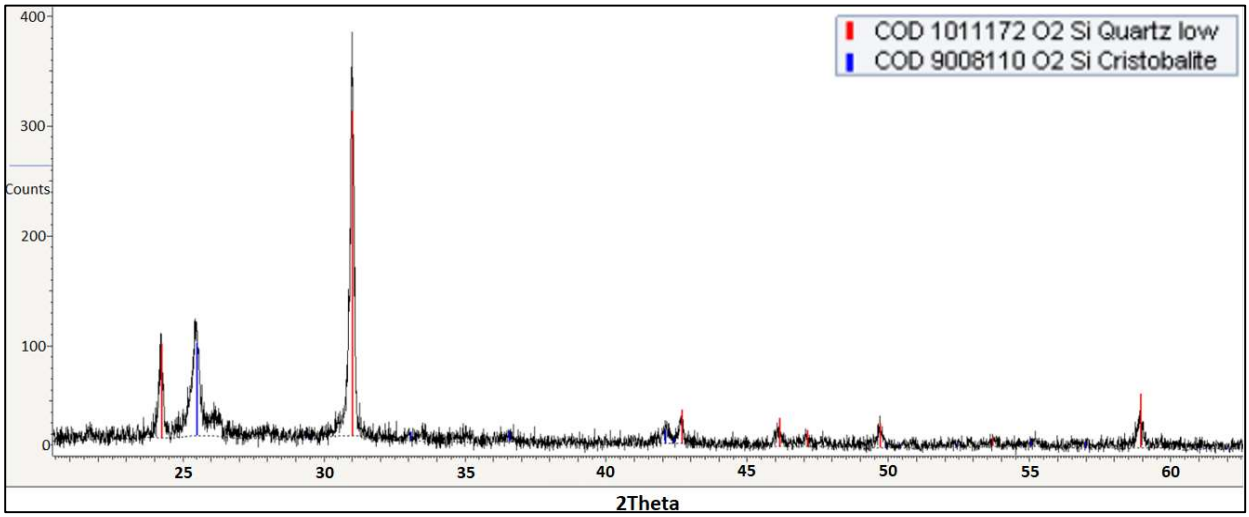

Figure 23: XRD analysis of gangue material showing a majority quartz and cristobalite.

SEM imagery of the isolated gangue shows sharp quartz grains surrounded by very fine quartz particles of a fibrous texture (**Figure 24**). 90% of gangue material is less than 38 microns.

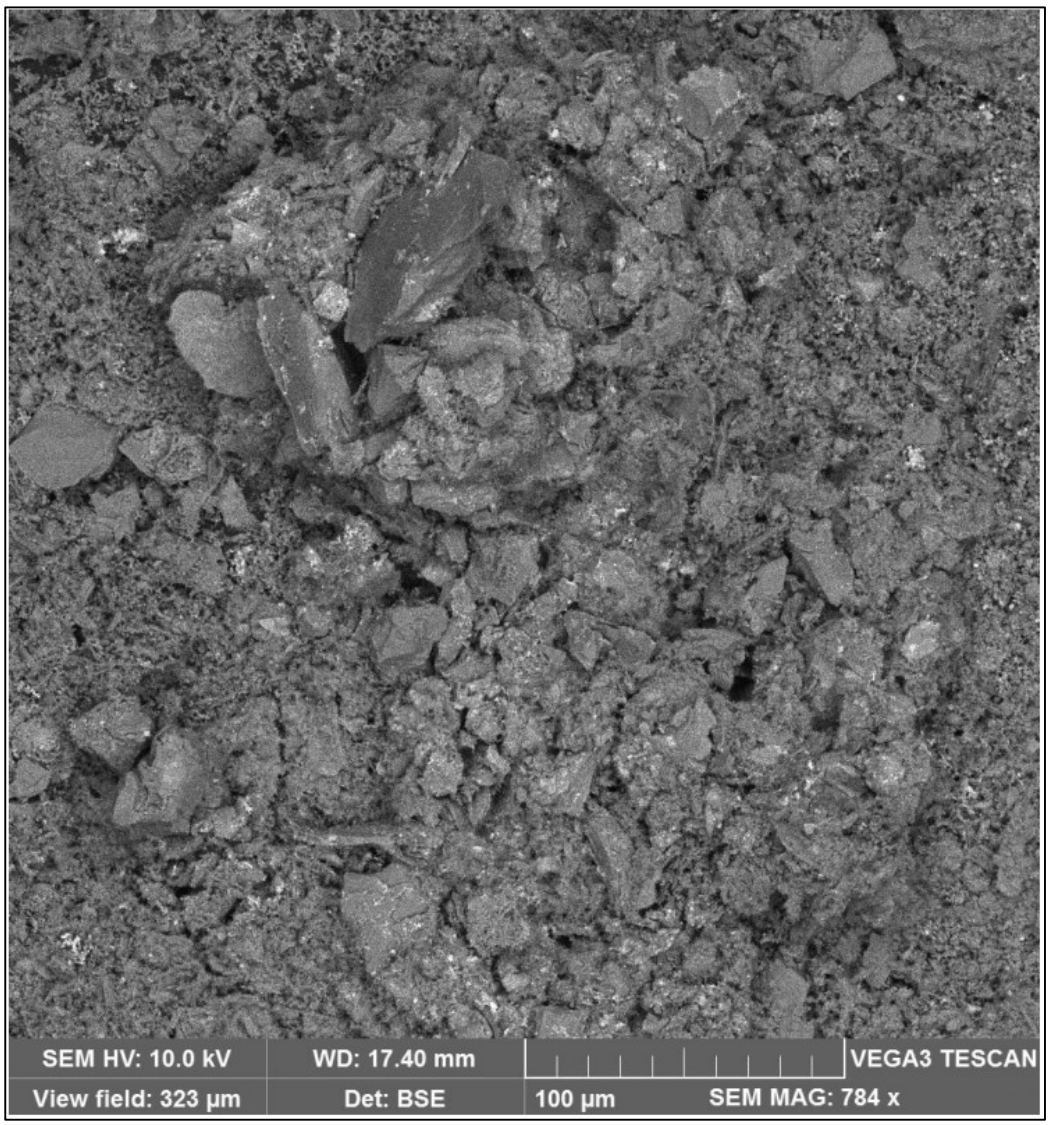

Figure 24: SEM of isolated gangue shows sharp quartz grains surrounded by very fine quartz particles.

4.3 Results of Ultrasonic Treatments Using Ultrasound Bath

Tests were conducted using an ultrasound bath for the first phase of this experimentation as a feasibility study for the process. Only the second cleaner feed slurry was used in these tests. Slurry was collected and homogenized while transplanted into a stainless-steel float cell, which was then submerged in the bed of the ultrasound bath filled with water. The ultrasound bath was set to 37 kHz for the whole duration of the test. Each test had a pretreatment of 2 minutes where the agitator ran to homogenize and de-settle the slurry without air nor ultrasound. Slurry was

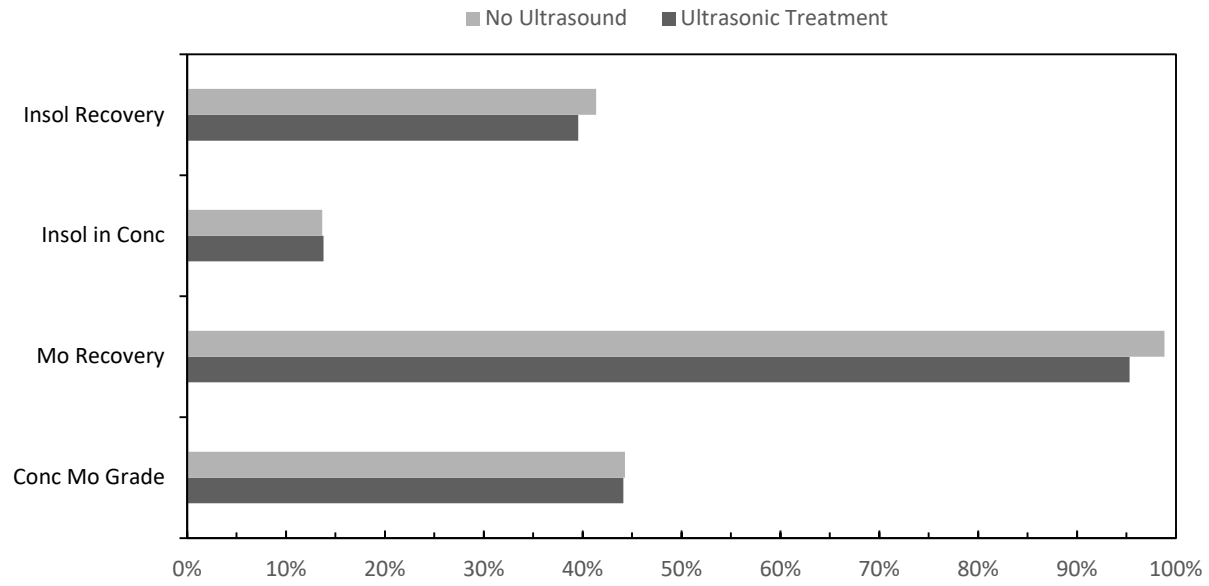

Figure 25: Results of feasibility study using the ultrasonic bath.

floated at 5 LPM for 8 minutes while being agitated at 1200 RPM and froth was collected using hand paddles. Concentrate, feed, and tailings samples were collected and were dried and prepared for assay and insol analysis. Each test revealed that recovery did not improve upon subjection to the ultrasonication using the bath as well as no improvement to molybdenum present in the concentrate. The only evidence of improvement using this system was a higher

gangue (insol) rejection rate, the ultrasonic testing showing an approximate 5% reduction in insol recovery.

Unfortunately, this feasibility study proved to show little improvement in recovery in grade in relation to the control tests. Likely this is due to the nature of the test which did not account for

Figure 26: The experimental set-up for using the ultrasonic bath.

changes in recovery over time. All recoverable material would be moved to the concentrate after enough time and so future experiments were altered to include separate concentrate samples at different time intervals in order to gauge the float kinetics using an ultrasonic probe. The ultrasonic waves may also have been hindered through reflection and/or adsorption by the need to pass through the stainless-steel enclosure of the float cell as it was submerged in the bath. Although according to literature the attenuation of steel with regards to ultrasound is minimal. The power of the ultrasonic bath may have not been adequate for this application as baths usually are powered low to prevent damage to their enclosures after extended use. Using a probe inserted directly into the slurry would have eliminated this potential issue.

Additional problems were encountered by using a bulk supply of slurry to be used with each experiment. As each day progressed, the pH level of the bulk slurry gradually decreased from 7.7pH to 5.8pH. This is due to the mine-drainage effect as the water in the slurry slowly leached the sulfides into sulfuric acid. As froth flotation is greatly affected by pH, the decision to use a freshly collected sample was then done to avoid this effect. Since molybdenite flotation favors solutions that are slightly alkaline, the changing of pH to become more acidic likely also hindered the results of this feasibility study using the ultrasonic bath.

4.4 Results of Ultrasonic Treatments Using Ultrasonic Probe

Tests were conducted to ascertain the effects of an ultrasonic probe on the froth flotation kinetics of molybdenite slurry from two streams: a rougher concentrate and feed from a second stage cleaner. The slurry for both streams were approximately 14% solids mass, was consistently about 7.8 pH on average, and was at an ambient temperature of 68°F. The 24 kHz ultrasonic probe was inserted into the float cell during the test along with injecting air at 5 LPM and agitated at 1200 RPM. The effects on recovery and grade from using the probe during separate

stages of the test were discovered. For the kinetics experimentation, concentrate was collected by hand paddle at 1-minute, 2-minute, 4-minute, and 8-minute intervals to elucidate a kinetics profile of the system. Concentrate, feed, and tailings samples were dried and prepared for ICP-OES assay and insol analysis.

Figure 27: The experimental setup using the ultrasonic probe.

4.4.1 Feasibility Study

A study was performed to ascertain the feasibility of using an ultrasonic probe to improve the recovery and grade of molybdenite slurry float tests on two different streams: a second cleaner and a rougher concentrate. The results of this study are detailed in this section.

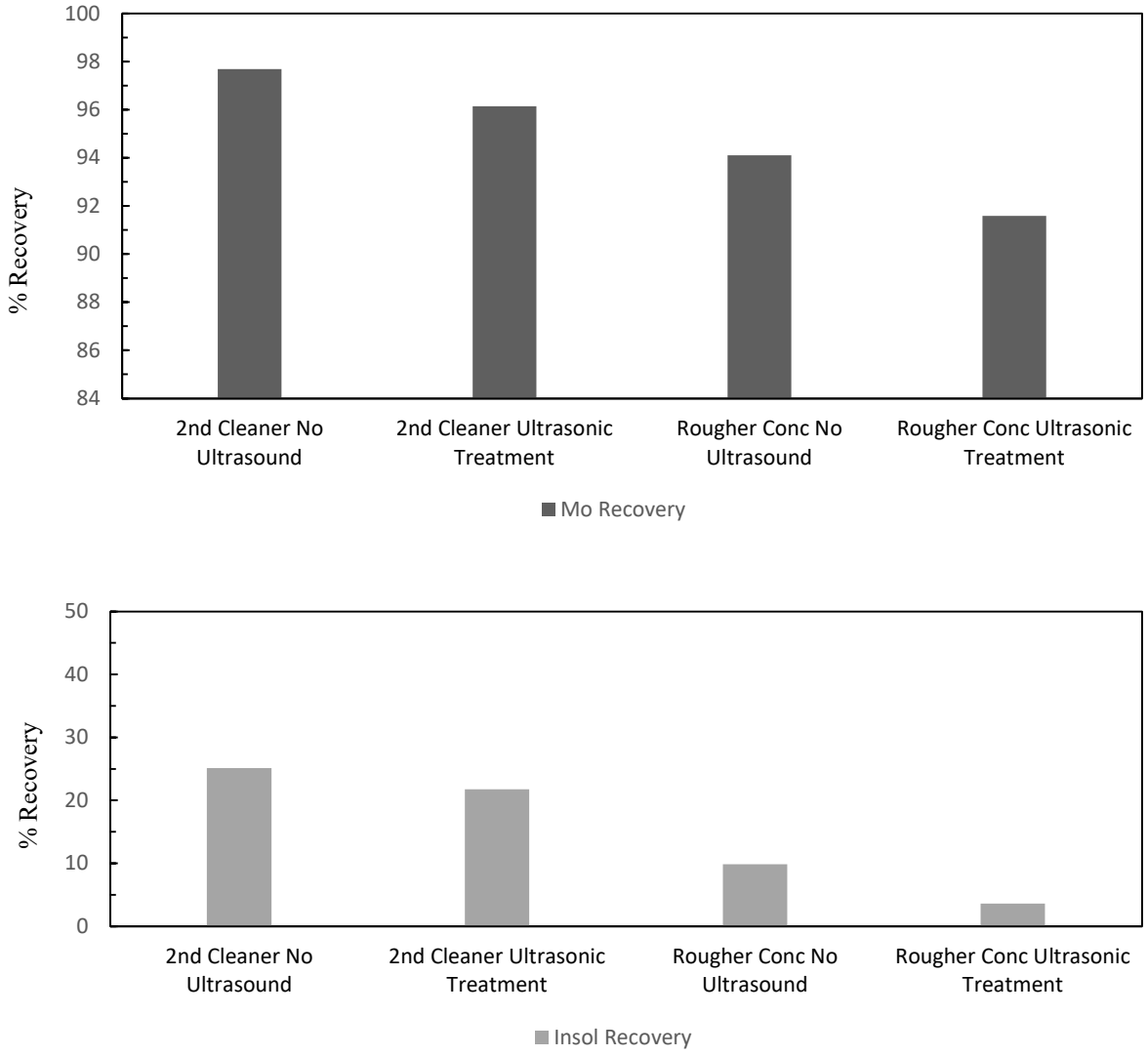

Figure 28: Molybdenum recovery (top) and gangue (insol) recovery (bottom) of the feasibility study using the ultrasonic probe.

Results show that ultrasonic treatments resulted in a lower overall molybdenum recovery but also decreasing the amount of gangue (insol) recovered in the concentrate. Second cleaner ultrasonicated tests showed a 96.1% Mo recovery with a 21.7% insol recovery, with non-ultrasonicated tests showing 97.6% Mo recovery with a 25.1% insol recovery. Ultrasonicated rougher concentrate testing showed 91.6% Mo recovery with a 3.5% insol recovery, with non-ultrasonicated testing showing 94.1% Mo recovery and 9.8% insol recovery. These results show promise to the method of ultrasonication as a whole to improve the grade of molybdenite floatation due to the almost 4% reduction in insol recovery for the 2nd cleaner stream and 6% reduction in the rougher concentrate tests. In addition, while there was a decrease in molybdenum recovery, ultrasonic treatments produced a consistently higher molybdenum grade in the concentrate.

While the feasibility study showed promise for the ultrasonic method of flotation, kinetics studies were needed to elucidate just how the method can produce concentrate at a given time interval since a regular test on a long enough time scale will recover all material. A kinetics study can show if an adequate concentrate can be collected after a certain time with any improvements due to ultrasonication.

4.4.2 Kinetics Experiments on Second Cleaner Feed

Kinetics tests were conducted on second cleaner feed samples with and without an ultrasonic probe. For ultrasonicated tests, the probe was initialized two minutes prior to the start of the injection of air while the agitator was running, for a two-minute ultrasound pretreatment. Concentrate was collected at 1-minute, 2-minute, 4-minute, and 8-minute time marks and assayed along with gangue (insol) analysis. Feed samples were analyzed as well with the tailings sample, and results were averaged to create a composite recovery profile.

Molybdenum recoveries showed that the ultrasound treatment slowed down recovery with a slightly lower level of overall recovery. Recovery at the one-minute mark showed the greatest difference in recoveries, with about a 17% lower recovery for the ultrasonic tests. Molybdenum recoveries over the course of the test began to equalize between the two tests eventually, with the ultrasonic tests having an end recovery of 93.8% compared to the tests without ultrasonic as 97.6% recovery. While overall molybdenum recovery was slightly less in the ultrasonic tests, the molybdenum content of each concentrate was higher than each in the tests without ultrasonication (**Figure 30**).

Figure 29: Image showing the paddling of 2CF froth into concentrate container.

Acidity of the slurry did not change over the duration of the test. However, there was a change in temperature of approximately 3°C over the course of the 8-minute test. This was expected due to the effects of the cavitation bubbles, each one's local temperature reaching approximately 5000°C as the cavitation bubble implodes, together contributes to a rise in temperature. However, a change in temperature, while does increase reaction rate according to

the Arrhenius equation, did not likely contribute much to the end result of these experiments as the temperature change was minimal.

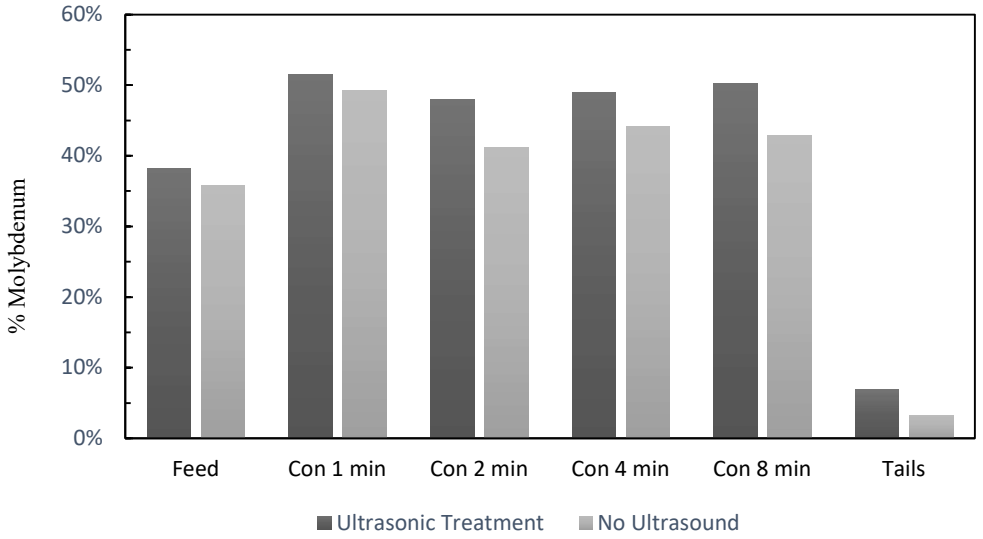

Figure 30: Comparison of the percent molybdenum in the concentrate at each time interval for each test.

Recovery for the ultrasonic tests was hindered by the amount of molybdenum that remained in tailings, which was about 6.2% of total Mo versus 2.4% for the non-ultrasonic tests. In some situations, having a larger amount of molybdenum and/or solids in the tails could be beneficial as some operations utilize a recirculating load whose function is to slow down the circuit and improve grade. Overall, ultrasonic tests regarding molybdenum recovery showed a substantially lower amount of recovered mineral at the one-minute mark, 58% recovery for ultrasonicated versus 75% recovery for non-ultrasonicated, along with a larger amount of mineral remaining in tailings after the experiment concluded. These results are possibly the result of the ultrasonication causing a deagglomeration of all particles in the slurry. While deagglomeration was an initial aim in order to separate gangue particles from molybdenite particles, it seems that molybdenite flotation in particular can benefit from agglomeration. Fine molybdenite particles aggregated around reagent oil droplets can lead to beneficial flotation

kinetics [31]. Disruption of these aggregates would lead to a lower recovery, as fine molybdenite particles have lower floatability due to their limited hydrophobicity and can take advantage of being in agglomerates. In these experiments, albeit doubling the time it took for the non-ultrasonic tests, the ultrasonicated molybdenum minerals eventually went into the concentrate as only there was only a minimum difference in overall recovery between the two tests.

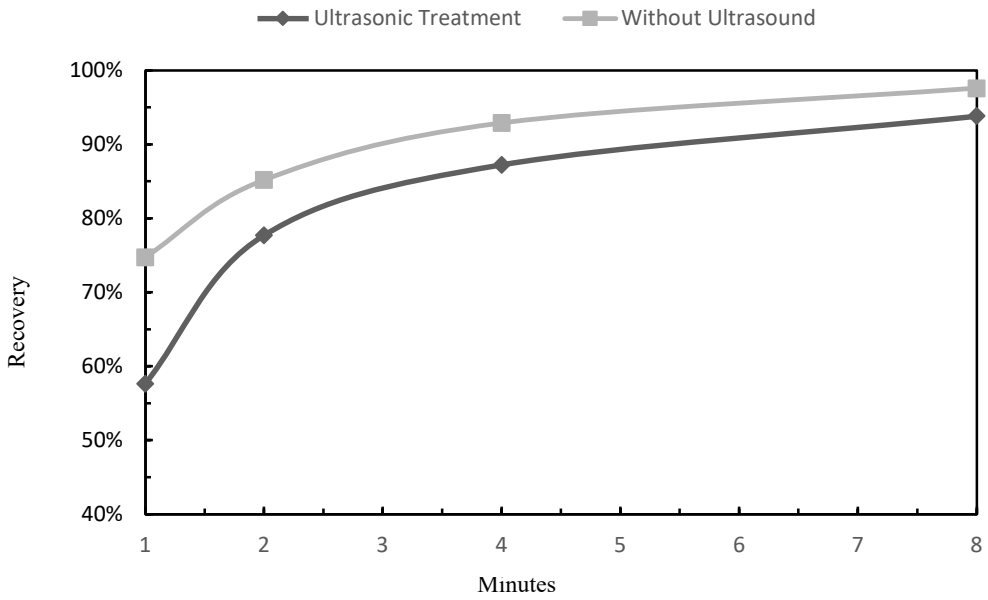

Figure 31: Cumulative recovery of molybdenum over the course of the test.

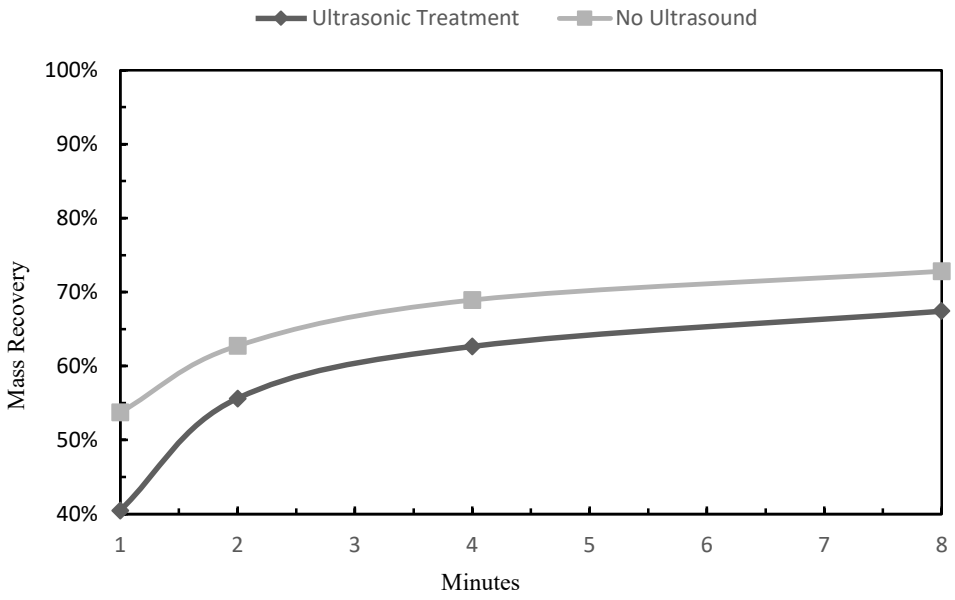

Figure 32: Cumulative mass recovery of the course of the test.

Cumulative mass recovery over the course of the experiments showed similar results to molybdenum recovery, with ultrasonic testing showing a slightly lower mass pull at every time interval.

While molybdenum recovery showed slower kinetics and an overall less recovery, the effects of ultrasonication on gangue (insol) were dramatic. Results showed a substantially lower gangue recovery in the concentrate throughout the kinetics experiment at every time interval, with an overall recovery in gangue for the ultrasonic tests at 19.5% and that increased to 28.2% for the tests without ultrasonication, with an overall reduction in approximately 9% gangue recovery.

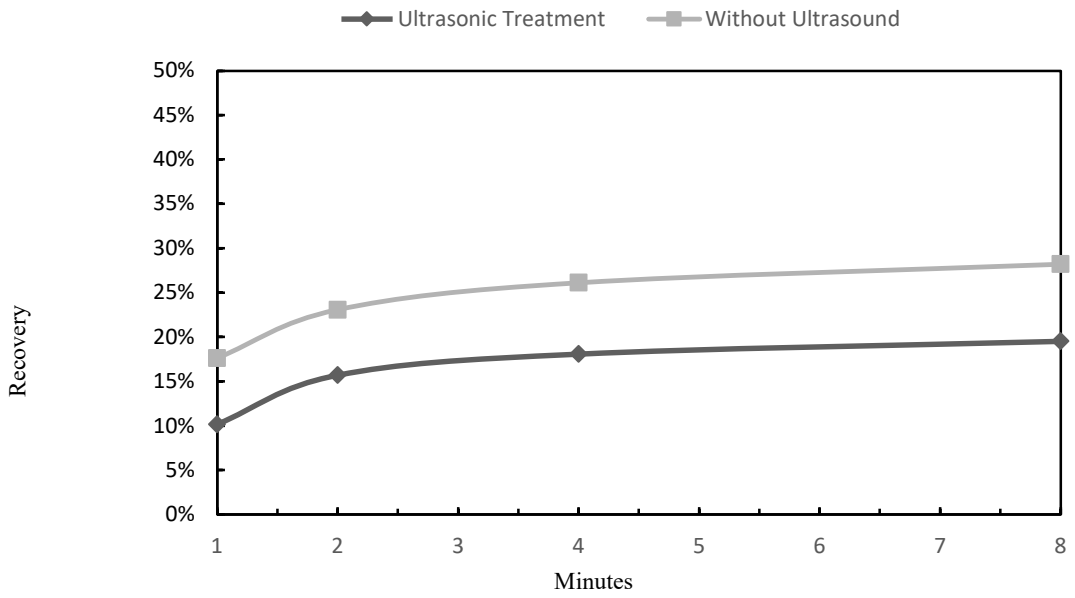

Figure 33: Cumulative gangue (insol) recovery over the course of the test.

The increase in gangue rejection for the ultrasonicated experiments could be attributed to the deagglomeration of molybdenite encapsulated quartz particles. In addition, SEM analysis of ultrasonicated samples will shed light on the topography changes to quartz particles and will be

discussed later in this chapter. As the amount of gangue entrainment is related to water recovery, a look into the water recovery profile for these experiments is necessary.

Water recovery in the ultrasonic tests proved to be about 2% less at each time interval. While less water recovery overall should account for some gangue entrainment reduction, this does not account for all the effects of gangue reduction in the ultrasonic tests. It is important to note that there is less water recovery for experiments subjected to ultrasonication. This may be due to a slightly increased level of drainage in the froth zone due to vibrations.

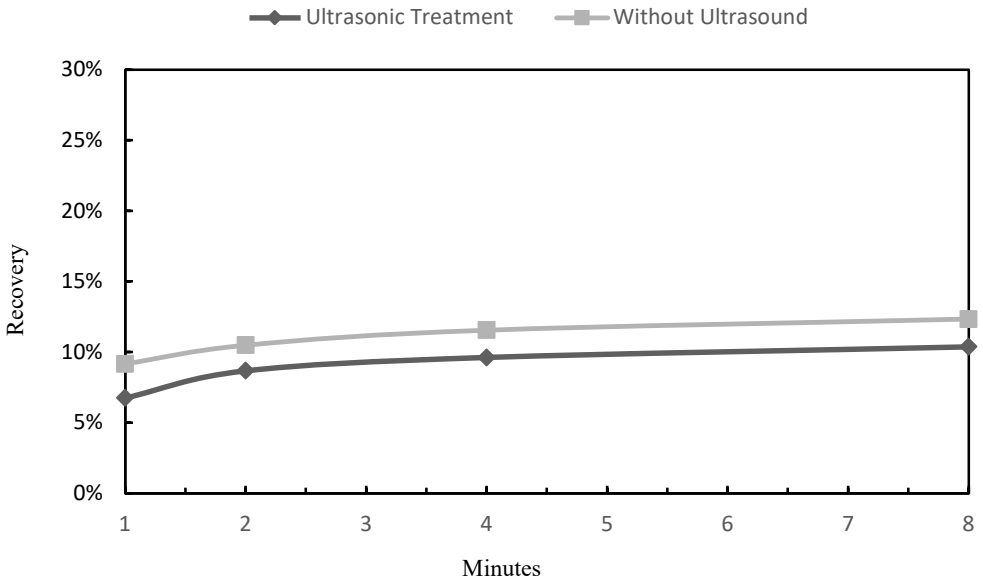

Figure 34: Cumulative water recovery over the course of the test.

Another aspect of this testing is to observe the effects that ultrasonic treatment had on the recoveries of trace elements. Trace elements are undesired in concentrate production and their recoveries are reduced as much as possible. There can be customer specifications for how much of a trace element can remain in the product and if values are too high (i.e. copper, iron, zinc) the product can be refused. In addition, other elements such as lead can lead to a disruption in the downstream processing of molybdenum oxide concentration. Lead can remain in the concentrate

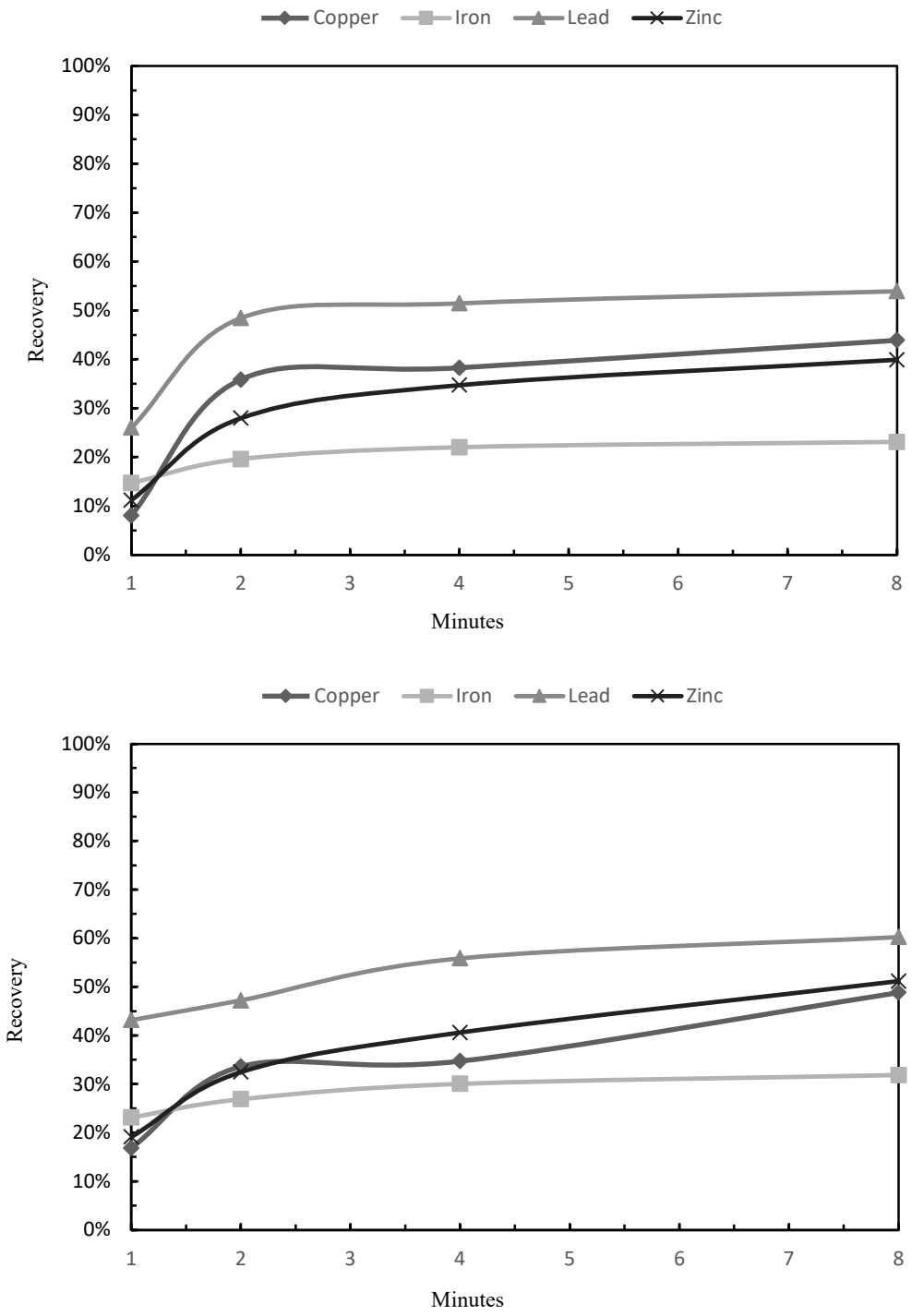

Figure 35: Cumulative recovery of copper, iron, lead, and zinc with ultrasonication (top) and without ultrasonication (bottom).

as it is relatively difficult to dissolve without a dedicated acid treatment. Copper, iron, lead, and zinc were tracked to see the differences in how well their floatability was affected by ultrasound throughout the experiment. Overall, each element showed a decrease in recovery with the exception of copper, which showed a slight increase of 5% in recovery with the ultrasonic treatment.

These results may be due to the effects that ultrasound had on the reagents in the system. Dispersing or diffusing the reagents in the system more effectively would increase their depressive abilities in the float test. In addition, applying the ultrasonication might have cleared the slime layer or oxidative surfaces on these minerals, allowing for reagents to land on their respective reactive sites. Reasons for copper's counter activity may be simply due to its such low presence in the sample causing a margin of error, with a total of copper mass being on average about 0.007 grams in the entire system for these tests.

4.4.3 Kinetics Experiments on Rougher Concentrate

A rougher concentrate slurry was tested with the same conditions as the second cleaner stream, with the hope to elucidate the differences the results would have on another stream. Rougher concentrate would have a larger percentage of gangue material with a coarser particle size.

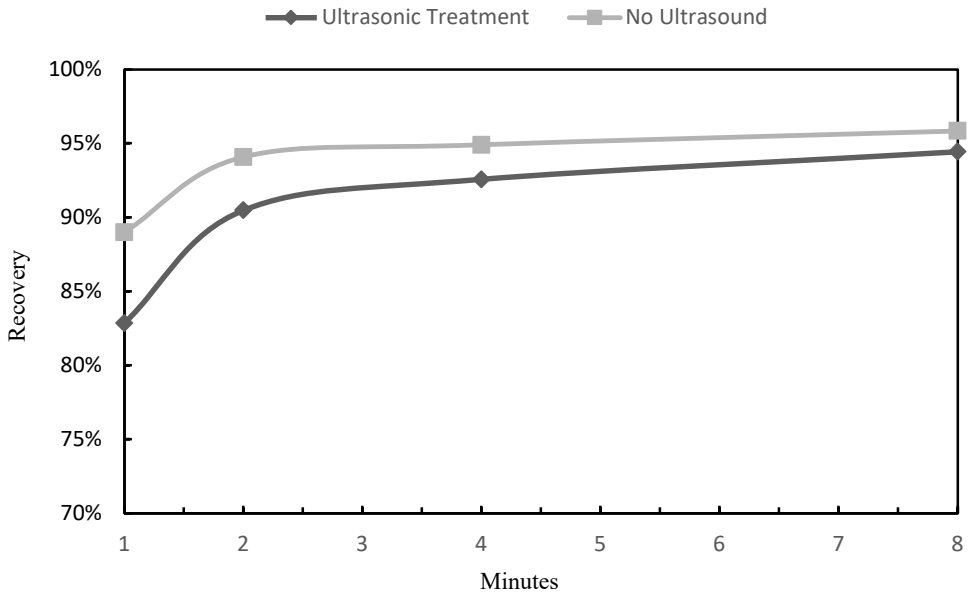

Figure 36: Cumulative recovery of molybdenum over the course of the test.

Charting the cumulative molybdenum recovery reveals that the rougher concentrate stream, although still lower in recovery for the ultrasonic testing, is much more similar in overall recovery. The non-ultrasound tests showed only a higher overall recovery at 95.8% versus 94.4% for the ultrasonic tests. The 1-minute interval does show similar results to the second cleaner molybdenum recovery, although not as considerable with the ultrasonic treatment having approximately 6% less molybdenum recovery at the beginning of the kinetics test. This may still be due to the deagglomeration effects of the ultrasound to fine molybdenum particles causing detriment to molybdenum recovery kinetics, although perhaps not as dramatic in this case as not much molybdenum is as fine as the second cleaner stream. Like the testing with the second cleaner stream, molybdenum recovery was less in the ultrasonic tests, but the molybdenum content of each concentrate was higher.

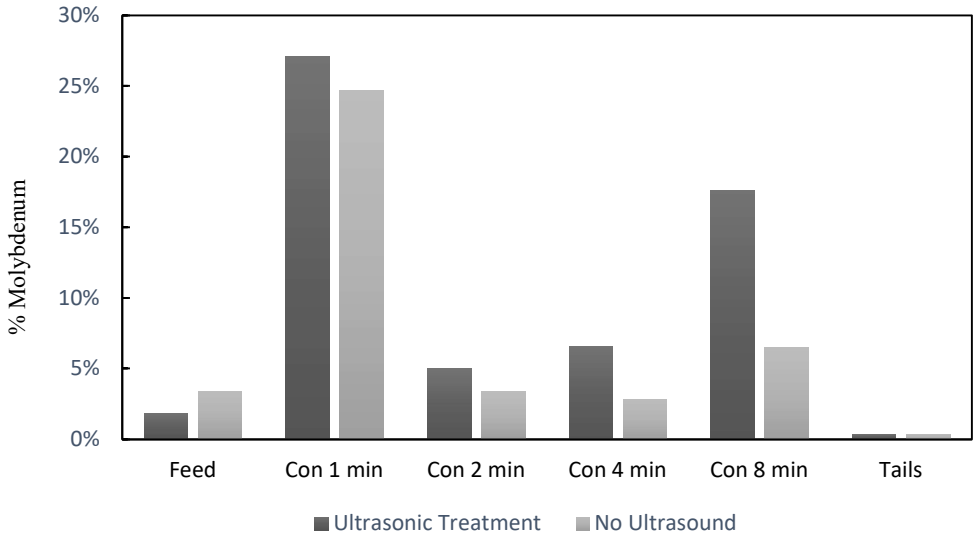

Figure 37: The percentage of molybdenum in each concentrate at 1, 2, 4, and 8 minutes with and without ultrasonication.

Analysis of the gangue (insol) in the kinetics profile of the tests with rougher concentrate also showed in improvement with the ultrasonic treatment. Overall there was a 5.3% reduction in insol recovery versus the tests without ultrasound. Water recoveries also showed similar results, with the ultrasonic testing having about 4% less water recovery than the testing without ultrasound.

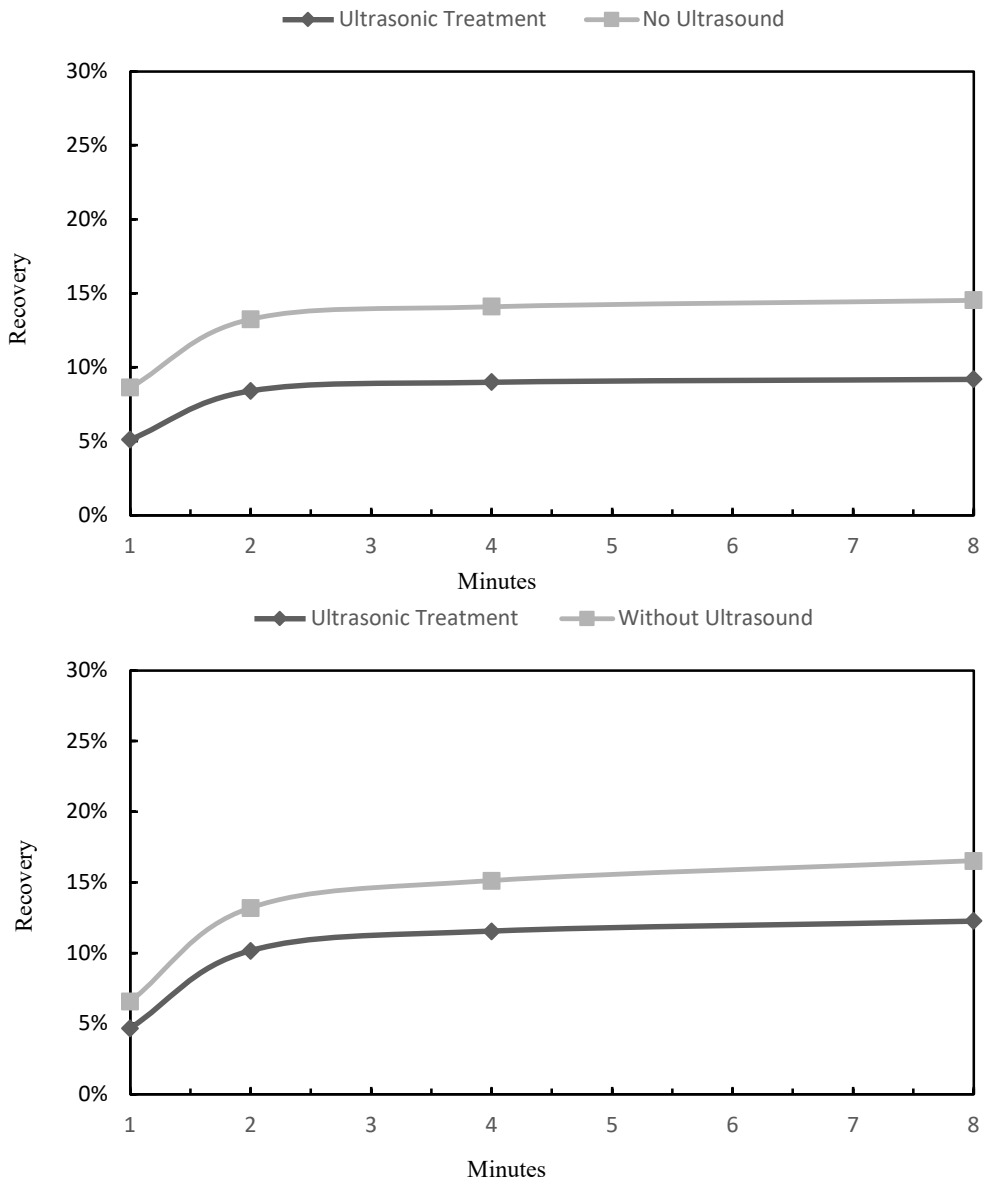

Figure 38: Cumulative gangue/insol recovery (**top**) and water recovery (**bottom**) over the course of the testing on rougher concentrate.

Analysis of copper, iron, lead, and zinc all showed lower recoveries in the testing with ultrasonic treatment. Copper had an overall decrease of 12.5% in recovery, iron a 7.2% decrease, lead a 8.5% decrease, and zinc a decrease of 13.1%. These decreases are likely due to the efficiency improvement on reagents in the system by ultrasonication. In addition, deagglomeration of

minerals adjoined to the more floatable molybdenum could have occurred in the case, contributing to the decrease in these trace elements' recoverability.

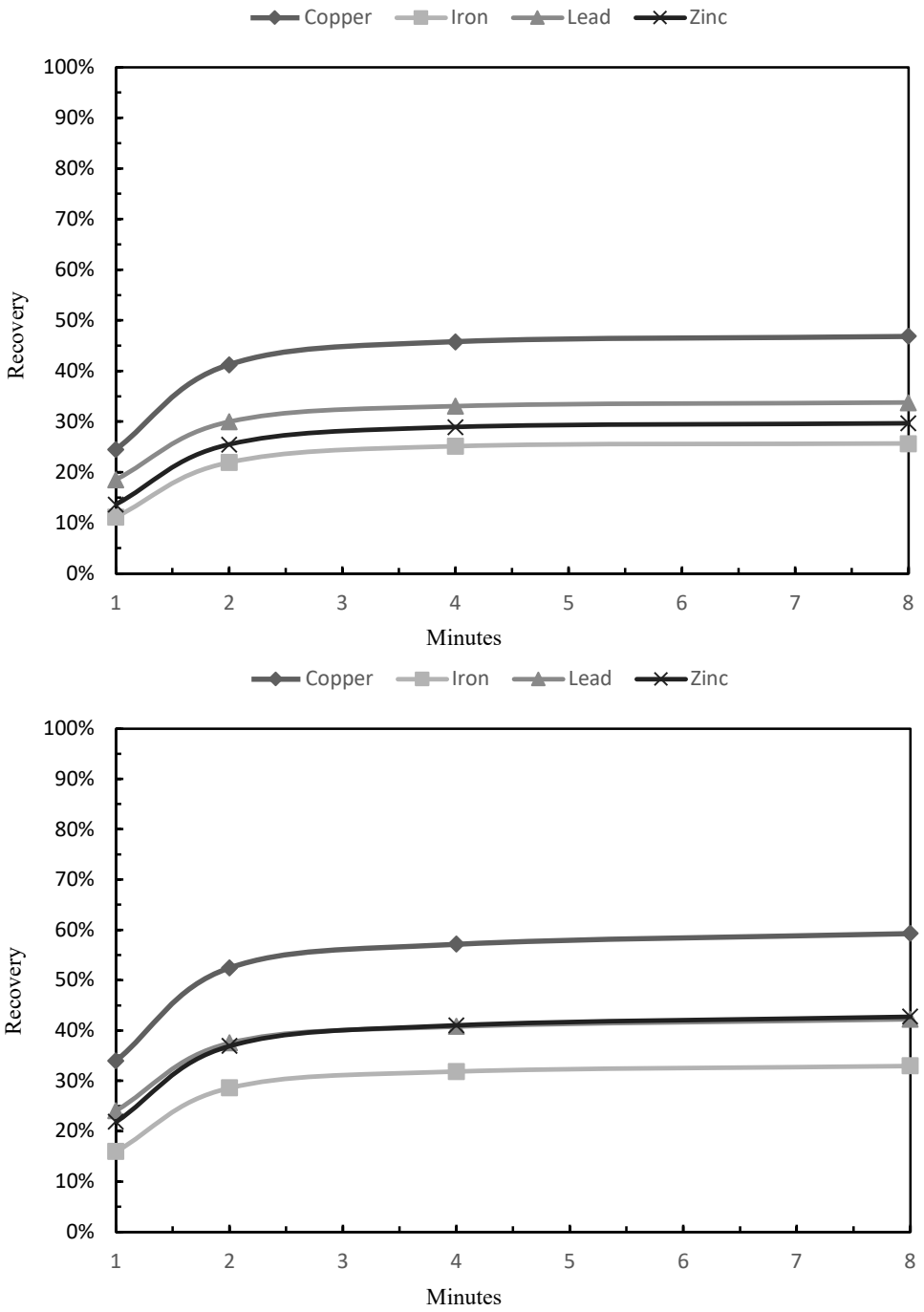

Figure 39: Cumulative recovery of copper, iron, lead, and zinc with ultrasonication (**top**) and without ultrasonication (**bottom**).

4.4.4 Effects of Ultrasonic Pre-treatment

The experiments performed thus far consisted of using ultrasonication throughout the duration of the float test. However, some literature suggests that an ultrasonic pretreatment is all that is necessary to provide the desired results [79]. Float tests were conducted on only second cleaner slurry using only the ultrasonic probe for a 2-minute pretreatment prior to the test and was turned off for the following 8 minutes. Concentrate collected at 1-minute, 2-minute, 4-minute, and 8-minutes were assayed and analyzed for gangue.

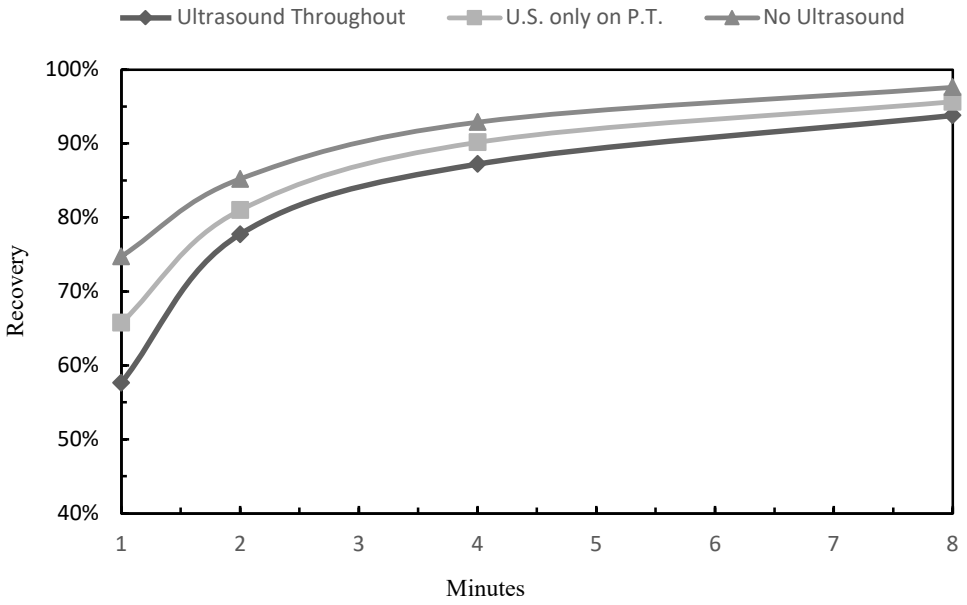

Figure 40: Cumulative recovery of molybdenum over the course of the test.

Using the ultrasonic probe for only a 2-minute pretreatment yielded a better molybdenum recovery than when it was used for the entire duration of the test, but still slightly less than the testing without the probe. Using the pretreatment method seems to help close the gap with the float kinetics.

While improving molybdenum recovery slightly, this method almost completely preserves the beneficial gangue (insol) rejection that occurs when using the ultrasonic probe.

While only hindering the effects by about 1-2%, the amount of reduction in insol recovery is still considerable while using a great deal less energy. These lead to a deduction that a slurry pretreatment of at least 2 minutes is all that is needed to reduce gangue considerably in a float concentrate, rather than running the ultrasonication continuously.

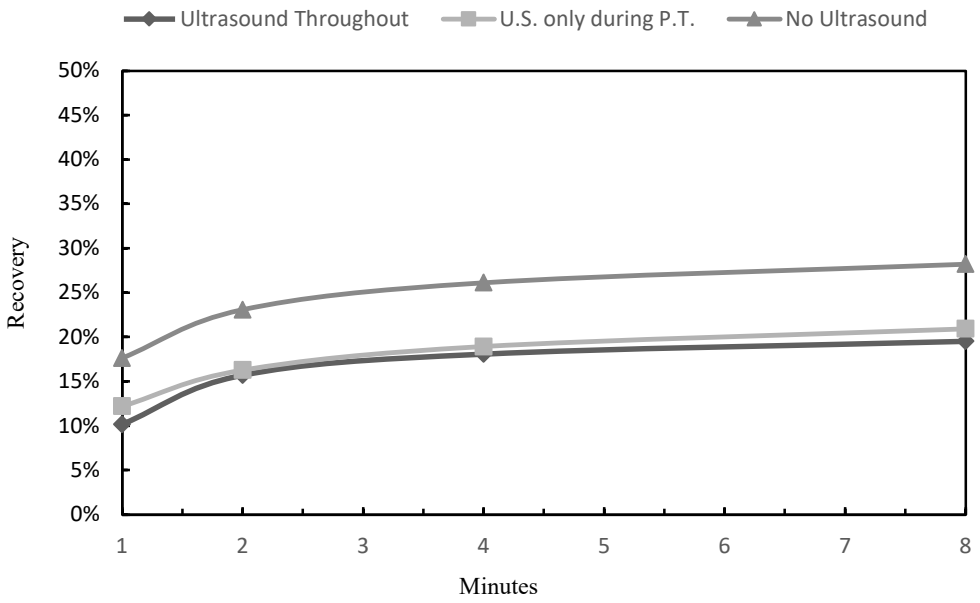

Figure 41: Cumulative gangue (insol) recovery over the course of the test.

Recovery of trace elements and water recovery were also very similar to the results from using the ultrasonic probe for the entire duration of the test. The beneficial effects of ultrasonication seems to occur in the two-minute pretreatment of the slurry and are only slightly improved when continued for the duration of the test.

4.4.5 Challenges

When considering the results of a small-scale flotation experiment for engineering a large-scale pilot test, one must recognize the challenges that exist with a small-scale test. A small-scale experiment does have limitations. Grade-recovery curves are subject to experimental error [80]. There exists a variability in how the concentrate is collected during the test (in these

experiments, the hand paddle was drawn across the surface over the course of 5 seconds per swipe). In addition, the repeatability of the test for further research depends on the original test's documentation of all variables: the dimensions of the float cell, agitator speed, temperature, pH, and in these experiments the size and shape of the ultrasonic probe and positioning in relation to the floatation cell. A large-scale plant will also be most likely a continuous operation while the small-scale experiment is a batch test and considerations must be taken accordingly.

There were challenges for this experimentation that should also be taken note of. The original planning called for a bulk slurry solution to be pulled from for each test, in the hope that the feed remained homogenous throughout the course of the testing. However, the bulk slurry grew more acidic over time, due to the mine drainage effect of the sulfides gradually leaching in the slurry and turning into sulfuric acid. As a changing pH was detrimental to the results of testing as the acidic slurry was less favorable to flotation as well as the changing of chemistry within the slurry, the decision was made to collect slurry from the active circuit and was tested in the float cell five minutes after sampling. This also must be considered as the circuit, while having mainly an overall consistent constituency, pH, and temperature, there was some variability in the feed for each test performed. Reagents added to the circuit in various points prior to the sampled slurry would likely have some variability but care was taken to have all conditions be as consistent as possible. A feed sample was taken for each and every test in order to calculate appropriate recovery rates in order to overcome this potential liability.

Another possibility for variability in the experiments with the ultrasonic probe might lie in the dimensions of the froth surface area. The probe was inserted near the back of the slurry and there was a region of about 1 to 1.5 square inches where the hand paddle was unable to draw

Figure 42: Probe prevents the paddle from accessing about 1.5 in^2 of float cell.

from, leading to a slightly less floatable surface area for the cell. Creating a custom-built flotation cell with transducers designed in the sides of the cell would overcome this obstacle. However, the costs of creating and maintaining a custom-made cell might be much larger than the ultrasonic probe, especially if used in a large-scale pilot test.

While these experiments show promise in the improvement of grade and reduction of gangue material in the concentrate, there are considerations to take when planning for implementation of ultrasonication on a large-scale operation. Current ultrasonic probes degrade with continuous use, and so a design for large-scale application could pulse the probe or have a series of probes that alternate being powered on over a period of time. This would increase the lifetime of the probe(s) but not extend it indefinitely, and replacements/maintenance would need

to be planned for. Another factor to consider is how much slurry throughput is in the operation and how large the stages are, as an ever-increasing amount of power is needed to provide an ultrasonic field in the slurry to prevent attenuation through slurry distance. A series of probes at relatively lower power at periodic distances could overcome that hinderance. The slurry would also need to be in contact with the ultrasonic field for a long enough period of time for the ultrasonication to be effective. A chamber or sump in which the slurry residence time was at least two minutes would be a good option to consider, although depending on the throughput this chamber's size could be significant. Another issue that could arise in implementing ultrasonication on a large-scale operation would be its effects on the lining of the floatation cells, as over time they would be degraded by cavitation bubbles. In order to overcome this, careful planning as to the positioning of the probe would have to be considered; if the probe(s) were at a sufficient distance from the lining, the intensity of the sonic waves could be reduced enough through attenuation in the liquid as so the damage could be minimized or eliminated completely. Advantages to the implementation of ultrasonication in a large-scale flotation operation would be of course the improvement of grade and reduction of gangue in concentrate. Moreover, the deagglomeration effects that ultrasonication provides may prove beneficial to operations that use regrind mills which act mainly to deagglomerate slurry. Some regrind mills do not necessarily reduce particle size significantly but improve floatability of the slurry down the circuit through the polishing and deagglomeration of the particles. Ultrasonication in theory could replace the need for these types of mills, saving energy, maintenance costs, as well as the time taken in shutting down the mill for maintenance.

While the molybdenite recovery kinetics was slowed in these experiments, one could strategically place an ultrasonication treatment in a flotation circuit so that it is not present in the

heads, but instead only in the middle and scavenger cells. In this way, the extremely floatable material that exists in the first part of the stage can quickly by recovered, and the middlings and tail end of the stage which typically recovers the higher amount of gangue in the concentrate can be subjected to ultrasonication and improve their concentrate's grade.

4.4.6 Further Discussion

These experiments suggest that an ultrasonic probe is more effective at obtaining the desired results than an ultrasonic bath, likely due to a better power capability as well as direct contact with the slurry. In addition, a pre-treatment of ultrasonication in the slurry using an ultrasonic probe was best at achieving the desired results: increasing concentration grade and increasing gangue rejection in the system. These results are likely due to the deagglomeration effects of the ultrasonication treatment affecting the route by which gangue can travel into the froth phase and concentrate in agglomerations. These agglomerations are likely broken up by the ultrasonication and gangue material is released. Although gangue was reduced in the concentrate and grade was increased, the kinetics were slowed. This can also be attributed to the deagglomeration effects of ultrasonication disrupting the fine molybdenite aggregates, which the particles by themselves are slow to float due to a high face to edge surface ratio.

4.5 SEM Topographical Analysis of the Ultrasonication Effects

Slurry from the two streams, 2nd cleaner feed and rougher concentrate, were collected and subjected to ten minutes of ultrasonication using the 2000 W probe at 24 kHz while the slurry was agitated in the small-scale float cell. After ten minutes of ultrasonication, the treated slurry was collected and pressure dried along with samples of slurry that were not ultrasonically treated. The samples were de-oiled using an acetone wash and prepped for scanning electron microscopy (SEM) as carbon coated pin stub specimens. The quartz particles in these samples

were observed under the SEM at various magnifications in order to see any topographical disturbances that might have been caused by bubble cavitations induced by the ultrasonic probe. This was of particular interest since literature has suggested that the rejection of quartz in a flotation system could be increased by way of ultrasonication through disruption of the mineral's surface causing a reduction in contact angle [79]. Quartz being notoriously hard could have damage to its surface from the bubble cavitations creating powerful jet streams directed at its surface. Images were captured with backscattered electron to discern elemental differences as well as secondary electron images to refine topographical information.

4.5.1 Non-Treated Second Cleaner Feed

Specimens from second cleaner feed slurry that were not ultrasonically treated were first observed under the SEM for topographical analysis. Quartz particles make up approximately 14% of the mass in this stream and can exist as liberated minerals, unliberated, or as extremely fine particles in agglomerations.

Quartz particles in this stream typically can display conchoidal fractures but otherwise show a relatively smooth surface on its flat regions. There are finer particles that can cover the surface which, in this ore body, usually consist of fine molybdenite, pyrite, or orthoclase feldspar. Some voids can be found on the untreated mineral's surface which are indicative of air voids. Larger angular cavities can be present which are indicative of the separation of a quartz grain, likely occurring during the grinding process. Orthoclase feldspar particles can also

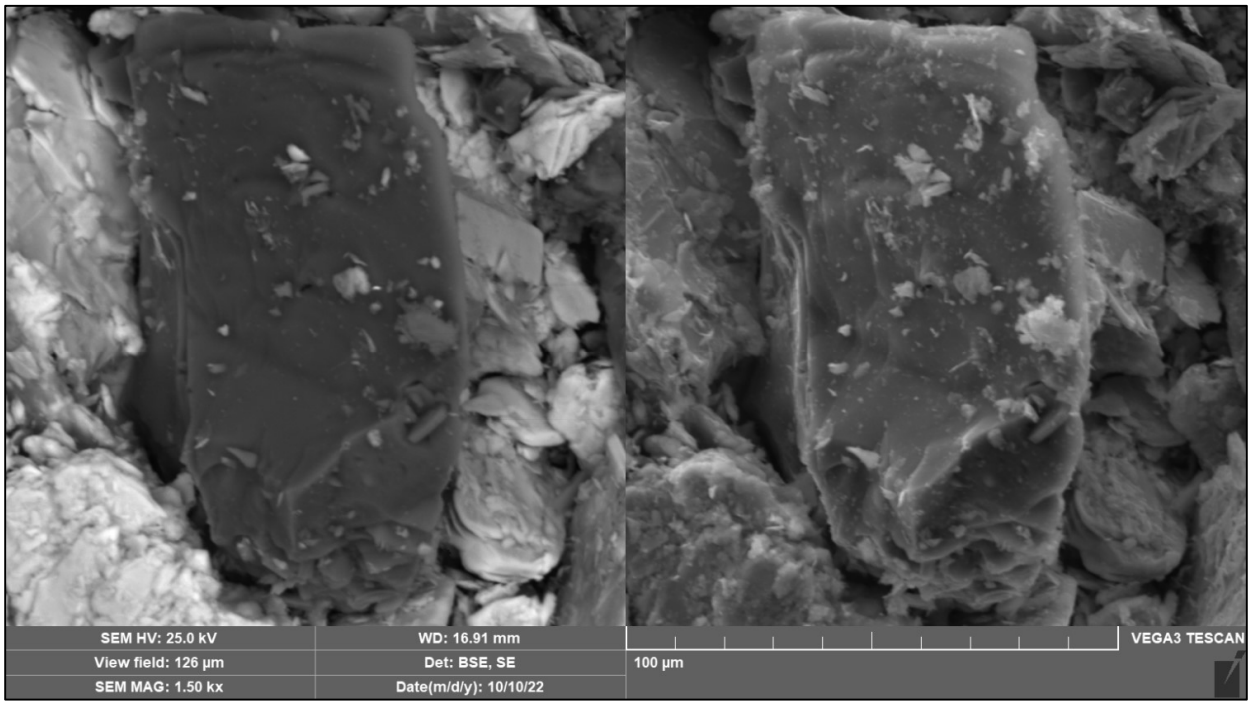

Figure 43: BSE (left) and SE (right) images of a quartz particle in untreated second cleaner feed specimens, surrounded by molybdenite particles.

be found in these streams for this ore body which display a more splintered surface as that mineral is much more susceptible to fracture than quartz [80]. While depressions and fractures were observed in feldspar and molybdenite particles for all samples for both streams, conclusions could not be drawn as to how ultrasonication affected their topography since the grinding process can cause imperfections in these samples and no susceptible difference was observed between non-ultrasonicated and ultrasonicated samples for those minerals. In addition, since quartz made up the majority of gangue material in the final product and the aim of this research was to reduce quartz floatability, the main focus of this topographical analysis was on quartz particle surfaces.

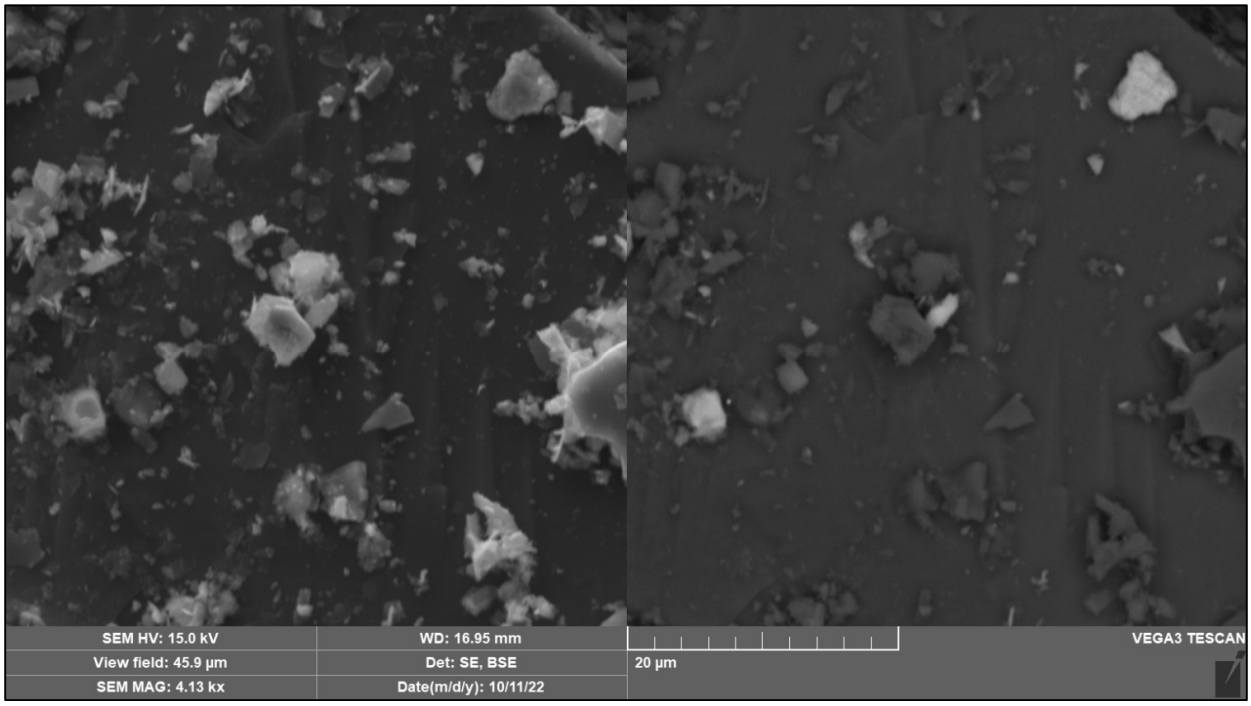

Figure 44: SE image (left) and BSE image (right) under SEM of a quartz particle surface, showing the mineral coverage by finer particles, majority of which are fine molybdenite, pyrite, or orthoclase feldspar, along with other finer quartz particles. Conchoidal fractures can be observed on the mineral surface.

A survey of quartz particles in the non-ultrasonicated second cleaner feed samples display similar topographies, with imperfections on their surfaces being conchoidal fractures likely created during the grinding/milling process. Craters could be observed but only as isolated, circular depressions that is indicative of air voids that are naturally present in quartz crystals. Larger indentions in their surfaces are indicative of a crystal grain removal or "plucking" that occurs during the grinding process.

Agglomeration is prevalent throughout all samples for both streams, treated and non-treated. Since deagglomeration was one of the main effects of ultrasonication, there was hope

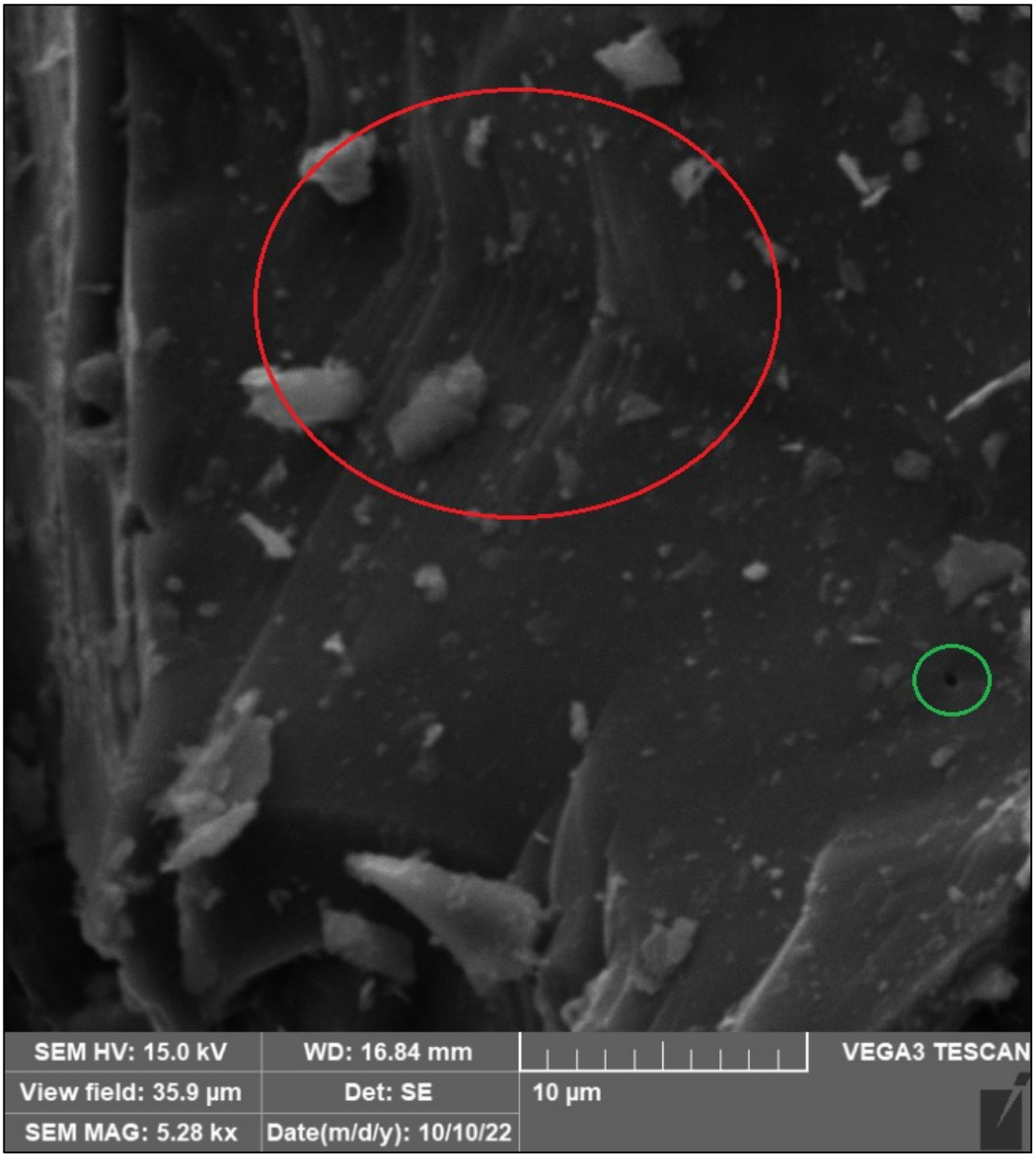

Figure 45: SEM imagery of quartz surface. Conchoidal fractures (circled red), along with an air void (circled green). Flat surfaces are relatively smooth.

that differences could be observed. However, sample drying and preparation would cause particles to reagglomerate and so calculations could not discern a difference. Molybdenite is particularly susceptible to agglomeration and occurs quickly, likely in the time in takes from the experiment ending and samples being weighed. An agglomerate under SEM appears in Figure 13.

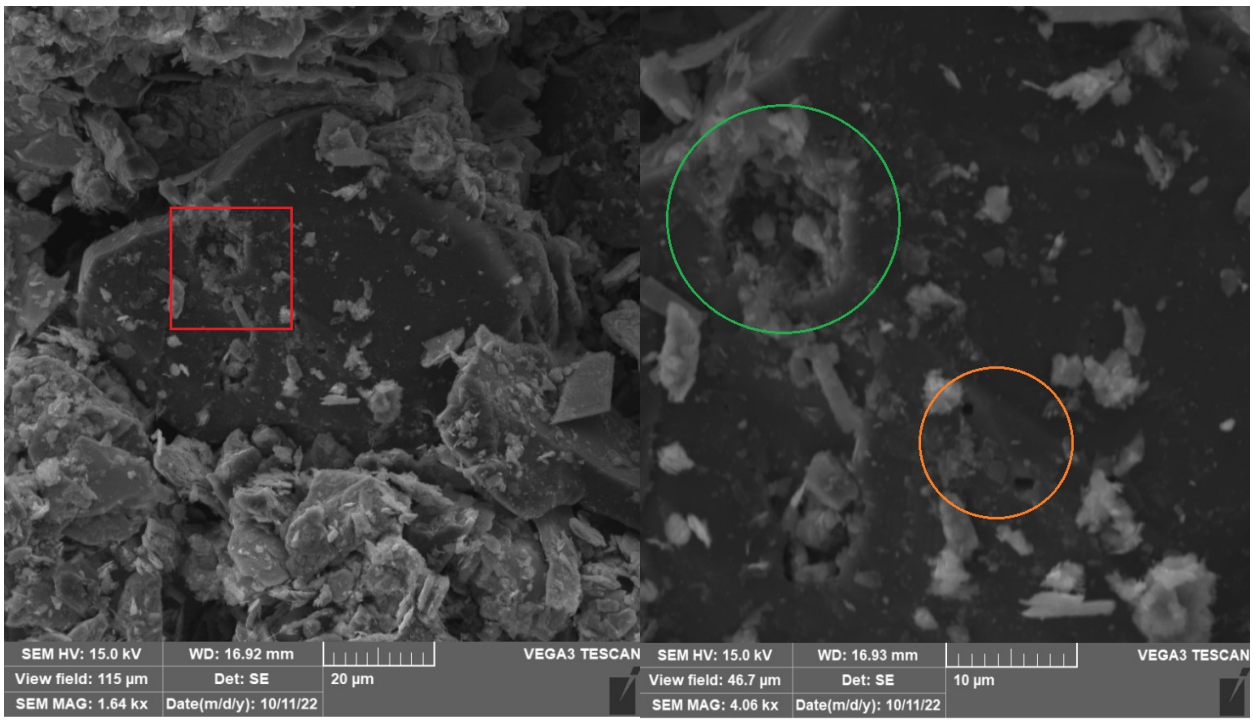

Figure 46: SEM images taken of a quartz particle (left), increased magnification of region (red) shows two air voids (circled orange) and a "plucked" grain (circled green).

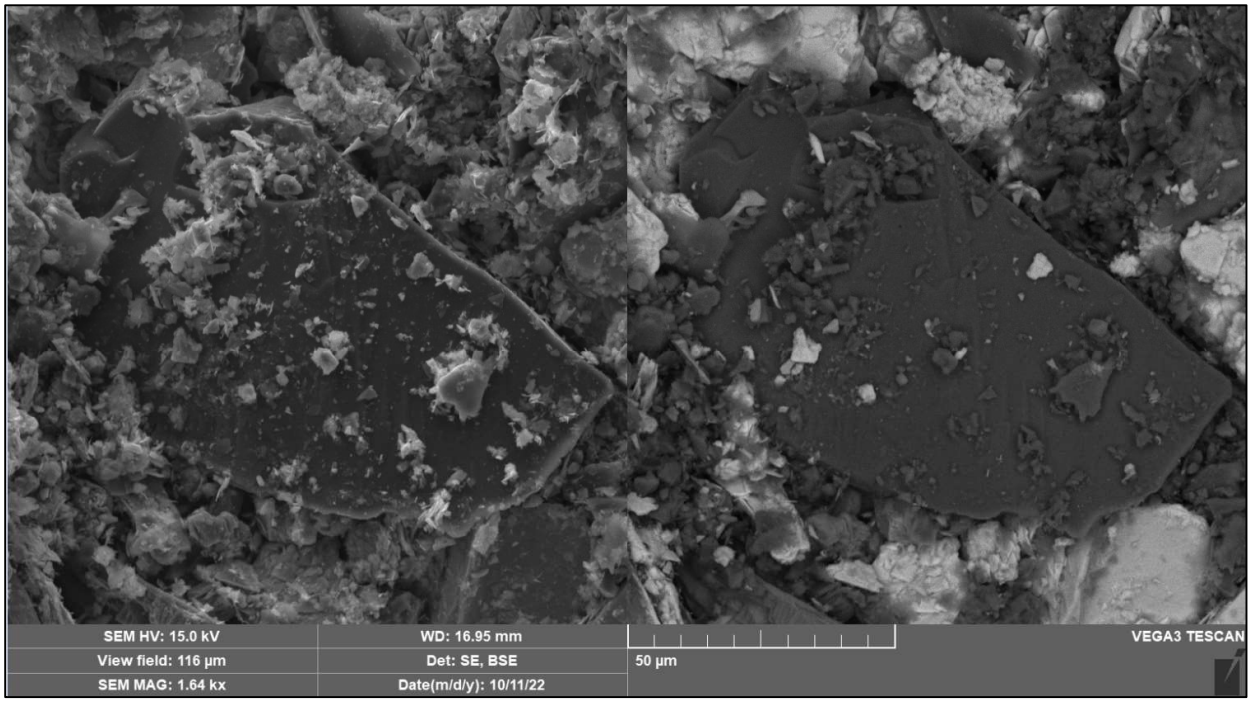

Figure 47: Surfaces of this quartz particle showing conchoidal fractures but otherwise smooth surface.

4.5.2 Ultrasonicated Second Cleaner Feed

SEM images were taken of second cleaner feed slurry subjected to ultrasonication for ten minutes at 24 kHz using a 2000 W probe while the small-scale float cell was agitated at 1200 RPM. No air was introduced in the system. A survey of the quartz particles in the samples revealed dimples displayed on their surfaces. Craters that are associated with air voids are typically circular and isolated. While air voids were observed in these samples, more irregularly shaped dimples were found on quartz surfaces. The dimples were approximately one micron in diameter. These topographical changes would contribute to lowering the floatability of quartz by reducing the contact angle a bubble adhered to the surface would form. A lower contact angle produces an adhesion force more susceptible to disruption [9].

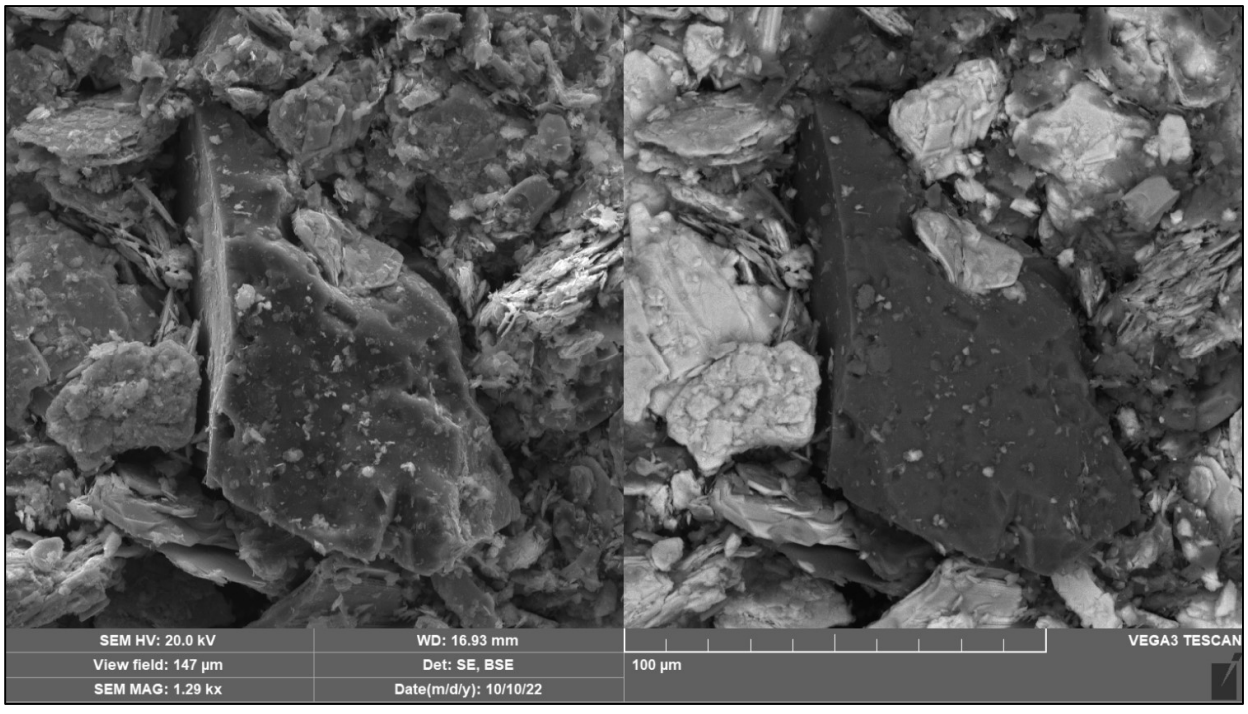

Figure 48: SE image (left) and BSE image (right) of quartz particle after ultrasonication, displaying dimples.

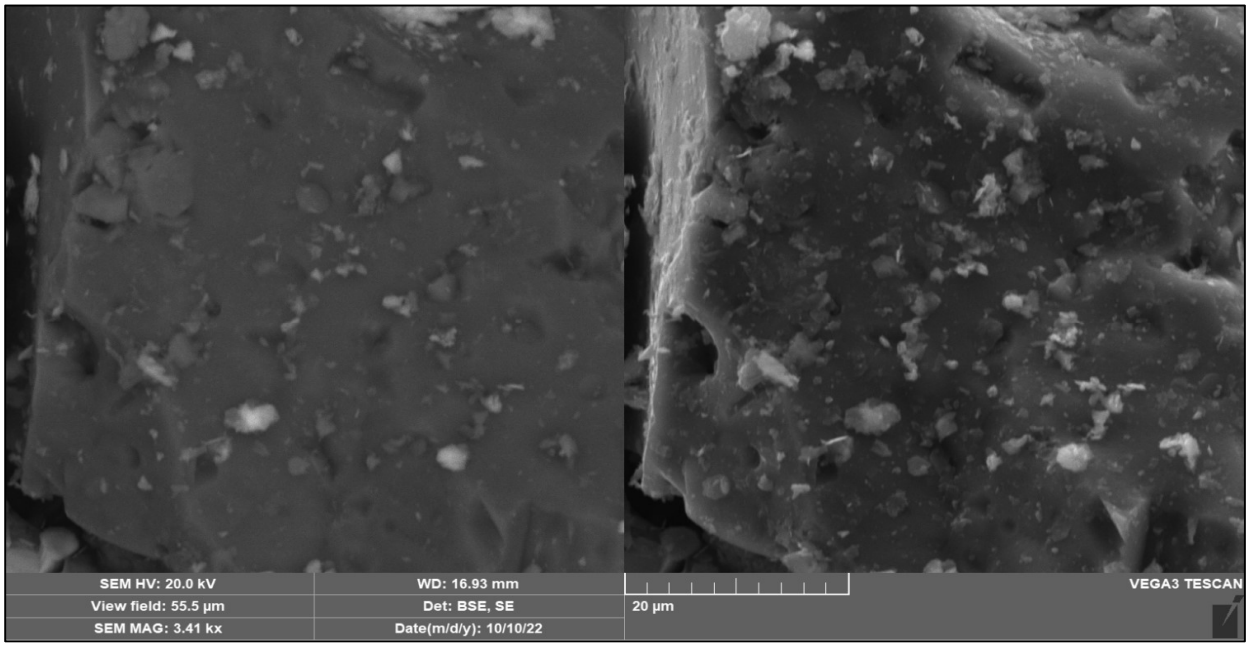

Figure 49: Increased magnification at the surface of a quartz particle displaying dimples.

There is a difference in surface topography between these observed quartz particles in the ultrasonicated slurry versus the untreated slurry. While the untreated quartz displayed a smoother surface marked by conchoidal fractures and air voids, the ultrasonicated quartz showed surfaces that were also periodically spotted by dimples and craters.

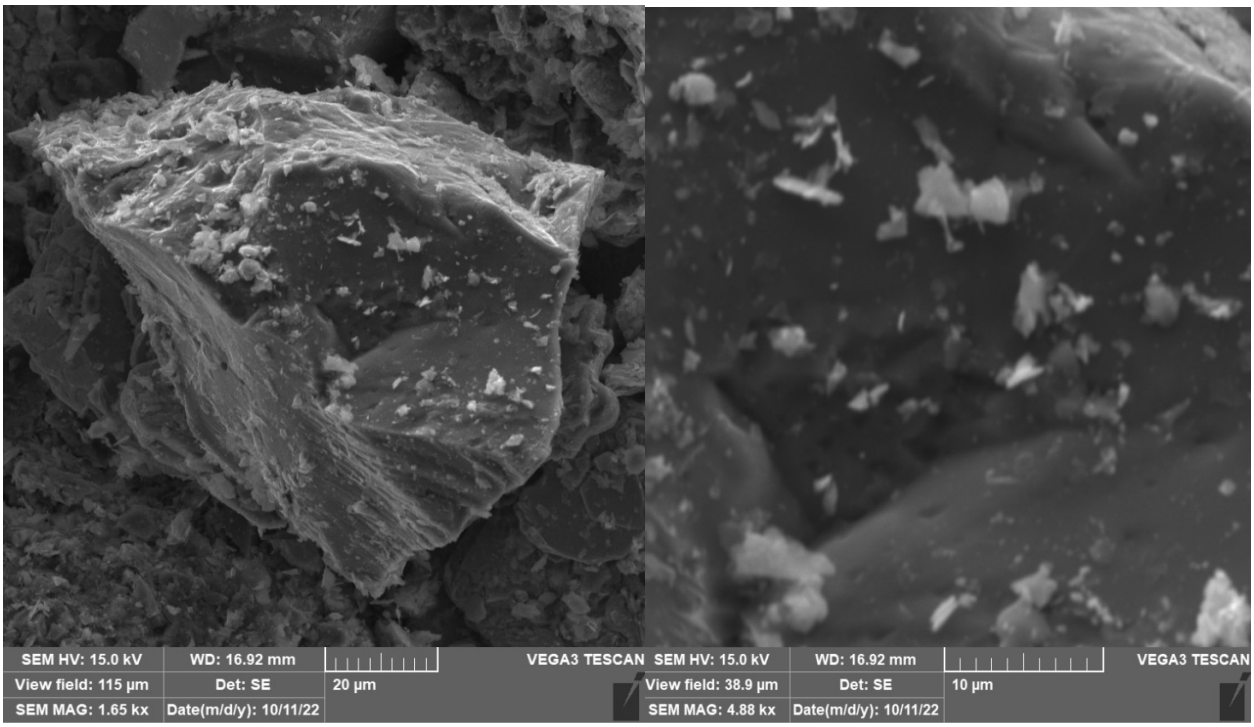

Figure 50: SEM image of quartz particle (left) with increased magnification (right) displaying surface dimples.

4.5.3 Non-treated Rougher Concentrate

SEM images were captured of rougher concentrate samples that were not subjected to ultrasonication. Quartz composes much more of this stream than the second cleaner slurry at approximately 45% of total dry mass.

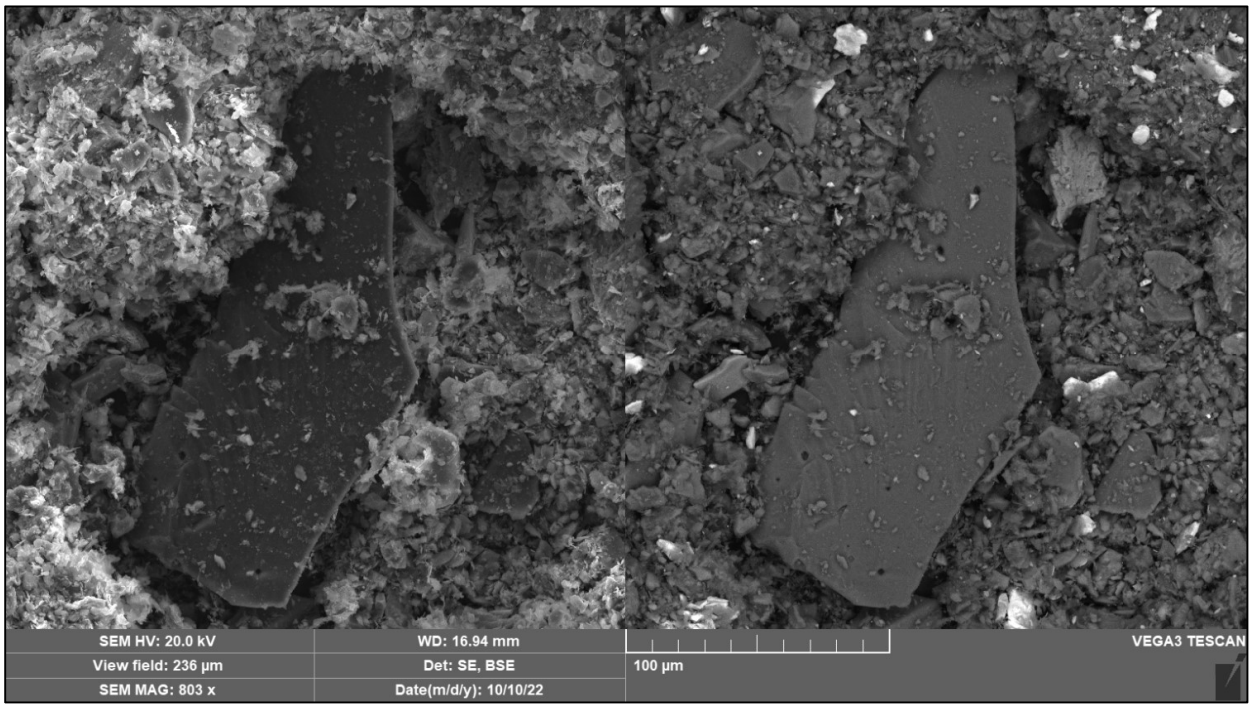

Figure 51: SE image (left) and BSE image (right) for a quartz particle in untreated rougher concentrate. Conchoidal fractures and air voids can be observed.

Similar to the second cleaner feed specimens not subjected to ultrasonication, the quartz surfaces of the rougher concentrate display imperfections of conchoidal fracture and air voids, but no regularly spaced dimples were apparent. Quartz particles in the rougher concentrate had a larger average particle size than the second cleaner feed and possessed a higher percentage of pyrite and orthoclase feldspar. This rougher concentrate had only passed through one mill while the 2nd cleaner feed had potentially been through many milling cycles. Less molybdenite was less liberated in the rougher concentrate and was less prevalent, making up about 2-4% dry mass.

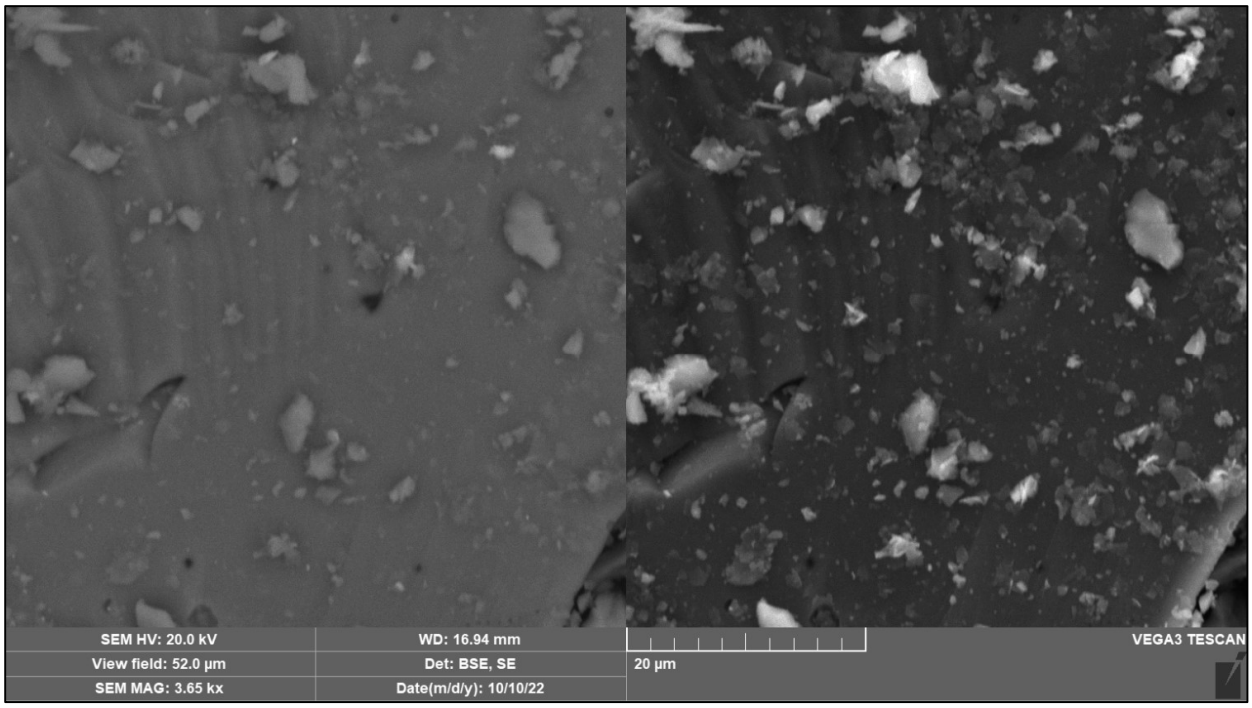

Figure 52: Increased magnification of a quartz particle's surface. BSE (left) and SE (right) images display conchoidal fractures and air voids on the surface, along with finer particulate.

The topography of quartz in these samples do compare similarly to other studies regarding the fracture of quartz [81, 82], possessing conchoidal fractures and small circular or euhedrally shaped craters. Conchoidal fractures can be identified as a smooth fracture with a ribbed appearance like a sea-shell and are a result of mechanical breakage, such as grinding. The euhedral craters, in addition to the circular air void craters, are likely to be small plucked quartz grains that fell out during the grinding process.

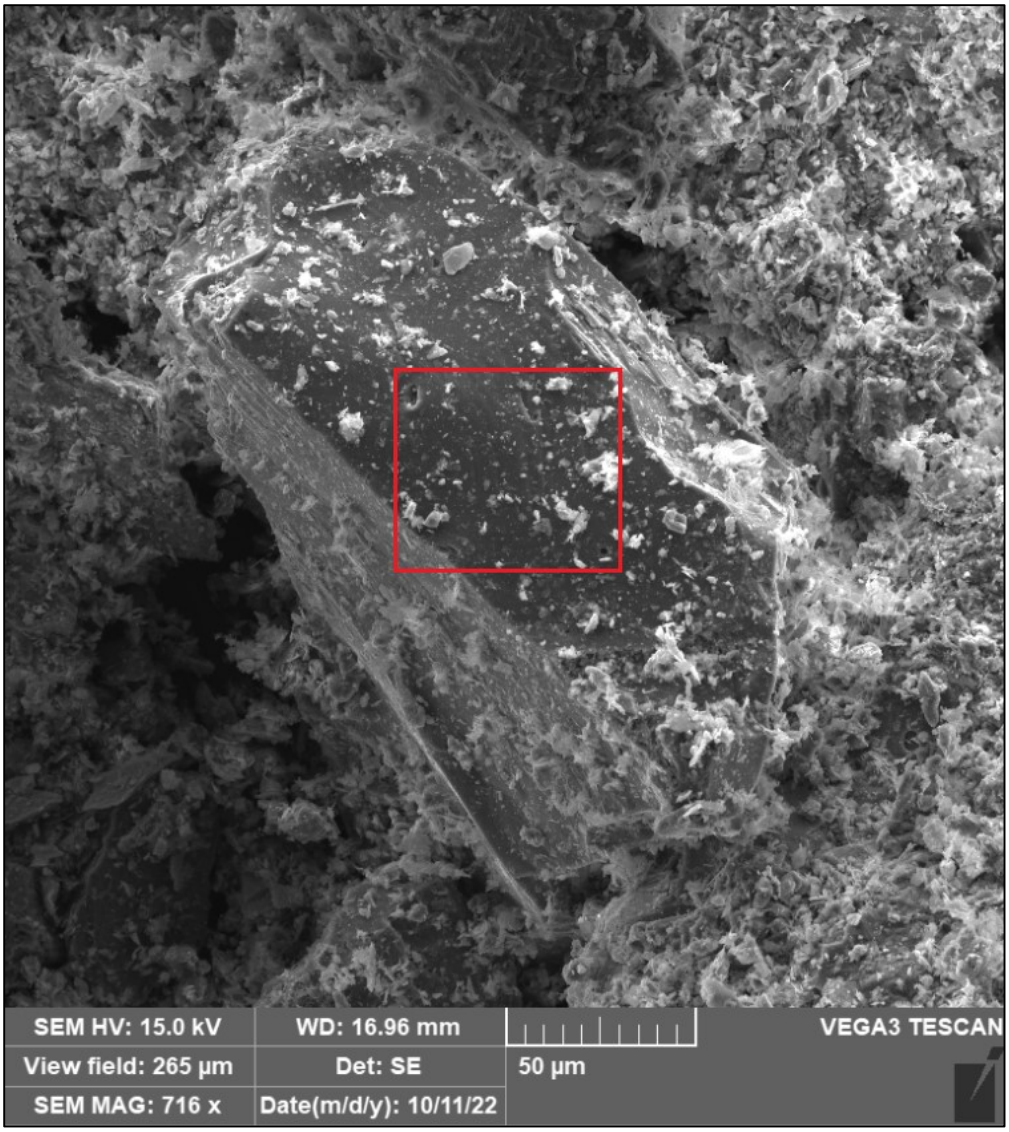

Figure 53: SE image of quartz particle under SEM. Particle displays relatively smooth surfaces and is surrounded by fine particulate composed of finer quartz and molybdenite.

Topographical features on finer quartz particles (<1 micron) in the samples were unable to be resolved using the SEM. Since dimpling that occurred during ultrasonication had diameters of approximately one micron, it might be unlikely to see ultrasonication effects on that small of a particle which are more likely to be broken apart as a result of cavitation rather than slight modifications to their surfaces.

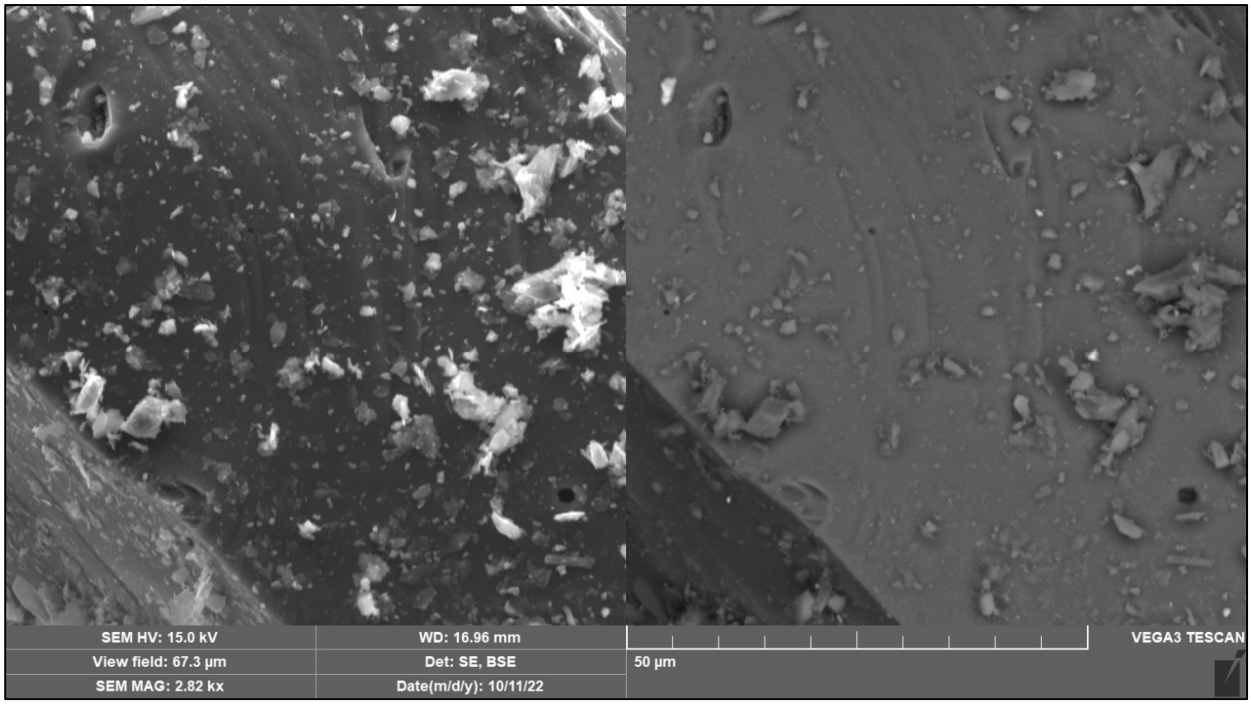

Figure 54: Magnification of red squared region on figure 50. Surface shows conchoidal fractures, air voids, and "plucked" grains.

4.5.4 Ultrasonicated Rougher Concentrate

SEM images were taken of rougher concentrate samples that were subjected to 24 kHz ultrasonication for ten minutes. While the ultrasonication effects found on the treated second cleaner samples were not as prevalent in the treated rougher concentrate, dimples of approximately one micron in diameter were observed at high magnification for a number of quartz particles surveyed. These show promising results in that it is probable that cavitation induced by ultrasonication does alter the topography of quartz particles subjected to it under these conditions, thereby reducing contact angle lowering floatability.

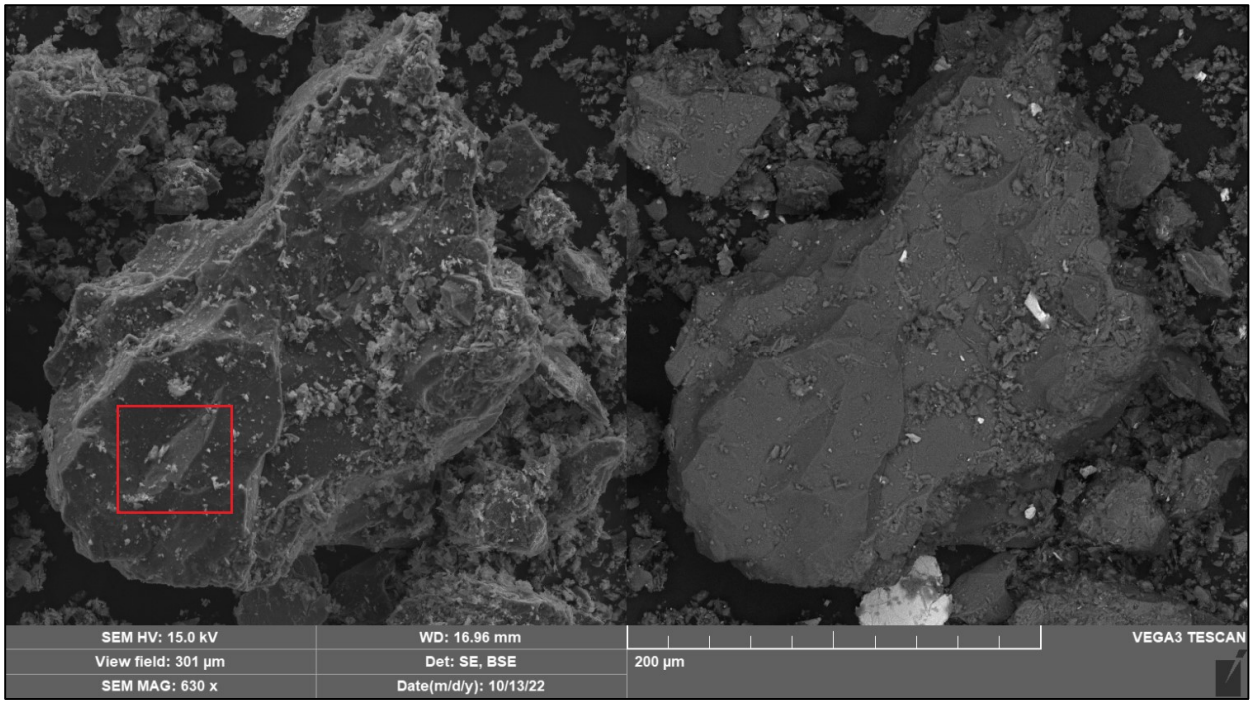

Figure 55: SE (left) and BSE (right) images of a quartz particle in the ultrasonicated rougher concentrate.

While particle sizes in the rougher concentrate are larger than the second cleaner feed, once magnification was increased on surfaces, dimples were able to be observed. The surface in figure 53 gave an advantage at displaying dimples due to its angle to the electron detector offering a higher contrast to view the surface imperfections. This might lead to a supposition that dimples/cratering due to cavitation were more prevalent but were unable to be seen clearly without that contrast. In either case, dimpling on the surface was apparent in the ultrasonicated samples for both streams as opposed to the non-treated samples, and makes a good case that contact angle is affected for the surface of quartz, leading to diminished floatability.

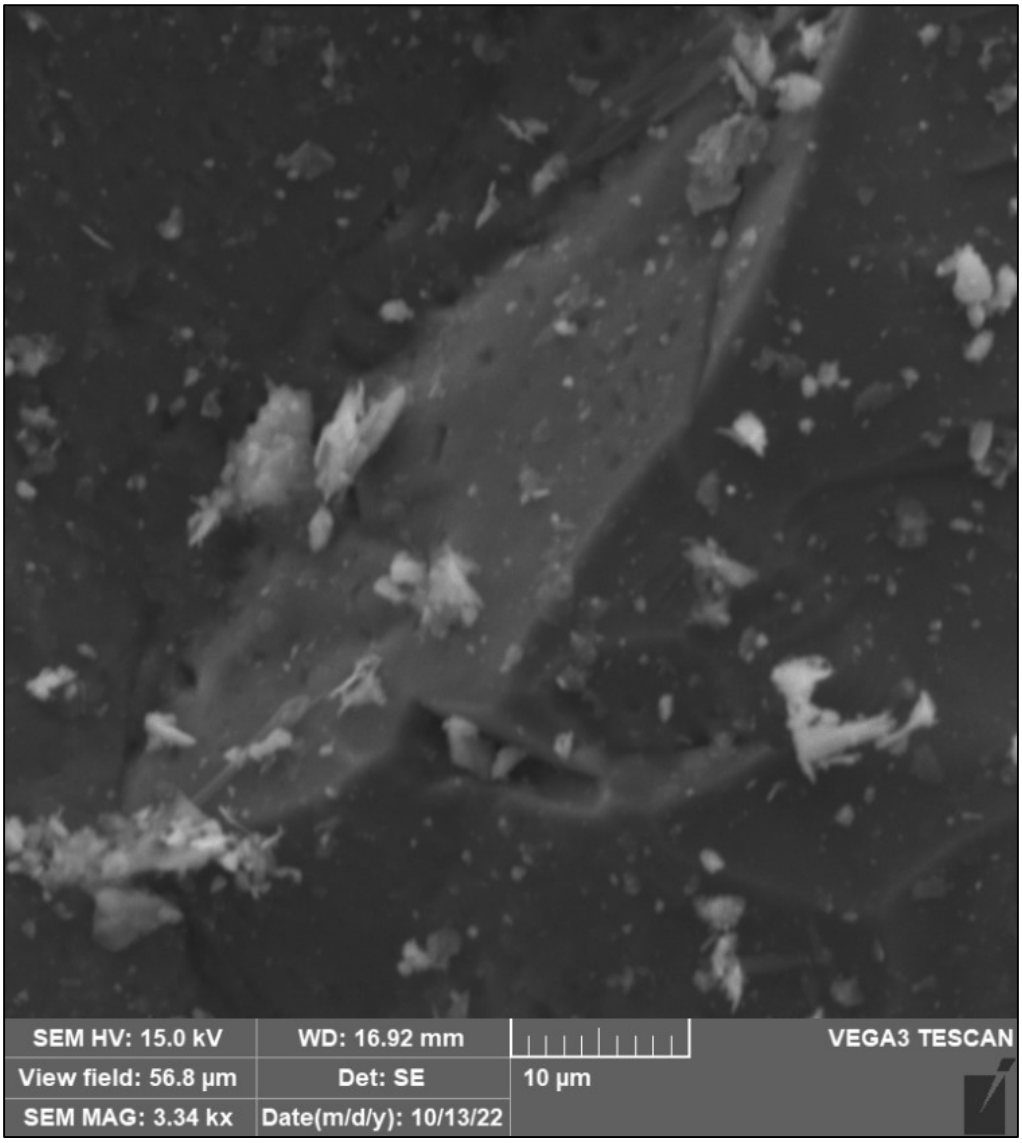

Figure 56: Magnified region from figure 52. SE imagery shows dimples at the surface.

Chapter 5: Conclusions

A series of experiments that subjected two different molybdenite streams, a second cleaner feed (2CF) and a rougher concentrate (CRC), to ultrasonication treatment during small-scale flotation tests were conducted. These experiments intended to elucidate the effects of ultrasonication on molybdenite floatability, gangue reduction, and kinetic improvement. As previous literature suggested that cavitation bubbles favor formation on hydrophobic surfaces, molybdenite flotation was a good candidate to study the effects of ultrasonic cavitation. Goals were to improve flotation kinetics and reduce gangue through the coalescence of cavitation bubbles with flotation bubbles, the increase of reagent dispersion and efficacy, and deagglomeration of particle groupings to release trapped gangue.

Experimentation on the two streams consisted of both testing with a float cell submerged in an ultrasonic bath at 37 kHz as well as running a 2000 W ultrasonic probe at 24 kHz immersed directly in the slurry. Testing using the ultrasonic bath, which entailed applying an ultrasonic treatment for the duration of the test (8 minutes), gave results that showed a slight detriment to molybdenum recovery but a minor improvement to gangue rejection. These results may be attributed to the low power of the ultrasonic bath being not enough to penetrate deep into the slurry due to attenuation, as well as the possibility that the ultrasonic waves must pass through the stainless-steel enclosure of the float cell. Another possibility may be due to not applying an ultrasonic pretreatment prior to the test. A great majority of concentrate is pulled within the first minute of the test, and the ultrasonic effects may not have had a long enough time to prove their effectiveness.

For testing using the ultrasonic probe, ultrasonication was applied for the duration of an 8-minute small-scale flotation test with a 2-minute pretreatment of ultrasound before air was

introduced. Testing found that ultrasonication slowed the kinetics of molybdenite recovery while at the same time improving the grade of the molybdenite concentrate and reducing the recovery of gangue material, which is composed mainly of quartz. These results could be explained by the deagglomeration effects of the ultrasound. Cavitation bubbles created by ultrasonic sound pressure will implode and cause powerful jet streams, where accumulated layers of molybdenite and gangue were separated through mechanical force. The breaking of these agglomerates, while allowing the gangue to escape, also likely caused a detrimental result in recovery kinetics. Fine molybdenite particle agglomerates join with oil droplets in the slurry which improves their likelihood of floating. The disruption of their agglomeration caused a slower molybdenite mass recovery over time since finer molybdenite possess a higher edge to face ratio in their structure, they are less hydrophobic and slower to float. Forming agglomerates with oil allows them to improve their float kinetics. Further research should be directed at calculating the amount of molybdenite agglomeration before, during, and after subjugation to ultrasonication in order to shed light on the likelihood of this theory. Due to sample preparation causing reagglomeration in these experiments, a clear picture of their proliferation before and after ultrasonication could not be obtained.

Although recovery was slowed, the difference in overall molybdenite recovery after the 8-minute test between the ultrasonically treated slurry and the non-treated slurry was minimal, while the ultrasound tests improved gangue rejection. In addition, the concentrate of the ultrasonicated experiments all had consistently higher molybdenum grade. Both the second cleaner feed and rougher concentrate streams benefitted; the positive effects of ultrasonication were more pronounced in the second cleaner stream than the rougher concentrate, leading to a

possibility that ultrasonication might be more beneficial on finer particles and less on coarser streams with a higher gangue percentage.

In addition to the experimentation involving ultrasonication that was operating for the entire duration of the float tests, testing that used the ultrasound probe for only the 2-minute pretreatment before the test was conducted on 2CF. Results found that the kinetics, while still slower than non-treated slurry, was faster than ultrasonicating for the duration of the 8-minute test. Concentrate was still higher in molybdenite grade and gangue rejection was still significantly higher in this pretreatment test than the non-ultrasonicated specimens, suggesting that a pretreatment of ultrasonication is all that is required to achieve favorable results. While ultrasonicating for the entire test did have better results, the difference between the pretreatment-only tests was very minimal and had an expenditure of energy five times higher.

SEM topographical analysis was conducted on the two ultrasonicated slurries and non-treated slurry for 2CF and CRC. The treated slurry had the 2000 W 24 kHz probe applied for ten-minutes while being agitated at 1200 RPM in the float cell. This was performed to inquire about the topological changes that might have occurred on quartz particles in the slurry. Literature had suggested that cavitation bubbles can theoretically cause imperfections on the surface of quartz, which is notoriously hard to fracture. These imperfections would lead to a smaller contact angle of the bubble to the surface of quartz, allowing the work of adhesion between bubble and particle to lessen, the separation easier, and floatability diminished. SEM secondary electron and backscatter electron images showed dimples and craters of one micron diameter in samples that were subjected to ultrasonication on the surface of quartz that were absent in the non-treated slurry. These observations give good plausibility to the effects of ultrasonic cavitation causing a reduction in floatability to quartz.

Overall, the results of ultrasonication regarding molybdenite flotation show positive results that can be improved upon with further research into the deagglomeration effects. Overcoming limitations to sample preparation for observation of differences in agglomerates would provide more insight. Furthermore, conditions for ultrasonication, such as probe positioning, float cell dimensions, intensity and frequency, can be manipulated in future testing to discover optimum conditions for this mineral's floatability.

The benefits to the mineral flotation industry of ultrasonication can be substantial. If results from these experiments translated to a large-scale operation, improvements in gangue reduction and concentrate grade could equate to great economic benefit to the operation in energy savings, faster tonnage throughput, and final product grade.

References

[1] U.S. Geological Survey, 2022, Mineral Industry Surveys: Molybdenum in May 2022 https://pubs.usgs.gov/periodicals/mcs2022/mcs2022-molybdenum.pdf (Accessed Sept 6, 2022).

[2] U.S. Geological Survey, 2022, Mineral commodity summaries 2022: U.S. Geological Survey, 202 p., https://doi.org/10.3133/mcs2022

[3] U.S. Geological Survey, 2021, Metals and minerals: U.S. Geological Survey Minerals Yearbook 2018, v. I, 15.1-15.12, https://doi.org/10.3133/mybvI.

[4] Donnet, C., et al. "Super-low friction of MoS2 coatings in various environments." *Tribology International* 29.2 (1996): 123-128.

[5] Gupta, Chiranjib Kumar. *Extractive metallurgy of molybdenum*. Routledge, 2017.

[6] Bulatovic, S. M., D. M. Wyslouzil, and C. Kant. "Operating practices in the beneficiation of major porphyry copper/molybdenum plants from Chile: Innovated technology and opportunities, a review." *Minerals engineering* 11.4 (1998): 313-331.

[7] Ralston, John, Daniel Fornasiero, and Nataliya Mishchuk. "The hydrophobic force in flotation-a critique." *Colloids and Surfaces A: Physicochemical and Engineering Aspects* 192.1-3 (2001): 39-51.

[8] Davis, William John Nankivell. "Method and apparatus for froth flotation." U.S. Patent No. 3,446,353. 27 May 1969.

[9] Wills, Barry A., and James Finch. *Wills' mineral processing technology: an introduction to the practical aspects of ore treatment and mineral recovery*. Butterworth-Heinemann, 2015.

[10] Shean, B. J., and J. J. Cilliers. "A review of froth flotation control." *International Journal of Mineral Processing* 100.3-4 (2011): 57-71.

[11] Ata, Seher. "Phenomena in the froth phase of flotation—A review." *International Journal of Mineral Processing* 102 (2012): 1-12.

[12] Bulatovic, Srdjan M. *Handbook of flotation reagents: chemistry, theory and practice: Volume 1: flotation of sulfide ores*. Elsevier, 2007.

[13] Crozier, Ronald D. "Flotation: theory, reagents and ore testing." (1992).

[14] Williams, J. J. E., and R. I. Crane. "Particle collision rate in turbulent flow." *International Journal of Multiphase Flow* 9.4 (1983): 421-435.

[15] Yoon, R-H. "The role of hydrodynamic and surface forces in bubble–particle interaction." *International Journal of Mineral Processing* 58.1-4 (2000): 129-143.

[16] Trahar, W. J. "A rational interpretation of the role of particle size in flotation." *International Journal of Mineral Processing* 8.4 (1981): 289-327.

[17] Jameson, Graeme J. "The effect of surface liberation and particle size on flotation rate constants." *Minerals Engineering* 36 (2012): 132-137.

[18] Smith, C., S. Neethling, and J. J. Cilliers. "Air-rate profile optimisation: From simulation to bank improvement." *Minerals Engineering* 21.12-14 (2008): 973-981.

[19] Rahman, Reza M., Seher Ata, and Graeme J. Jameson. "The effect of flotation variables on the recovery of different particle size fractions in the froth and the pulp." *International Journal of Mineral Processing* 106 (2012): 70-77.

[20] Chau, T. T., et al. "A review of factors that affect contact angle and implications for flotation practice." *Advances in colloid and interface science* 150.2 (2009): 106-115.

[21] Cooper, M., et al. "Impact of air distribution profile on banks in a Zn cleaning circuit." *CIM Bulletin* 97.1083 (2004): 1-6.

[22] Yoon, R-H. "Microbubble flotation." *Minerals Engineering* 6.6 (1993): 619-630.

[23] Waters, K. E., K. Hadler, and J. J. Cilliers. "The flotation of fine particles using charged microbubbles." *Minerals Engineering* 21.12-14 (2008): 918-923.

[24] Bloom, Frederick, and Theodore J. Heindel. "On the structure of collision and detachment frequencies in flotation models." *Chemical Engineering Science* 57.13 (2002): 2467-2473.

[25] Maldonado, M., et al. "An experimental study examining the relationship between bubble shape and rise velocity." *Chemical Engineering Science* 98 (2013): 7-11.

[26] Yianatos, J. B., and F. Henríquez. "Boundary conditions for gas rate and bubble size at the pulp–froth interface in flotation equipment." *Minerals Engineering* 20.6 (2007): 625-628.

[27] Crozier, R. D. "Sulphide collector mineral bonding and the mechanism of flotation." *Minerals Engineering* 4.7-11 (1991): 839-858.

[28] Cho, Yoon-Seong, and J. S. Laskowski. "Effect of flotation frothers on bubble size and foam stability." *International Journal of Mineral Processing* 64.2-3 (2002): 69-80.

[29] Chu, Pengbo, and James A. Finch. "Frother and breakup in small bubble formation." *Proceedings of the 52nd Conference of Metallurgists (hosted by Materials Science & Technology (MS&T) 2013): Water and Energy in Mineral Processing, The 9th UBC-McGill-U of A International Symposium on the Fundamentals of Mineral Processing, The Metallurgical Society of CIM*. 2013.

[30] Chu, P., M. Mirnezami, and J. A. Finch. "Quantifying particle pick up at a pendant bubble: A study of non-hydrophobic particle–bubble interaction." *Minerals Engineering* 55 (2014): 162-164.

[31] Yi, Gaosong, et al. "Recent progress on research of molybdenite flotation: A review." *Advances in colloid and interface science* 295 (2021): 102466.

[32] Lu, Zhenzhen, et al. "Probing anisotropic surface properties of molybdenite by direct force measurements." *Langmuir* 31.42 (2015): 11409-11418.

[33] Wang, Jingyi, et al. "Electrochemical investigation of the interactions of organic and inorganic depressants on basal and edge planes of molybdenite." *Journal of colloid and interface science* 570 (2020): 350-361.

[34] Miki, Hajime, et al. "Electrolysis oxidation of chalcopyrite and molybdenite for selective flotation." *Materials Transactions* 58.5 (2017): 761-767.

[35] Yarar, B., and J. Kaoma. "Estimation of the critical surface tension of wetting of hydrophobic solids by flotation." *Colloids and surfaces* 11.3-4 (1984): 429-436.

[36] Yianatos, J. B. "Fluid flow and kinetic modelling in flotation related processes: columns and mechanically agitated cells—a review." *Chemical Engineering Research and Design* 85.12 (2007): 1591-1603.

[37] Ross, V. E. "Flotation and entrainment of particles during batch flotation tests." *Minerals Engineering* 3.3-4 (1990): 245-256.

[38] Wang, Ly, et al. "A review of entrainment: Mechanisms, contributing factors and modelling in flotation." *Minerals Engineering* 70 (2015): 77-91.

[39] Wang, Lei. "Entrainment of fine particles in froth flotation." (2017).

[40] Zhang, Wei, J. E. Nesset, and J. A. Finch. "Water recovery and bubble surface area flux in flotation." Canadian Metallurgical Quarterly 49.4 (2010): 353-362.

[41] Martinez, Jose, Miguel Maldonado, and Leopoldo Gutierrez. "A Method to Predict Water Recovery Rate in the Collection and Froth Zone of Flotation Systems." *Minerals* 10.7 (2020): 630.

[42] Bradshaw, D. J., and F. Vos. "The development of a small scale test for rapid characterisation of flotation response (JKMSI)." *Proceedings of the Canadian Mineral Processors Operators Conference, Ottawa, ON, Canada*. 2013.

[43] Runge, Kym. "Laboratory flotation testing–an essential tool for ore characterisation." *Flotation Plant Optimisation: A Metallurgical Guide to Identifying and Solving Problems in Flotation Plants. Australasian Institute of Mining and Metallurgy, Spectrum Series Carlton, Vic* (2010): 55-173.

[44] Cheeke, J. David. "N. 2002 Fundamentals and Applications of Ultrasonic Waves." *CRC Series in Pure and Applied Physics*.

[45] Mason, Timothy J., and P. Cintas. "Sonochemistry." *Handbook of Green Chemistry and Technology*. Oxford: Blackwell, 2002. 372-396.

[46] Chatel, Gregory. *Sonochemistry: new opportunities for green chemistry*. World Scientific Publishing Company, 2016.

[47] Neppiras, E. A., and B. E. Noltingk. "Cavitation produced by ultrasonics: theoretical conditions for the onset of cavitation." *Proceedings of the Physical Society. Section B* 64.12 (1951): 1032.

[48] Ashokkumar, Muthupandian. "The characterization of acoustic cavitation bubbles–an overview." *Ultrasonics sonochemistry* 18.4 (2011): 864-872.

[49] Klassen, Villi Ivanovich, and Vladimir Alekseevich Mokrousov. *An introduction to the theory of flotation*. Butterworths, 1963.

[50] Blake, John R., and D. C. Gibson. "Cavitation bubbles near boundaries." *Annual review of fluid mechanics* 19.1 (1987): 99-123.

[51] Neppiras, Ernest A. "Acoustic cavitation." *Physics reports* 61.3 (1980): 159-251.

[52] Flynn, Hugh G. "Cavitation dynamics. I. A mathematical formulation." *The Journal of the Acoustical Society of America* 57.6 (1975): 1379-1396.

[53] Noltingk, B. Eo, and Eo A. Neppiras. "Cavitation produced by ultrasonics." *Proceedings of the Physical Society. Section B* 63.9 (1950): 674.

[54] Zheng, X., J. P. Franzidis, and N. W. Johnson. "An evaluation of different models of water recovery in flotation." *Minerals Engineering* 19.9 (2006): 871-882.

[55] Wrobel, S. "The adsorption of nuclear gas-its role in froth flotation." Mine Quarry Eng (1952): 313-317.

[56] Klassen, V. I. "Theoretical basis of flotation by gas precipitation." *The Proceedings of Vth IMPC, London* (1960): 309-322.

[57] Kursun, Hulya, and Ugur Ulusoy. "Zinc recovery from a lead–zinc–copper ore by ultrasonically assisted column flotation." *Particulate Science and Technology* 33.4 (2015): 349-356.

[58] Hassanzadeh, Ahmad, et al. "Effect of power ultrasound on wettability and collector-less floatability of chalcopyrite, pyrite and quartz." *Minerals* 11.1 (2021): 48.

[59] Chen, Yuran, et al. "A review of effects and applications of ultrasound in mineral flotation." *Ultrasonics sonochemistry* 60 (2020): 104739.

[60] Mørch, Knud Aage. "Reflections on cavitation nuclei in water." *Physics of Fluids* 19.7 (2007): 072104.

[61] Bandini, Paula, C. A. Prestidge, and J. Ralston. "Colloidal iron oxide slime coatings and galena particle flotation." *Minerals Engineering* 14.5 (2001): 487-497.

[62] Gurpinar, G., E. Sonmez, and V. Bozkurt. "Effect of ultrasonic treatment on flotation of calcite, barite and quartz." *Mineral Processing and Extractive Metallurgy* 113.2 (2004): 91-95.

[63] Altun, N. Emre, Jiann-Yang Hwang, and Cahit Hicyilmaz. "Enhancement of flotation performance of oil shale cleaning by ultrasonic treatment." *International Journal of Mineral Processing* 91.1-2 (2009): 1-13.

[64] Ozkan, Safak G., and Halit Z. Kuyumcu. "Investigation of mechanism of ultrasound on coal flotation." *International Journal of Mineral Processing* 81.3 (2006): 201-203.

[65] Özkan, Şafak G., and Halit Z. Kuyumcu. "Design of a flotation cell equipped with ultrasound transducers to enhance coal flotation." *Ultrasonics Sonochemistry* 14.5 (2007): 639-645.

[66] Ozkan, Safak Gokhan. "Further investigations on simultaneous ultrasonic coal flotation." *Minerals* 7.10 (2017): 177.

[67] Videla, A. R., et al. "Ultrasound treatment on tailings to enhance copper flotation recovery." *Minerals Engineering* 99 (2016): 89-95.

[68] Misra, M., A. M. Raichur, and A. P. Lan. "Improved flotation of arsenopyrite by ultrasonic pretreatment." *Mining, Metallurgy & Exploration* 20.2 (2003): 93-97.

[69] Cao, Qinbo, et al. "Surface cleaning and oxidative effects of ultrasonication on the flotation of oxidized pyrite." *Powder technology* 311 (2017): 390-397.

[70] Xu, Mengdi, et al. "Effect of ultrasonic pretreatment on oxidized coal flotation." *Energy & fuels* 31.12 (2017): 14367-14373.

[71] Feng, Dingwu, and Chris Aldrich. "Effect of ultrasonication on the flotation of talc." *Industrial & engineering chemistry research* 43.15 (2004): 4422-4427.

[72] Aldrich, C., and D. Feng. "Effect of ultrasonic preconditioning of pulp on the flotation of sulphide ores." *Minerals Engineering* 12.6 (1999): 701-707.

[73] Li, Chenwei, et al. "Effect of ultrasonication on the flotation of fine graphite particles: Nanobubbles or not?." *Ultrasonics Sonochemistry* 69 (2020): 105243.

[74] Filippov, L. O., J. J. Royer, and I. V. Filippova. "Improvement of ore recovery efficiency in a flotation column cell using ultra-sonic enhanced bubbles." *Journal of Physics: Conference Series*. Vol. 879. No. 1. IOP Publishing, 2017.

[75] Zhou, Z. A., Zhenghe Xu, and J. A. Finch. "On the role of cavitation in particle collection during flotation-a critical review." *Minerals Engineering* 7.9 (1994): 1073-1084.

[76] Zhou, Z. A., et al. "Role of hydrodynamic cavitation in fine particle flotation." *International Journal of Mineral Processing* 51.1-4 (1997): 139-149.

[77] Celik, M. S. "Effect of ultrasonic treatment on the floatability of coal and galena." *Separation Science and Technology* 24.14 (1989): 1159-1166.

[78] Feng, D., and Chris Aldrich. "Effect of preconditioning on the flotation of coal." *Chemical Engineering Communications* 192.7 (2005): 972-983.

[79] Napier-Munn, T. J. "Statistical methods to compare batch flotation grade-recovery curves and rate constants." *Minerals Engineering* 34 (2012): 70-77.

[80] Tromans, D., and J. A. Meech. "Fracture toughness and surface energies of minerals: theoretical estimates for oxides, sulphides, silicates and halides." *Minerals Engineering* 15.12 (2002): 1027-1041.

[81] Martinelli, Giovanni, et al. "Fracture Analysis of α-Quartz Crystals Subjected to Shear Stress." *Minerals* 10.10 (2020): 870.

[82] Stevic, Marijana. "Identification and environmental interpretation of microtextures on quartz grains from aeolian sediments: Brattforsheden and Vittskövle, Sweden." *Dissertations in Geology at Lund University* (2015).

Vita

Wayne Alexander Campbell first earned a Bachelor of Science in Biology with a double minor in chemistry and music from the University of North Texas. He worked as a microbiologist for a small company testing for microbial contaminants for three years, followed by working as a high school chemistry teacher for three years. In 2019, Wayne began his graduate degree in metallurgical engineering at the University of Texas at El Paso working under Dr. Guikuan Yue. Wayne worked as a teaching assistant while at UTEP and taught an introductory materials science course. He was the president of UTEP's chapter for the Society for Mining, Metallurgy, and Exploration (SME) during his time at the university. Wayne currently works as a metallurgist for Freeport-McMoRan as of 2022.